Development of a Wide-Band Gamma-Ray Camera Onboard a 50 kg-Class Small Satellite GRAPHIUM

WASEDA University[1], SCIENCE TOKYO[2], iMAGINE-X[3]

◎R.Mori[1], J.Kataoka[1], K.Tanaka[1], T.Suga[1], S.Ogasawara[1], K.Yamamoto[1], A.Joshi[1], T.Kanda[1], Y.Yatsu[2], H.Nakanishi[2], T.Chujo[2], T.Tomura[2], K.Miyamoto[2], K.Watanabe[2], H.Kobayashi[2], Y.Amaki[2], K.Takahashi[2], M.Yasuda[2], D.Kobayashi[2], K.Otsubo[2],Y.Arai[2], D.Yoshimura[2], Y.Ozeki[2], K.Tashiro[2], S.Hayatsu[2], Y.Kawaguchi[2], H.Yoshida[2], M.Fukuda[2], H.Seki[2], S.Joshima[2], M.Onishi[3], S.Takeda[3]

1. Research Background

◆ MeV gamma-ray astronomy

・Satellite observation is essential
・Cannot be imaged with lenses or reflectors
・Background dominated(Albedo, CXB)
⇨ "Last Window" for space observation

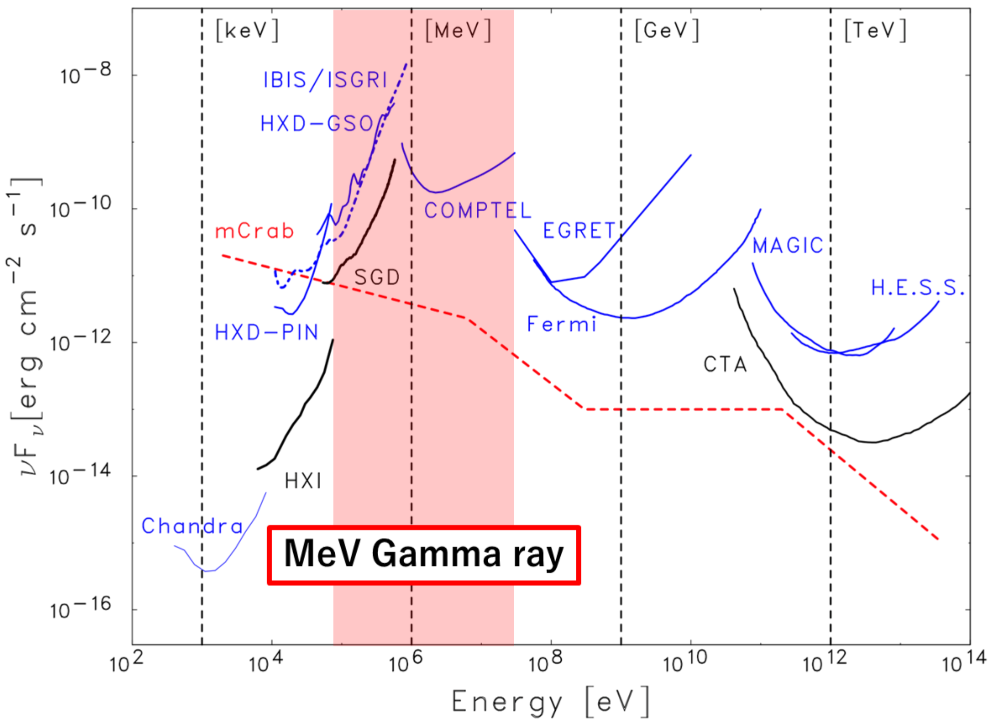

◆ MeV all-sky survey

・Transients like GRB, solar flares, kilonova
・The origin of heavy element synthesis
Au, Pt ++ (rare metals)

New science proved with MeV Gamma Ray Observations

2. MeV γ rays as nucleosynthesis probe

EMMI, GSI/Different Arts

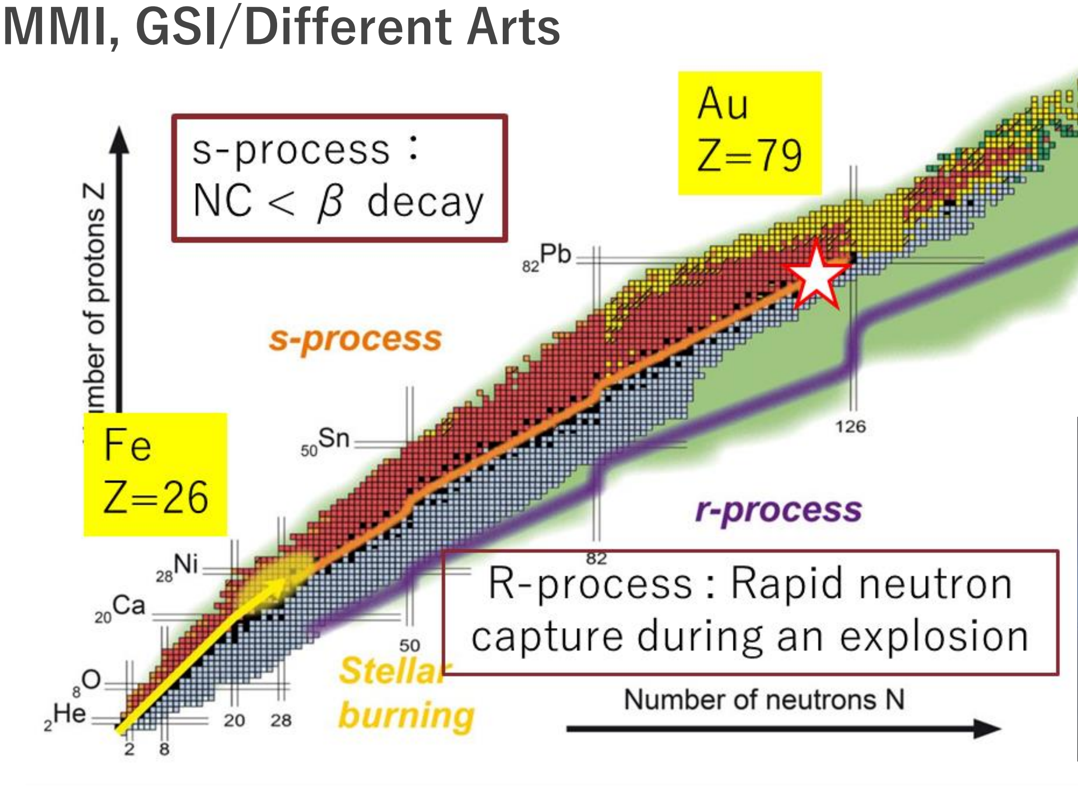

EMMI, GSI/Different Arts

LIGO collaboration 2017

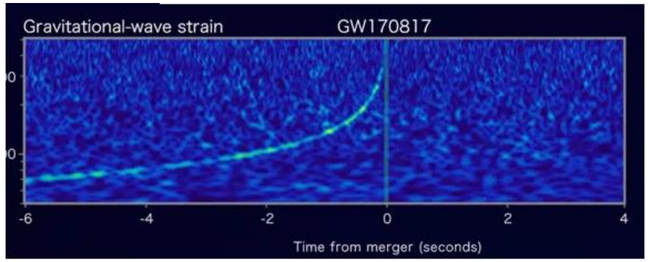

Hotokezaka et al. 2016

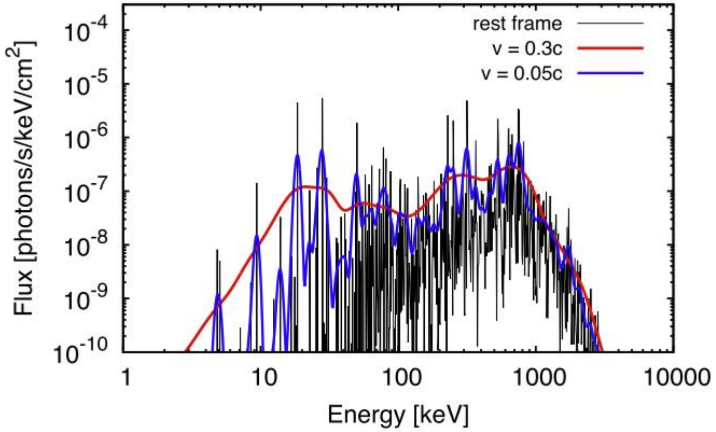

- Heavy elements than $_{26}$Fe are thought to be produced via NC by s-process, but origin of Pt , Au ++ (rare metals) remains mystery
- "Kilonova" is a candidate - also emit line γ rays at 30 keV – 3 MeV ?

3. Observation of Solar flare

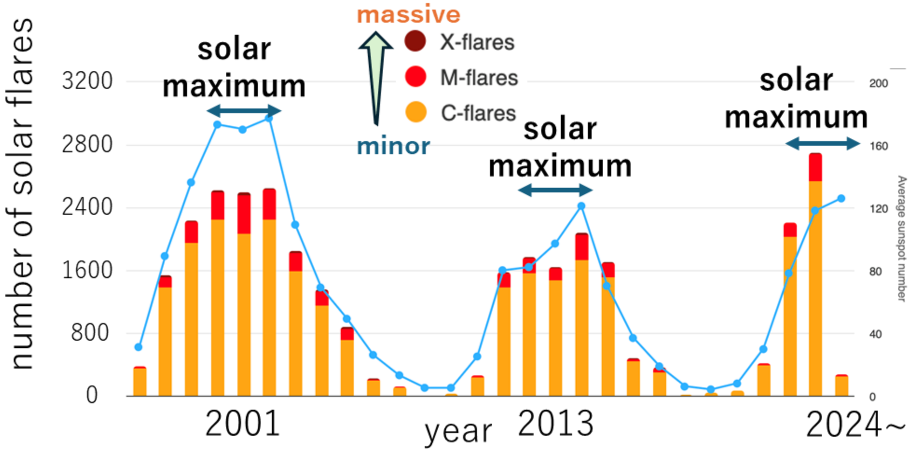

Ackermann et al. 2012

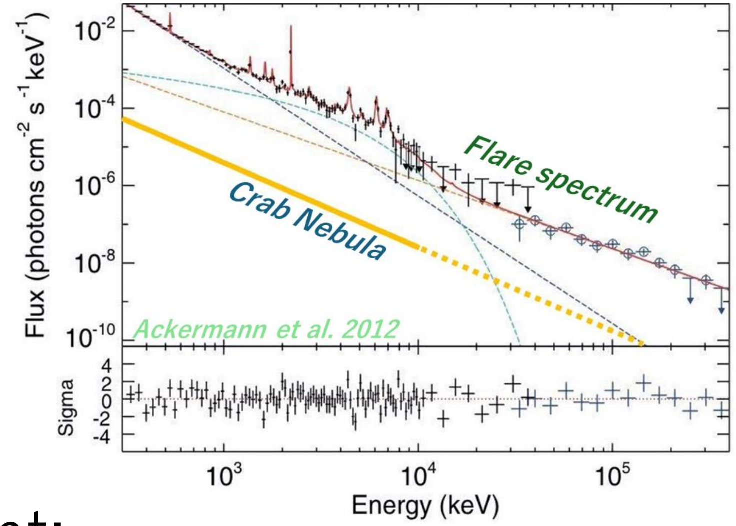

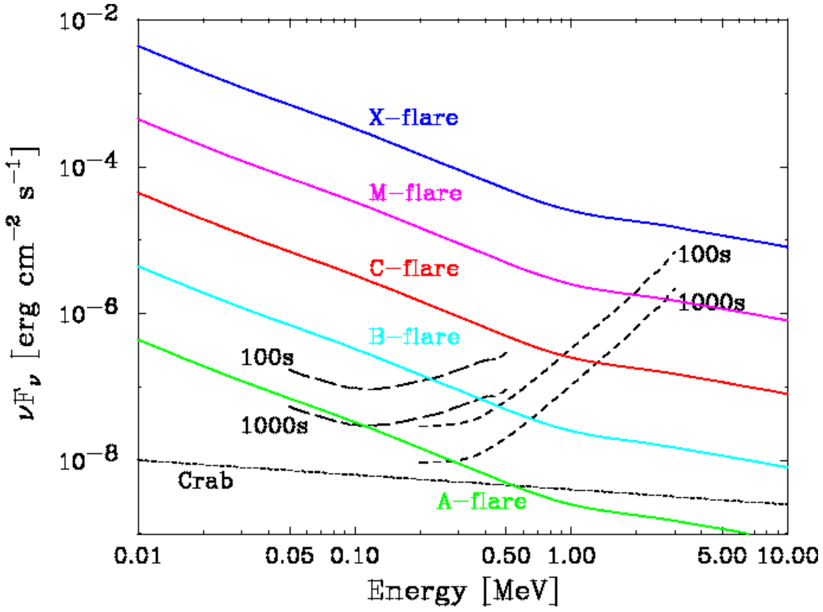

- Very bright and frequent:
  - ✓ ~5/day for C-class flare
  - ✓ ~0.7/day for M-class flare
- Various de-excitation lines along with non-thermal bremss: e^-e^+(511keV), ^{56}Fe, ^{24}Mg(0.5-2MeV), NC(2.2MeV), ^{12}C(4.4MeV)++

4. Our strategy for MeV observation

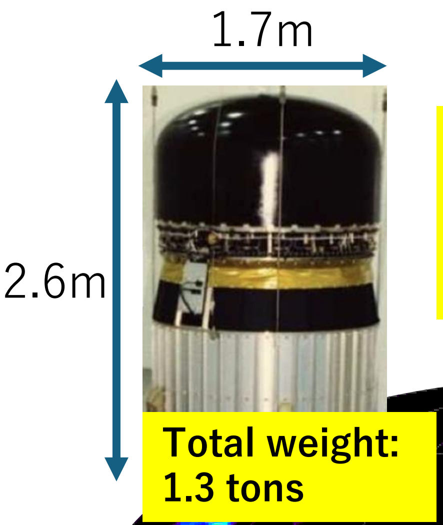

Cost: ~50 M USD
Development Period:
Over 10 years

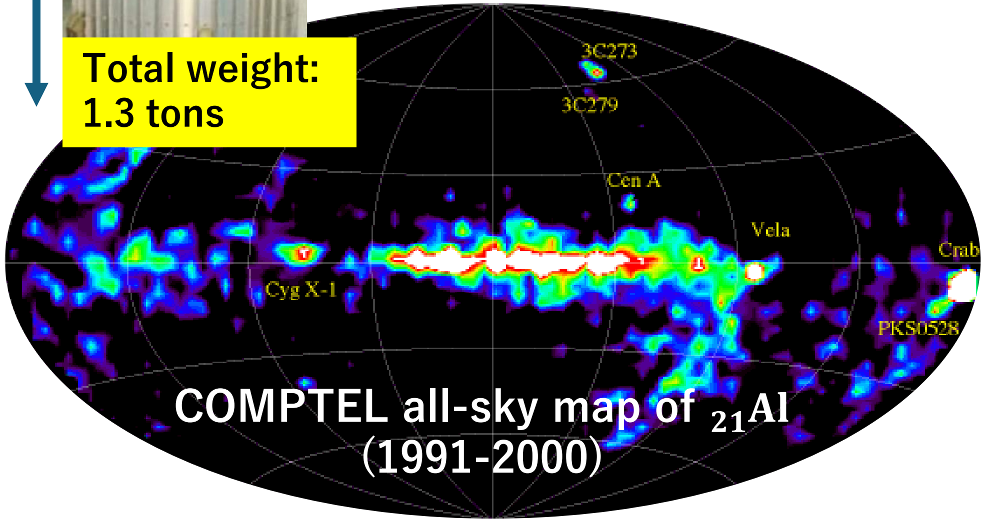

COMPTEL all-sky map of $_{21}$Al
(1991-2000)

◆ CGRO Satellite "COMPTEL"

・Compton camera for 1-30 MeV
・Developed by NASA, launched in 1991

△difficulties in terms of cost, manpower, development period, rocket etc···
⇨**30 years** of stagnation

◆ Our Motivation

・50 kg-class small satellite
⇒Low cost (~ 2 M USD)
 + short development period (~5 years)
 c.f., COSI : 400kg , ~90 M USD

New challenge for space science using small satellites

5. Wide-band imaging

◆ Hybrid CC

- "active pinhole" in the Scatter center:

✓ E < 200 keV as a pinhole camera

✓ E > 200 keV as a conventional CC

- Extend the energy range down to **30 keV**

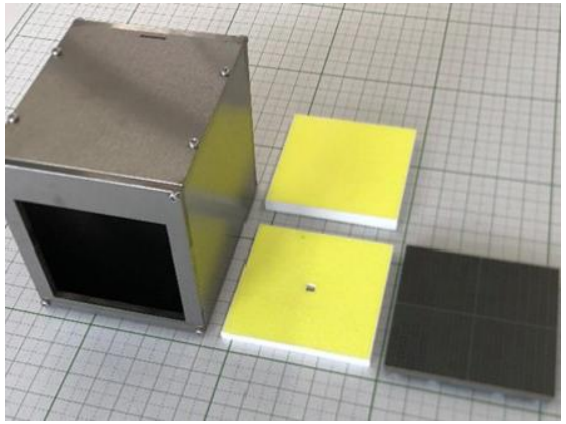

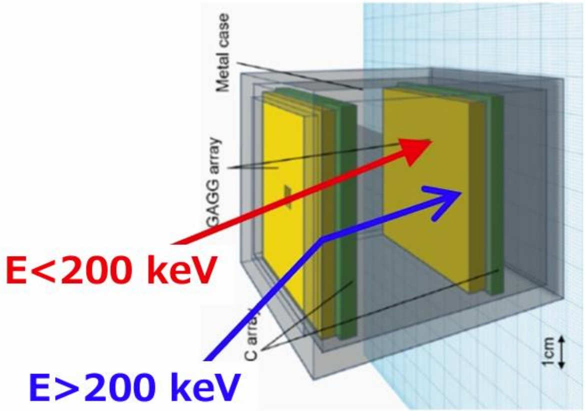

Omata et al. 2020; 2022, Sci. Rep.

◆ For Medical

- Confirming radiopharmaceutical Accumulation Externally
- Simultaneous Imaging of different radionuclides
- Broadband imaging in small animal experiments

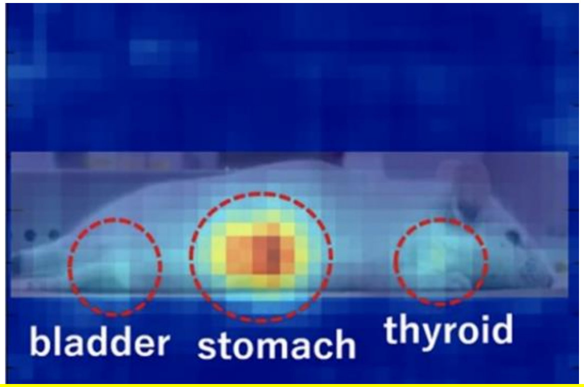

Pharmacokinetic Monitoring for Cancer Therapy

Deploying Compton Cameras for Space Applications!!

6. GRAPHIUM mission

HIBARI:2021

Demonstration of variable shape control

PETREL:2025

UV telescope and Earth monitor

GRAPHIUM:2027

MeV all-sky survey

INSPIRE

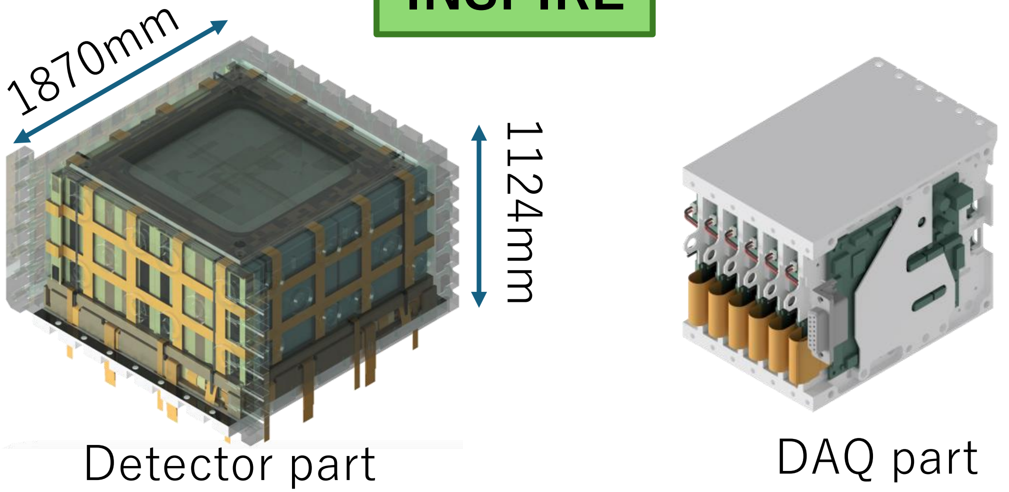

- 3rd Series of SCIENCE TOKYO satellite w/ 75kg and 50x50x50 cm in size
- **INSPIRE** : Hybrid Compton camera to monitor 30 keV – 3 MeV range w/ a single detector

7. INSPIRE : system configuration

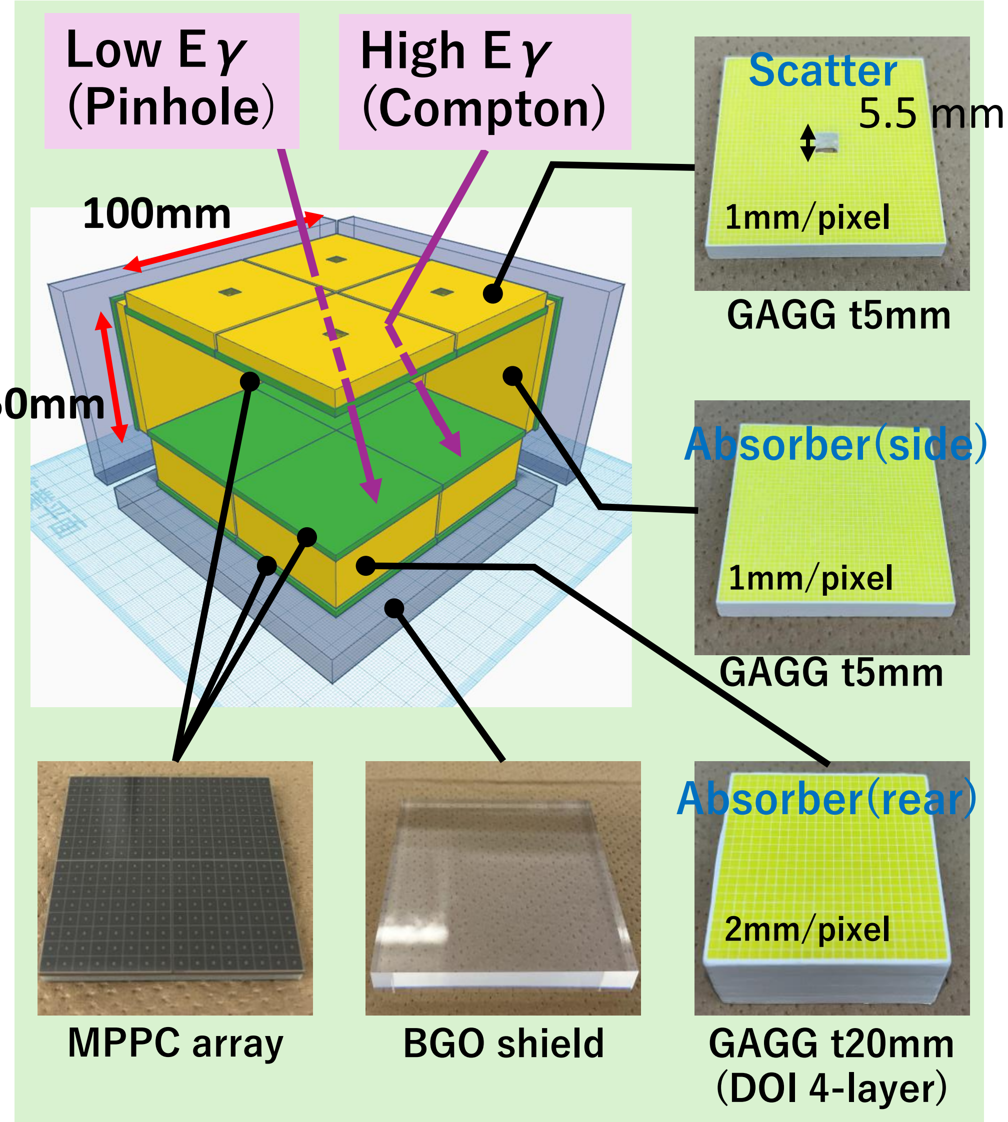

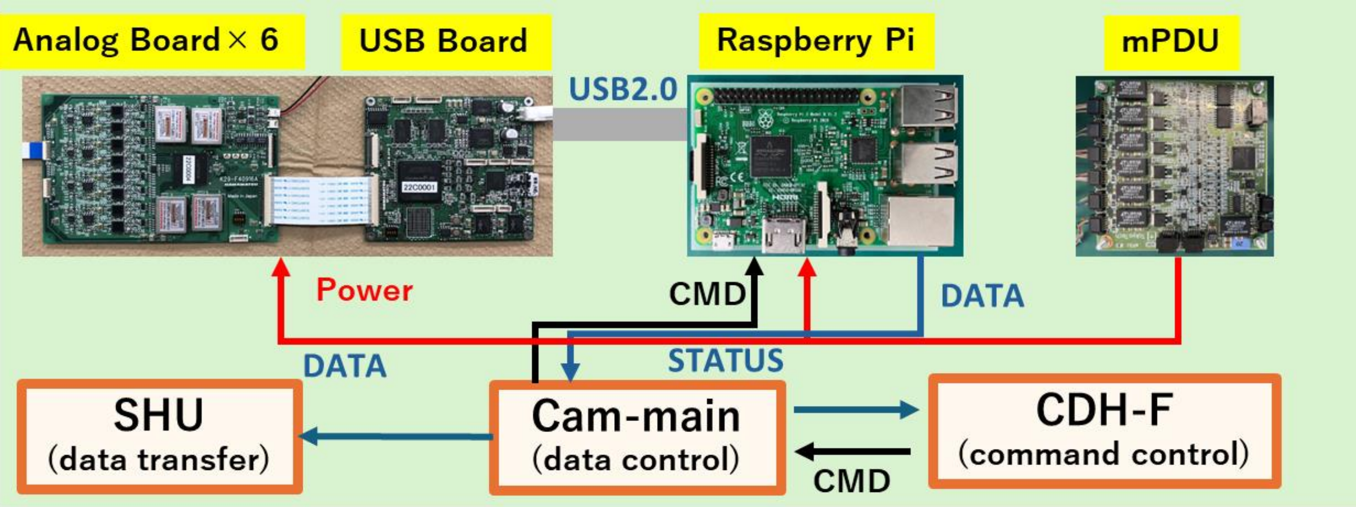

- Simultaneous X & γ-ray imaging:
  Pinhole(30-200keV)+Compton(150-3,000keV)
- Energy resolution(FWHM)
  GAGG : 7%@662keV　BGO : 16%@662keV
- 3D position sensitive Ce:GAGG array for absorber to improve resolution

8. Expected Performance -Geant4 Simulation-

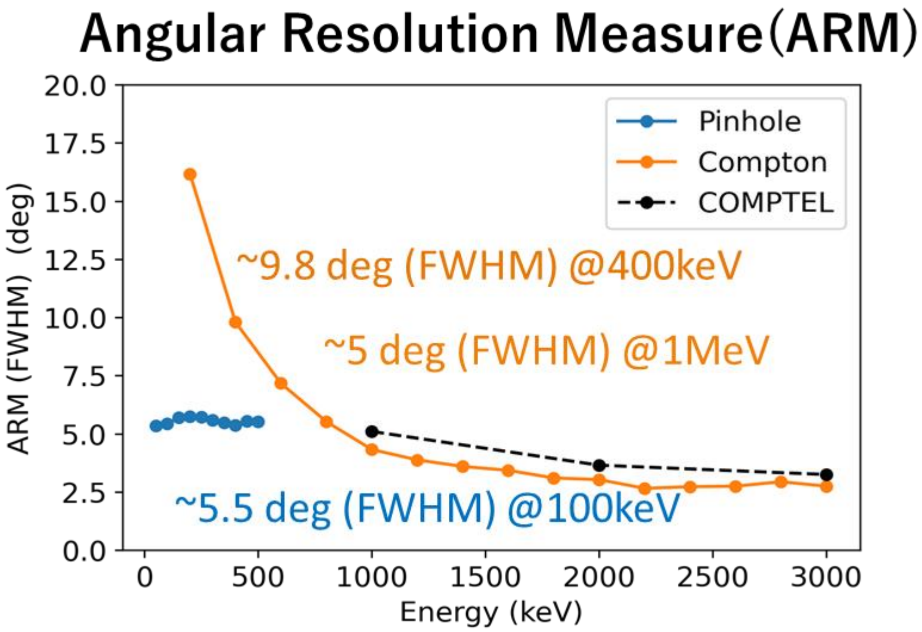

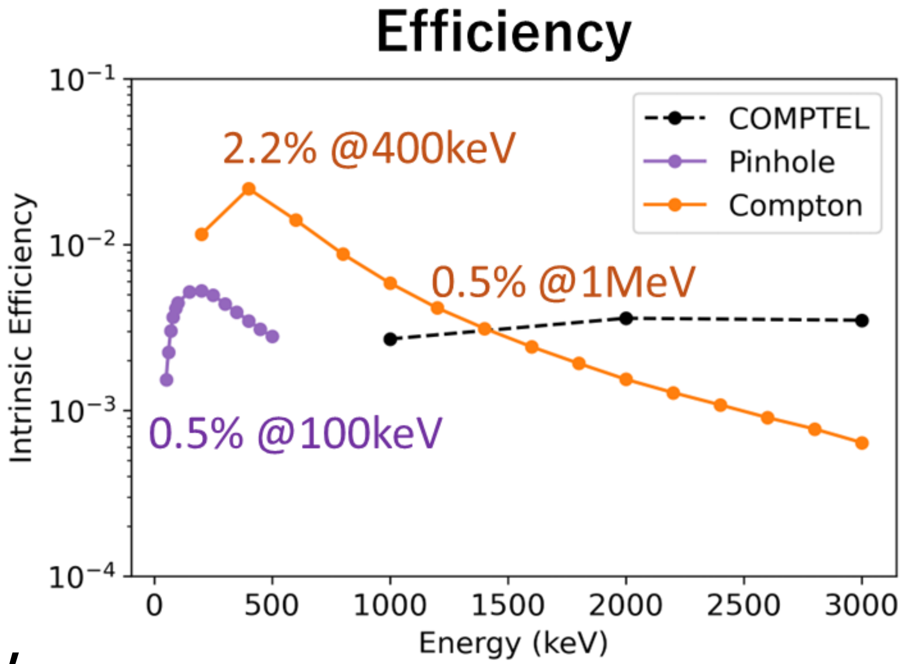

Kataoka et al. 2024, NIM-A

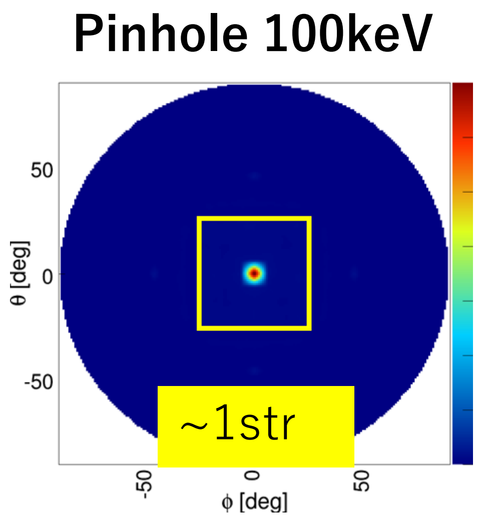

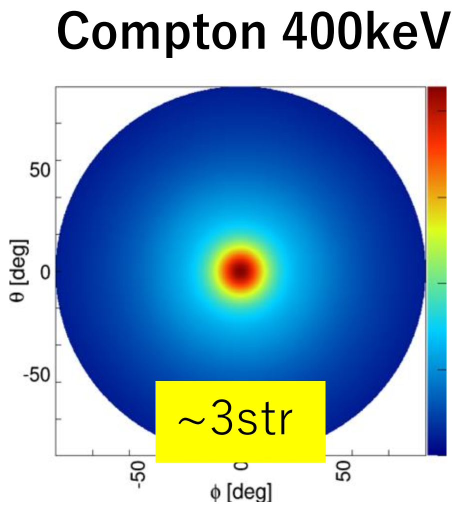

3D position sensitive GAGG

- ✓ Typical Angular resolution $\Delta\theta \sim 5^\circ$ @ 1MeV (FWHM)
- ✓ Wide FOV
  Pinhole：~1str　CC-Box：**~3str**

9. Expected sensitivity -Geant4 Simulation-

Continuum Sensitivity

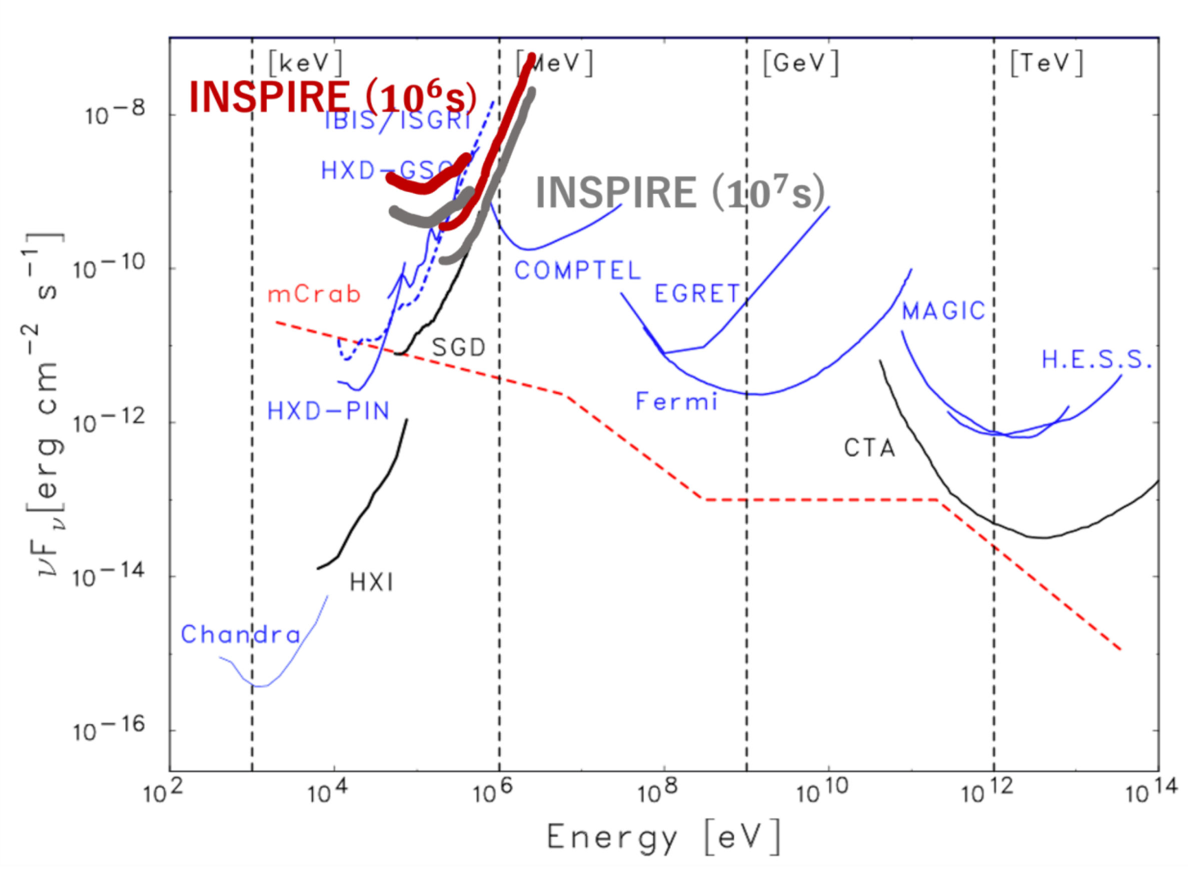

Takahashi et al. 2012

Line Sensitivity

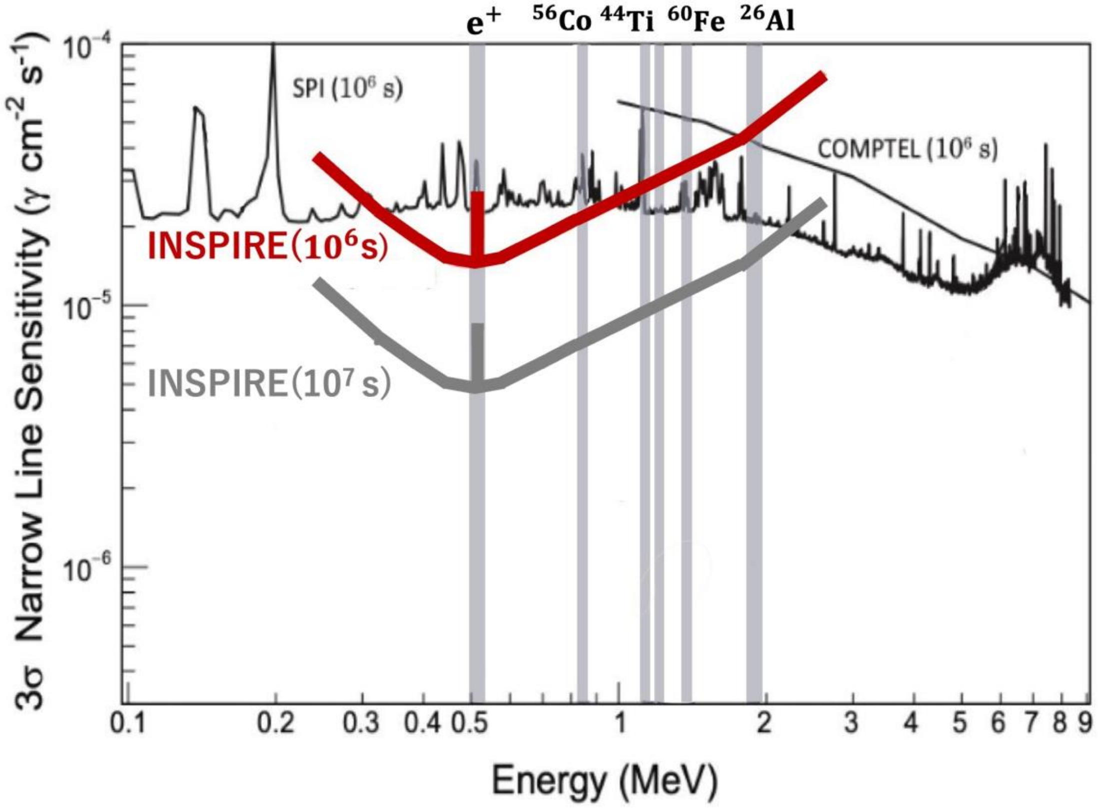

McEnery, J. et al. 2019

10. EM fabrication and testing

◆CC-configration

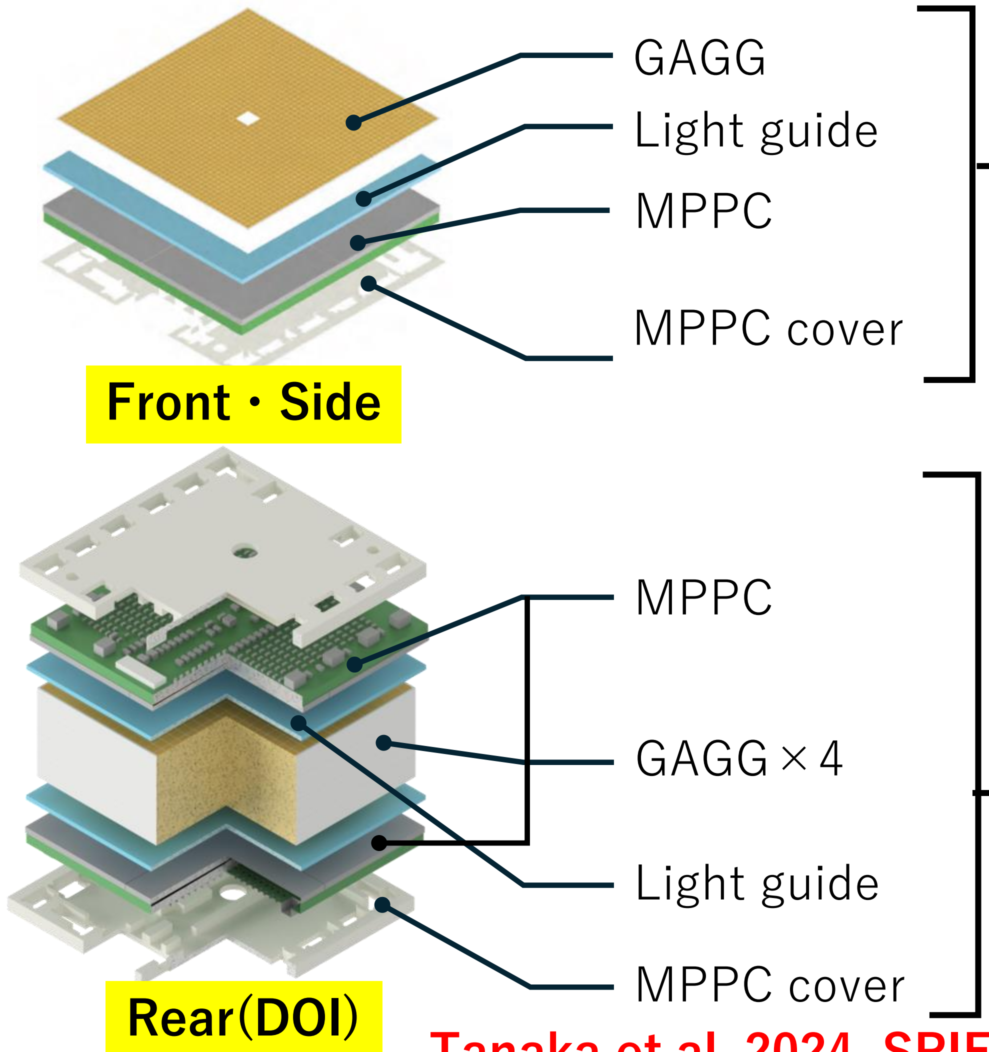

Tanaka et al. 2024, SPIE

◆Pixel Map(Calibration)

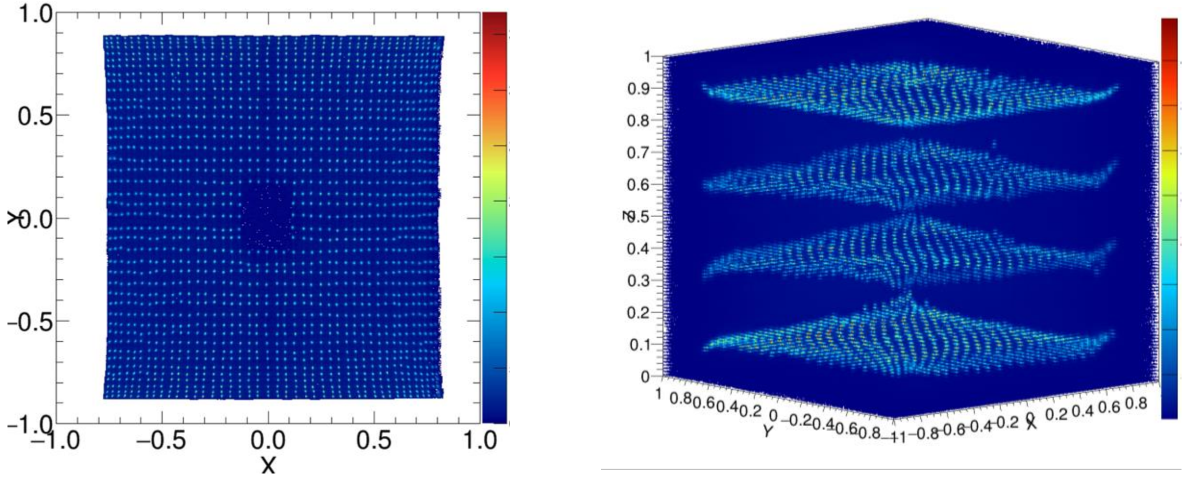

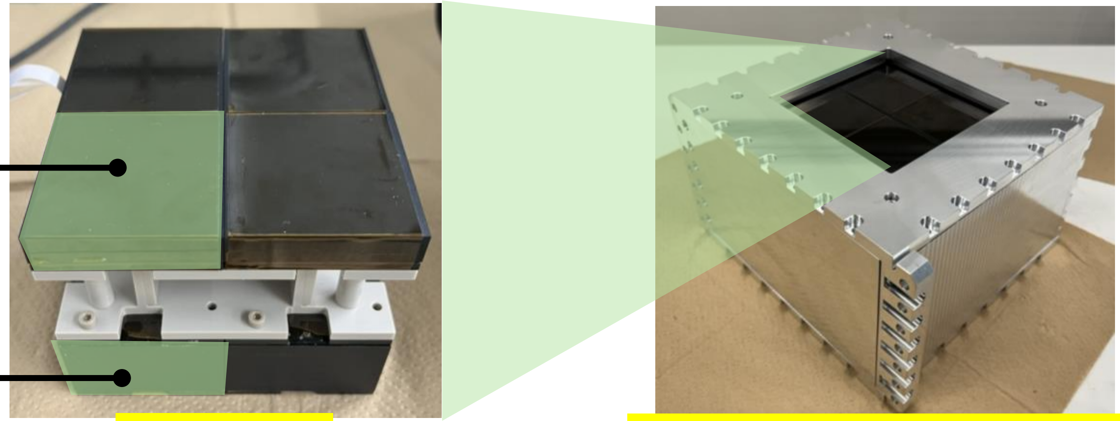

11. Imaging results of the EM

◆EM imging result(Compton mode)

^{137}Cs imaging

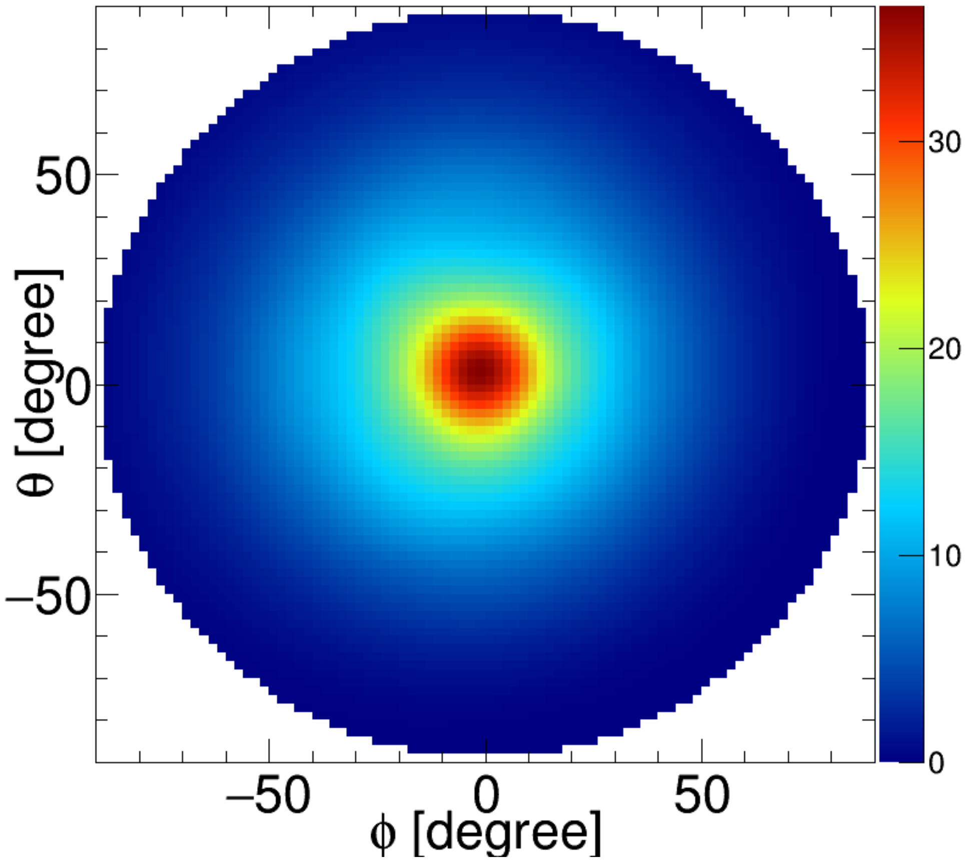

662keV

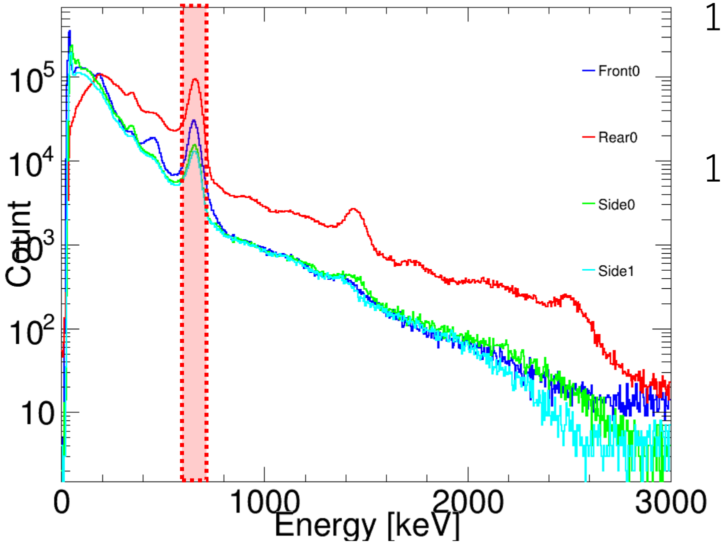

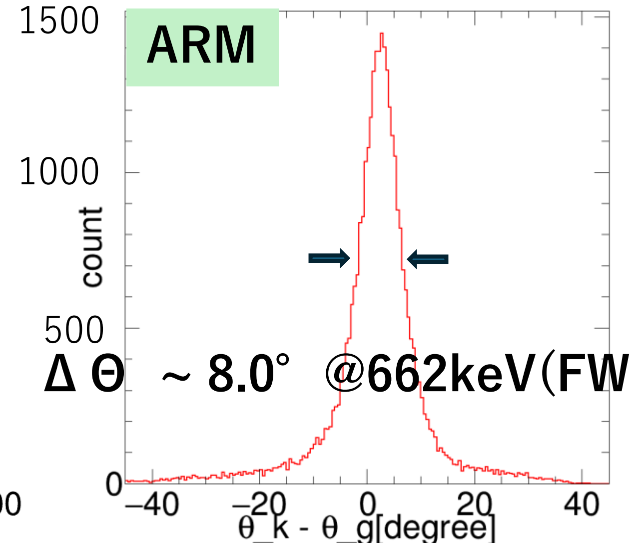

Δ Θ ~ 8.0° @662keV(FWHM)

12. Current status

◆development status

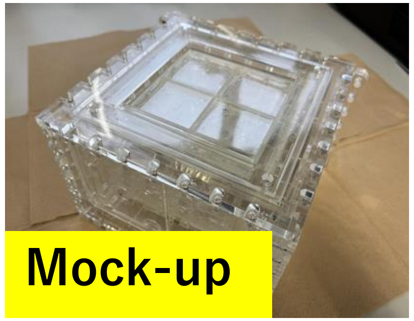
Mock-up

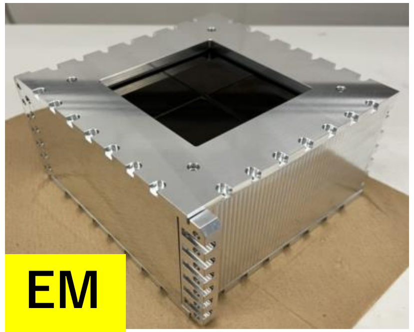
EM

Concept
↓
Basic design
↓
Detailed specifications
↓
EM
↓
FM
↓
Launch

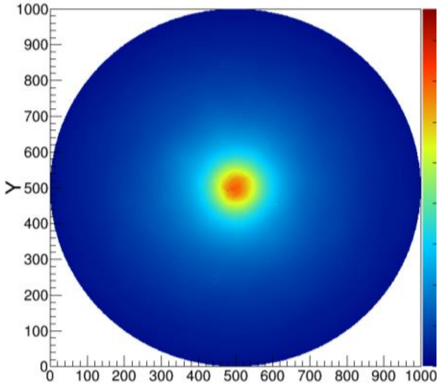

Simulation of Solar Flare Imaging

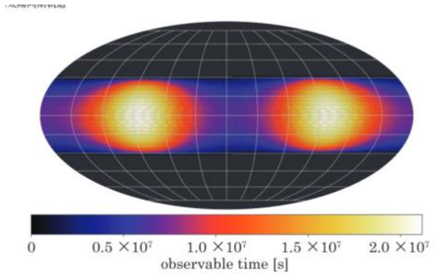

Estimated observation time

Development aimed at a launch in 2027

◆Various environmental tests

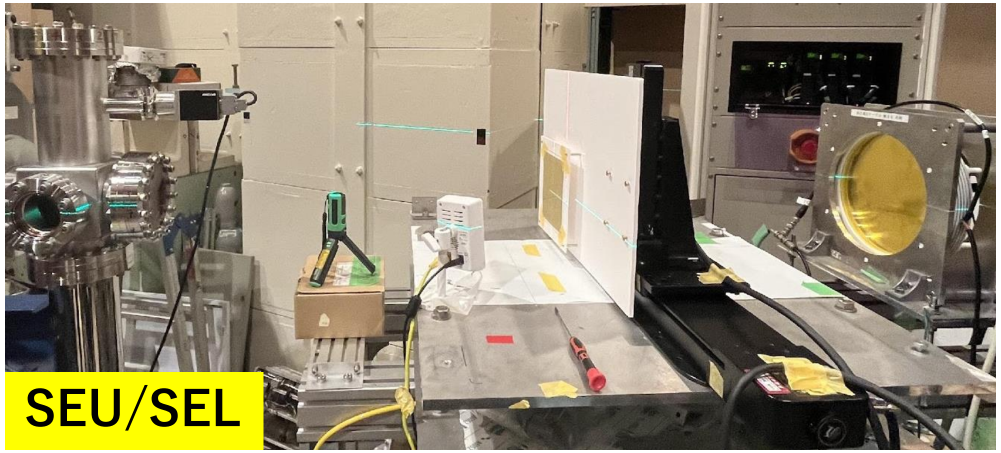
SEU/SEL

- **GAGG・BGO Temperature test**
  -40°C~85°C (15cycle：95min)
- **Electric Power Test**
  ～18W(steady-state)
  Reduction of Inrush Current

Vibration/thermal vacuum testing, and other tests are being planned.

13. Summary

◆MeV Compton camera onboard the GRAPHIUM satellite

- ✓ Equip 50-kg class small satellite, the successor to the Hibari and Petrel satellites, with a CC-Box.
- ✓ **Box-CC**(Pinhole-mode / Compton-mode)
- ✓ Energy range: **30keV to 3 MeV**
- ✓ Conduct source imaging with the Engineering Model.
- ✓ $\mathbf{\Delta E \sim 7\%@\,662keV}$ (FWHM), $\mathbf{\Delta\theta \sim 8.0° \,@\, 662keV}$ (FWHM) w/ EM

◆Future Prospects

- ✓ Pinhole Imaging w/ EM
- ✓ Conduct space environment resistance testing with the Engineering Model.

Thank you for listening!!

Appendix

1. Nuclear gamma rays -Galactic plane-

◆ ^{26}Al emission lines (1.809MeV)

$^{26}_{13}\mathrm{Al} \rightarrow {}^{26}_{12}\mathrm{Mg} + \mathrm{e}^{+} + \nu + 1.809\ \mathrm{MeV}$ (720000years)

✓ $^{26}_{13}$Al is produced in core-collapse supernovae
(Core-collapse supernovae also produce ^{60}Fe)

COMPTEL
^{26}Al (1.8MeV) map

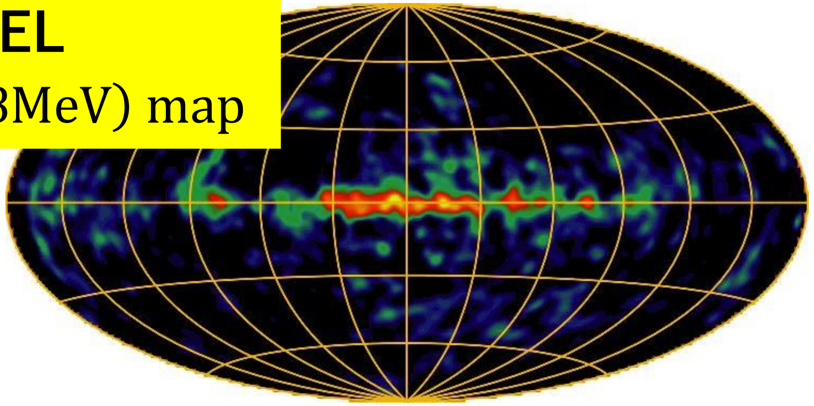

⇨ Determines the locations of element synthesis in the galaxy
⇨ Flux ratio of $^{60}\mathrm{Fe}/^{26}\mathrm{Al}$
→ Constrains theoretical predictions of element synthesis in supernovae

◆ ^{44}Ti gamma ray lines (1.16MeV)

$^{44}\mathrm{Ti} + e^{-} \rightarrow {}^{44}\mathrm{Sc} + \nu + 67.8, 78.4\ \mathrm{keV}$ (60years)
$^{44}\mathrm{Sc} \rightarrow {}^{44}\mathrm{Ca} + e^{+} + 1.16\ \mathrm{MeV}$ (3.97hours)

✓ ^{44}Ti is produced in supernova remnants

⇨ Pinpoints the locations of SNRs over hundreds of years
⇨Enables detailed studies of individual SNRs

◆ Annihilation Gamma Rays (511keV)

^{26}Al decay… Positron source
⇨ Positron annihilation with electrons

but... The distribution of ^{26}Al is not fully traceable

⇨ Understanding the unknown origins of positrons

2. The origin of heavy elements

Big Bang (13.7 billion years ago)

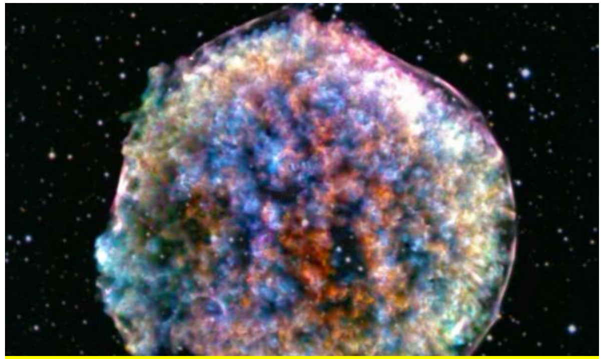

Supernova explosion

Rare metals like Au Pt

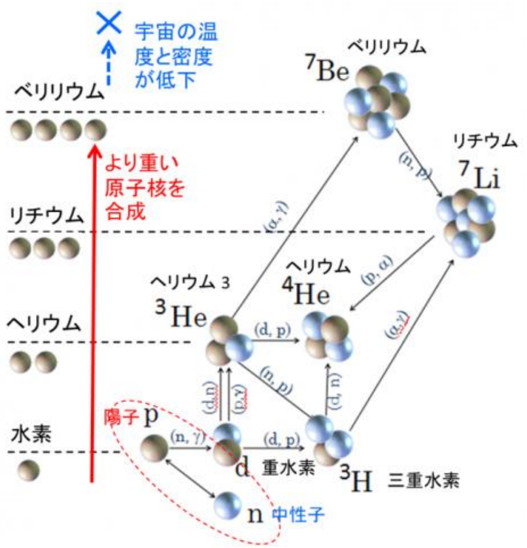

Synthesis of light elements (Li, Be)

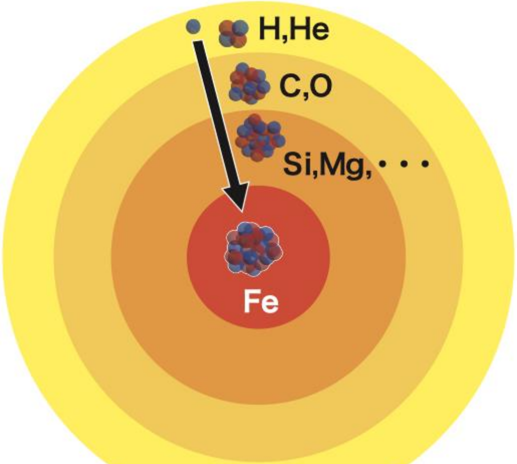

Synthesis of elements up to iron (Fe) through nuclear fusion

The origin is still unknown.

Gamma-ray observation is the key!

2. MeV γ rays as nucleosynthesis probe

◆ Element synthesis and gamma-ray emission

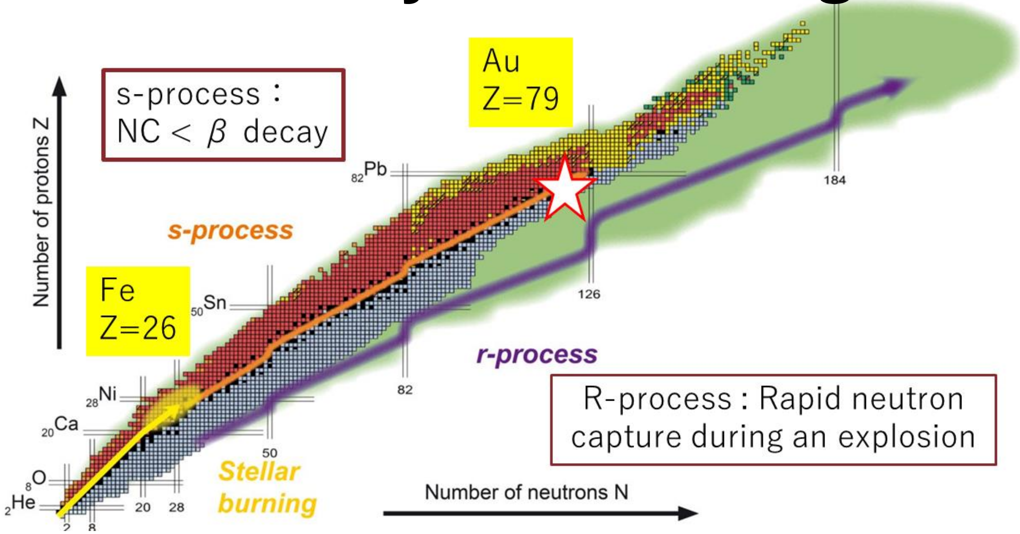

Kilonova

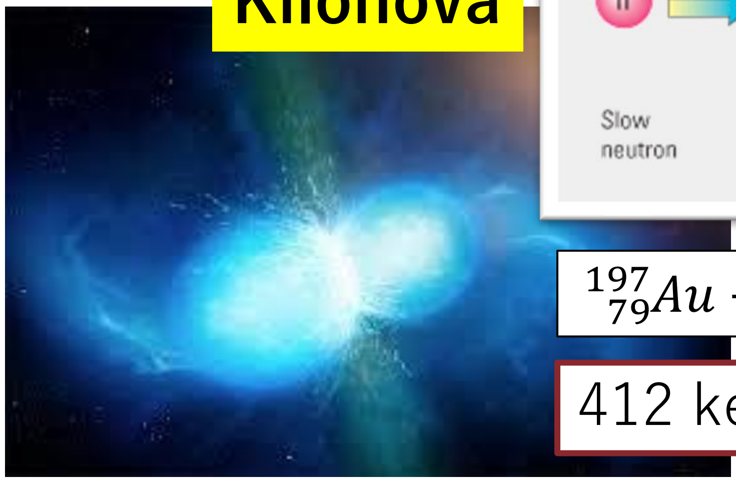

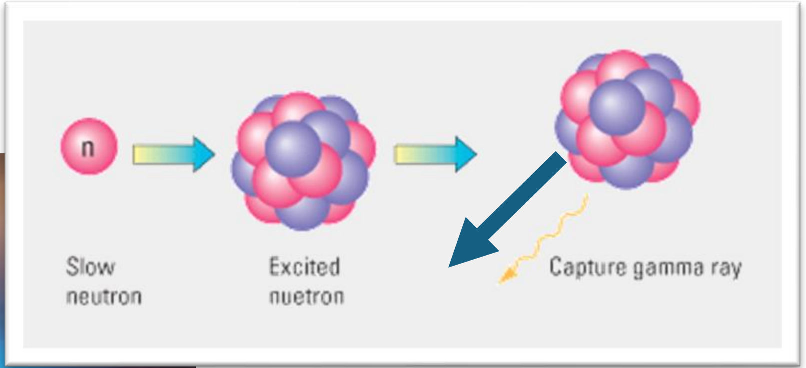

$${}^{197}_{79}Au + n \rightarrow {}^{198}_{79}Au + 412\ \text{keV}$$

412 keV ⇨ The origin of Au

- In the s-process, the slow neutron capture allows beta decay to occur immediately upon forming unstable isotopes, leading to stable nuclei.
- In the NC process that generates heavy elements, gamma rays are emitted during neutron capture. In the case of gold, it emits 412 keV gamma rays, and detecting this can serve as evidence.
- The r-process line reflects neutron capture, not the stable isotopes, which form later through beta decay.
- Gold production events like kilonovae are rare and often too distant to observe from Earth, making them highly challenging to study.

3. Observation of Solar flare

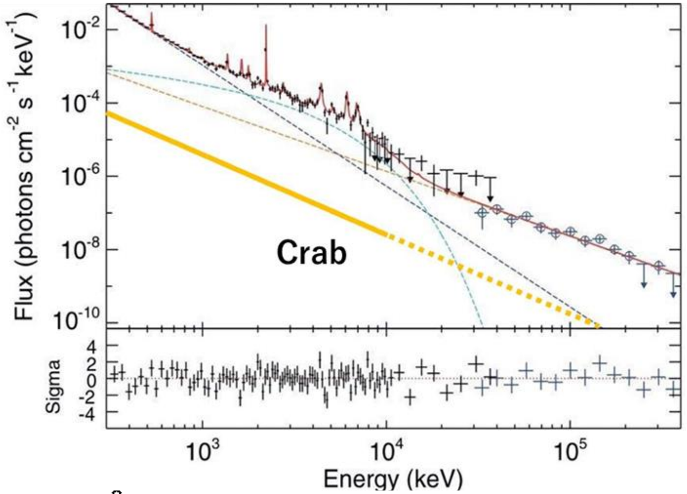

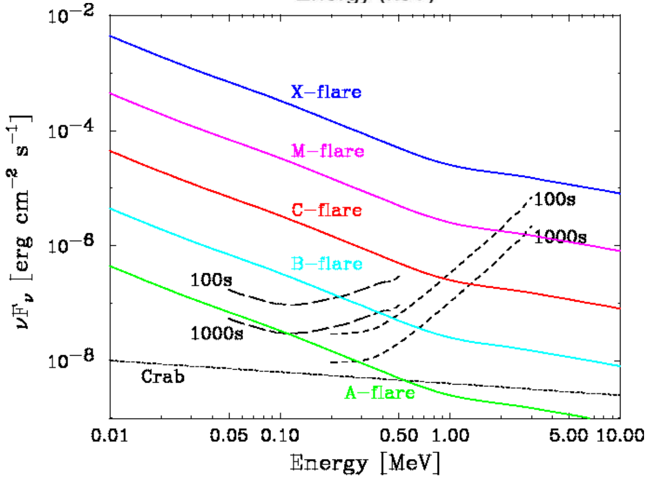

- ✓ It is exceptionally bright, even in comparison to the Crab Nebula.
- ✓ In addition to non-thermal bremsstrahlung, various de-excitation lines can be observed. e^-e^+, $^{60}\mathrm{Fe}$, $^{24}\mathrm{Mg}$ (0.5~2MeV) ⋯

- ✓ The launch period coincides with the peak phase.
  - ・C class flare ~5/day
  - ・M class flare ~0.7/day
- ✓ The dashed lines represent the 100s and 1000s continuum sensitivity in INSPIRE's pinhole and Compton modes.
- ✓ The effects of solar flares on the camera and the circuit board are currently under investigation.

Low-energy gamma rays (hundreds of keV to MeV) from bremsstrahlung and positron annihilation characterize the early stages of solar flares. Tracking these sources enables direct study of particle acceleration processes and energy release mechanisms

3A. Observation of Solar flare

◆ Gamma-ray emission mechanisms due to solar flares

① Occurrence of magnetic reconnection
→ Release of magnetic energy
② Plasma heating (thermal radiation)
+ Particle acceleration
③ Accelerated particles travel along magnetic field lines to the chromosphere
④ Interaction with chromospheric plasma
→ Non-thermal radiation

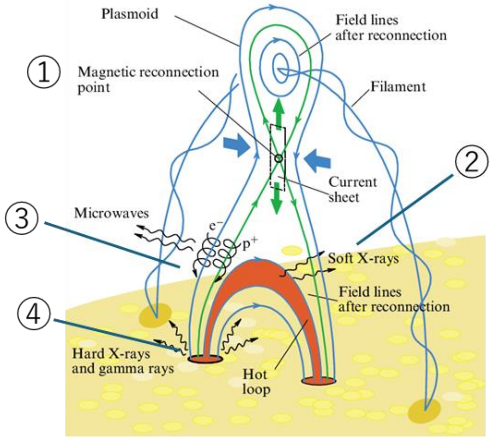

These emissions characterizing the initial stages of solar flares.

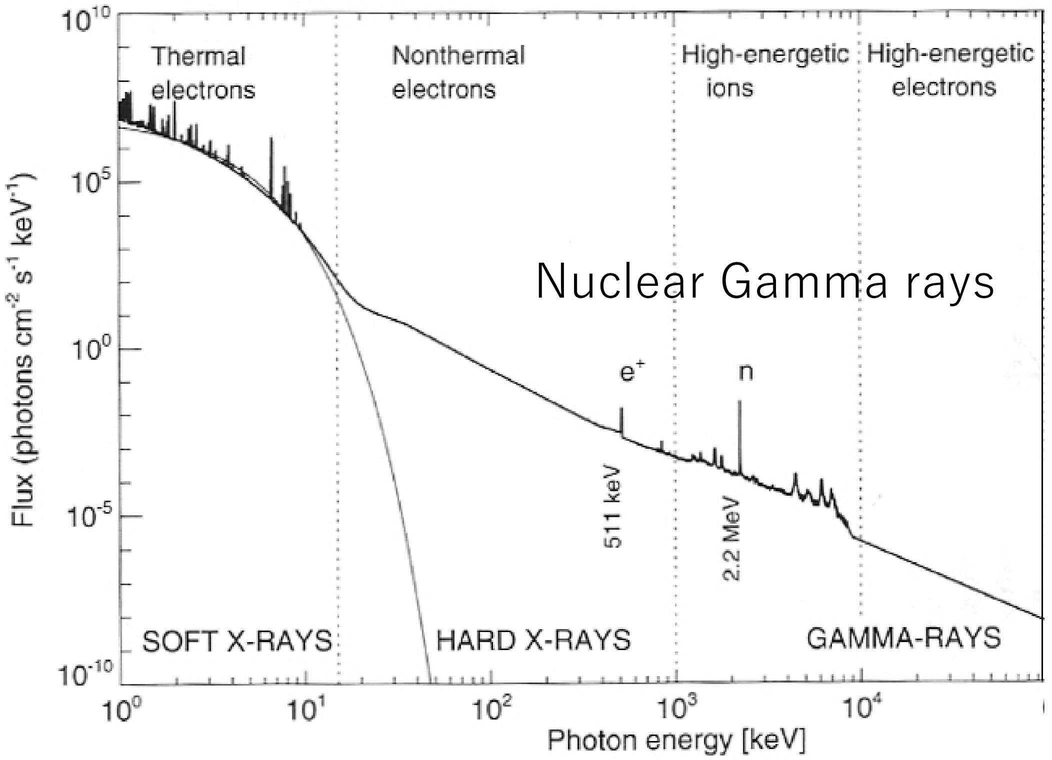

How electrons are accelerated in solar flares remains a mystery ⇨ MeV exploration

4. COMPTEL

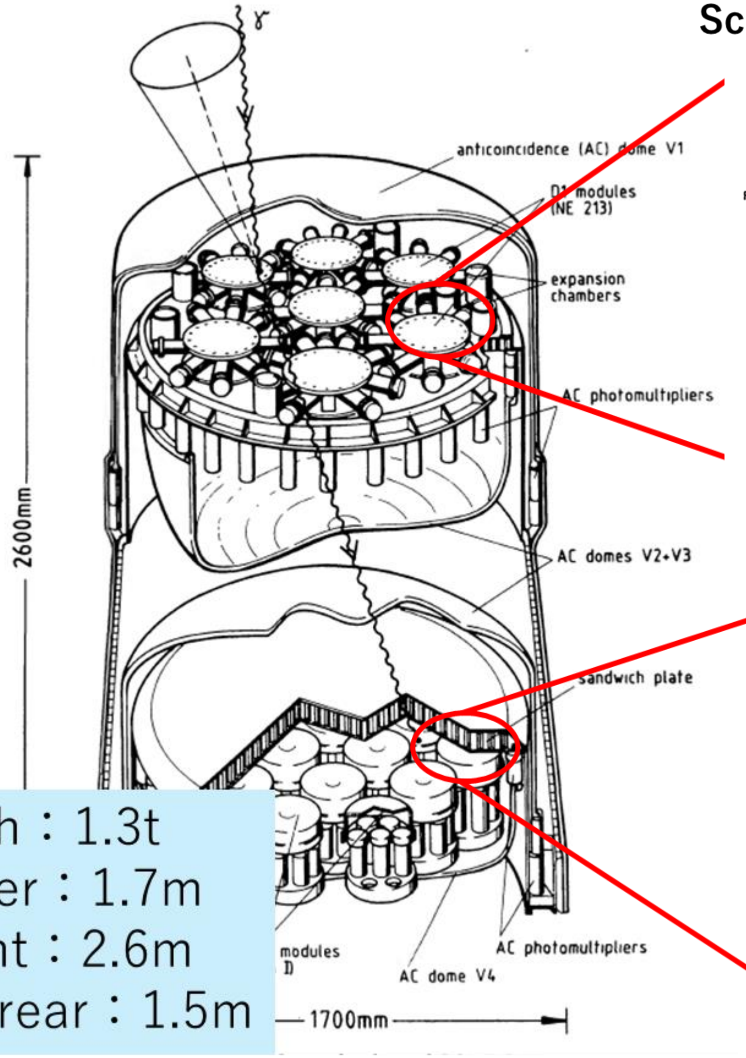

weigh：1.3t
diameter：1.7m
height：2.6m
front－rear：1.5m

Scatter：Liquid scintillator（NE213A）＋ PMT

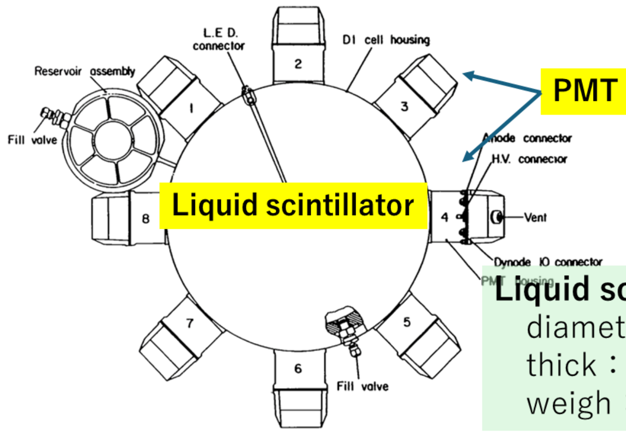

Liquid scintillator
diameter：28cm
thick：8.5cm
weigh：15.3kg

Centroid calculation with eight PMTs.
⇩
Position resolution: an average of 2.3 cm.

Absorber：NaI(TI)scintillater + PMT

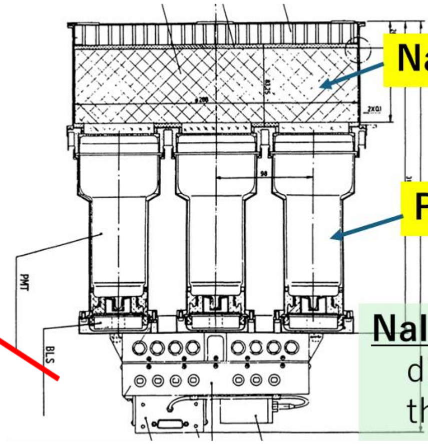

NaI(TI)scintillater
diameter：28.2cm
thick：7.5cm

Centroid calculation with eight PMTs.
⇩
Position resolution: an average of 2.3 cm.

4. COMPTEL

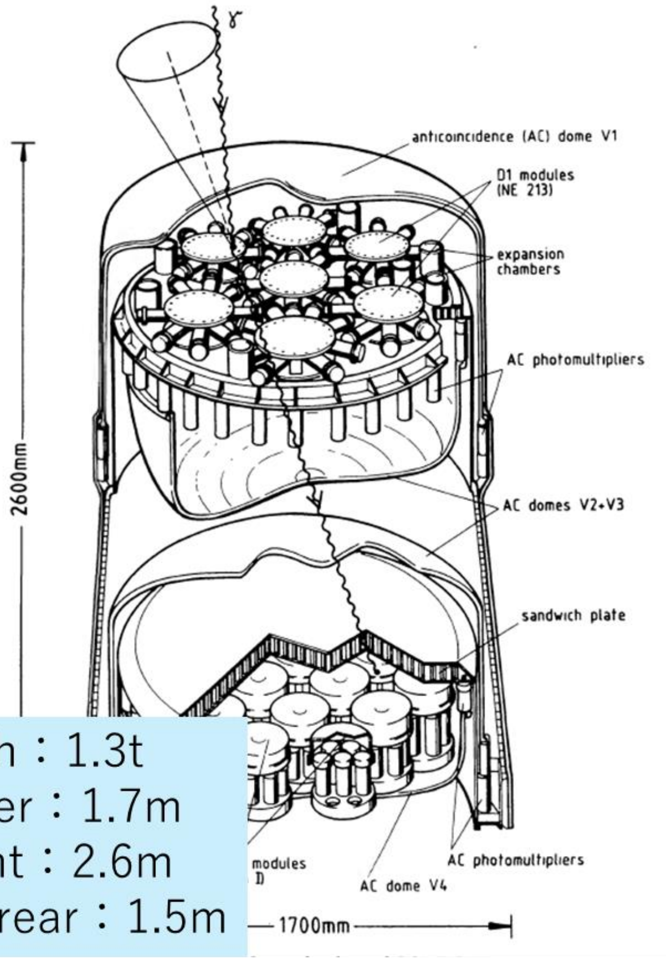

weigh：1.3t
diameter：1.7m
height：2.6m
front－rear：1.5m

Compared to COMPTEL

✓ COMPTEL is a large detector, but its position resolution of about 2 cm. So, COMPTEL required a 1.7 m distance between the scatterer and absorber to achieve sufficient image resolution. The same applies to the ARM. As a result, this led to reduced detection efficiency and a loss in sensitivity.

✓ INSPIRE, with millimeter-level position resolution, allows the scatterer and absorber to be placed just a few centimeters apart. This results in sensitivity, comparable to that of COMPTEL.

✓ However, for high-energy gamma rays (E > 3 MeV), INSPIRE's smaller size limits absorption, making COMPTEL superior in this range.

4. COSI

Compared to COSI

- ✓ Our camera can observe from 30 keV, lower than COSI's range.
- ✓ While our camera's energy resolution is inferior to HPGe detectors, COSI's integrated scatterer-absorber design results in similar angular resolution.
- ✓ It's also highly cost-efficient, at 1/100th the cost and 1/10th the weight of COSI, enabling easier future scaling up.
- ✓ **Observing transient events like kilonova** requires quickly launching multiple satellites to maximize opportunities. Small satellites are ideal for this.

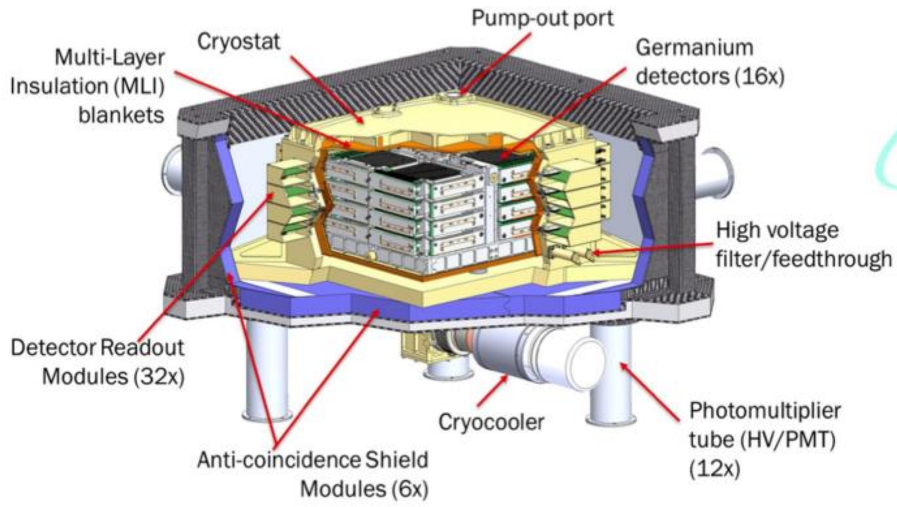

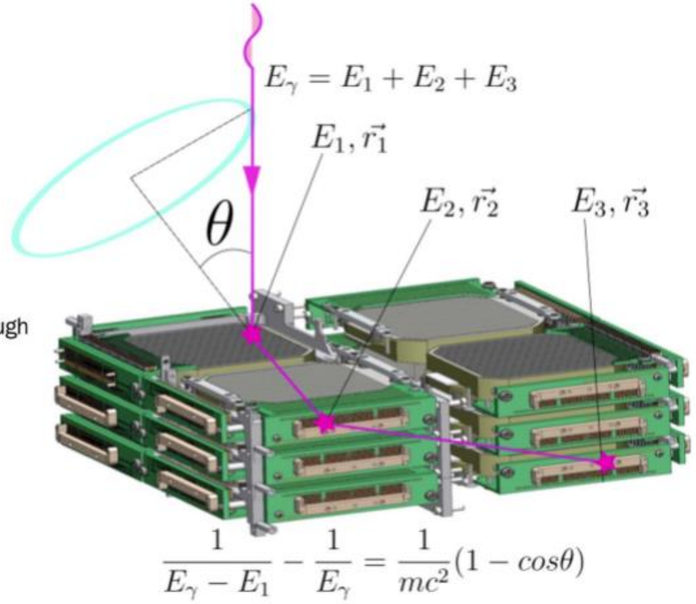

The detector of COSI adopts a structure that reads out germanium semiconductors using a cross-strip method.

4. Compared to other mission

◆Our main goal is to observe **transient events**,
like kilonovae, GRB, rather than steady sources.

◆INSPIRE has wide field of view compared to COMPTEL(1.0str).
⇒With a wider field of view, the chances of observing transient events increase.

◆The merit of small satellite
⇒For Increasing the probability observing these transient events, having multiple satellites increases the chances of detecting them.
Small satellites are well-suited for this purpose.

◆We also see INSPIRE as a testing ground for innovative science. If we succeed, it'll be easy to scale up this technology for larger satellites.

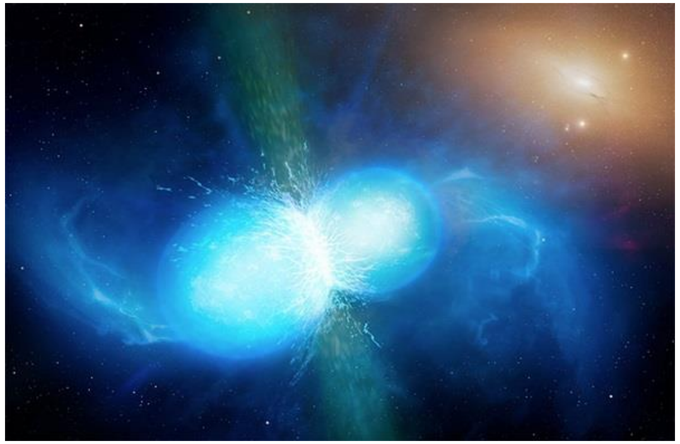

So, this mission is really an important first step—a proof of concept.

4. Compared to other mission

	COMPTEL (NASA: 1991~)	INTEGRAL SPI (ESA: 2002~)	Hitomi SGD (JAXA: 2016)	COSI (NASA: 2026~)	GRAPHIUM (2026~)
weight (Satellite)	~17,000 kg	4,000 kg	2,700 kg	~400 kg	75 kg
weight (detecter)	1,300 kg	1228 kg	316 kg	> 100 kg	10 kg
Energy Range	0.3 - 30 MeV	0.02 – 8 MeV	0.04 – 0.6 MeV	0.3 – 2 MeV	0.03 – 3 MeV
Effective area (@100 keV)	-	500 cm^2	30 cm^2	-	1 cm^2
Effective area (@1 MeV)	10 cm^2	150 cm^2	-	7 cm^2	1 cm^2
Imaging method	Compton	Coded Mask	Compton	Compton	Compton
Field of View	1.0 str	0.24 str	0.03 str	3.1 str	3.0 str
Cost (detecter)	~50M USD?	~100M USD?	~20M USD	~90M USD	~2M USD
Energy Resolution (FWHM @1MeV)	8 %	0.30 %	1.30 %	0.50 %	5 %
Angular Resolution (FWHM @1MeV)	7°	2.5°	3°	4.5°	5°

4. Success Criteria

	Achieved milestones.	Notes
Minimum success	・Power on the CC and operate it in orbit.	Space operation demonstration
	・Collect background data.	Orbital background and activation.
	・Detect gamma-ray bursts and solar flares.	Luminosity variation and spectrum
Full success	・Observe bright PSRs, AGNs, etc.	Crab, Vera, Cyg X-1, CenA, 3C273
	・Observe the Galactic center (511 keV).	point source
	・Observe diffuse gamma-rays from the Galactic plane.	diffuse source
Extra success	・Nuclear gamma-ray survey of the Galactic plane	^{10}B, ^{56}Fe, ^{44}Ti, ^{26}Al
	・Observation of bright SNRs and detection of nuclear gamma rays.	Tycho, Kepler, Cas A
	・Polarization observations of bright celestial objects.	Crab Nebula, Cyg X-1, Cen A, 3C273
	・Observation of gravitational wave sources and kilonova.	Evidence of the r-process.

7. Our strategy for MeV observation

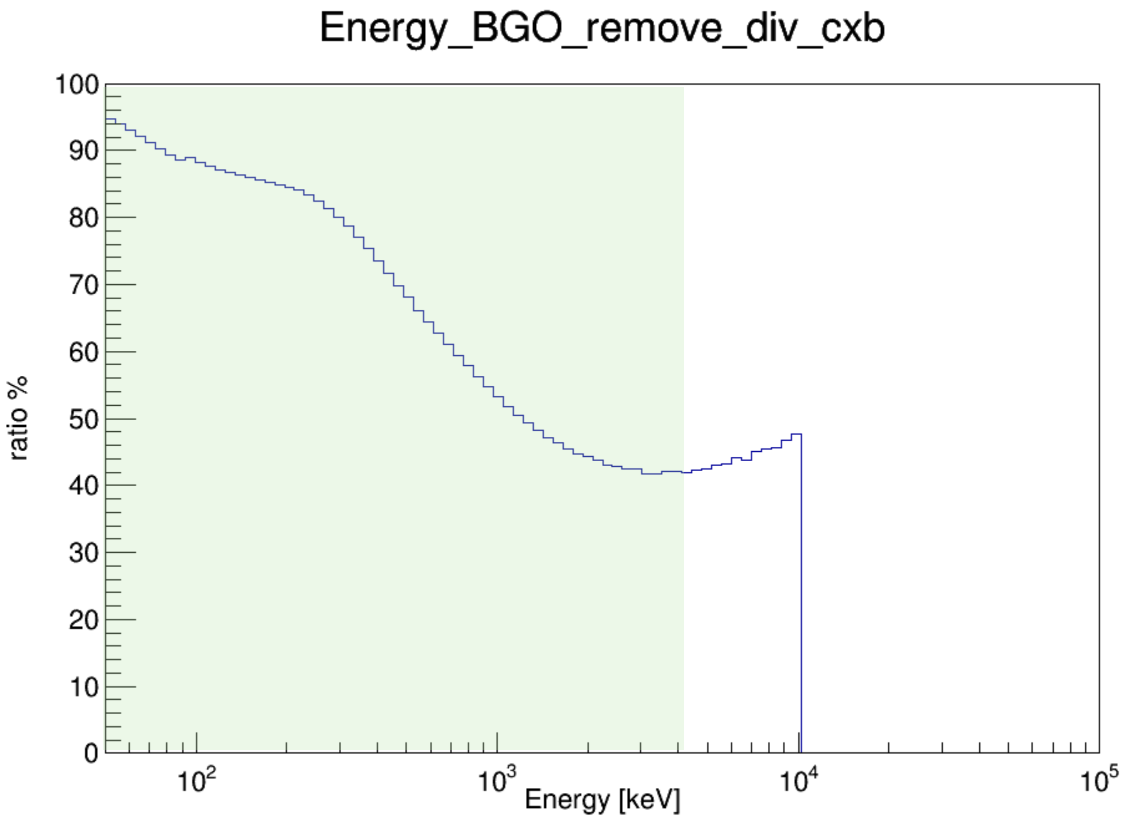

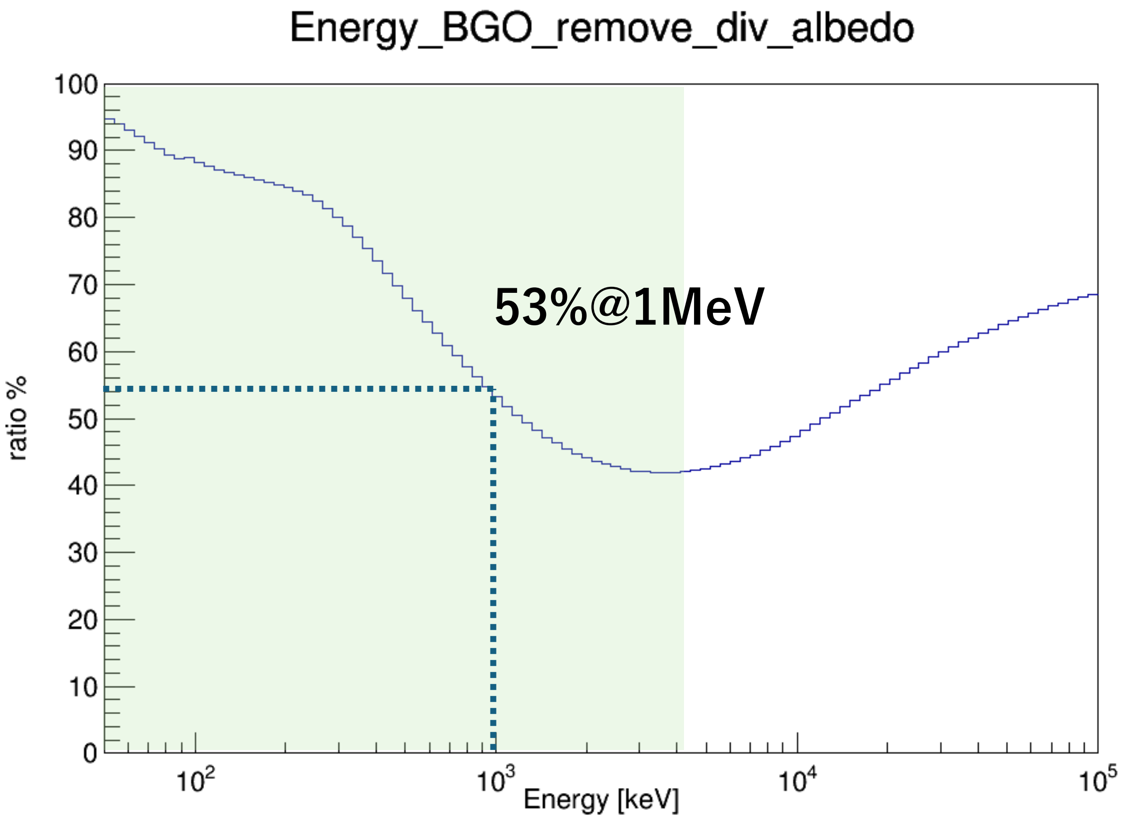

- ✓ This shows the CXB and Albedo removal rates for BGO, respectively.
  For albedo, BGO can eliminate 53% of albedo at 1 MeV.
- ✓ Due to the small satellite size, it is difficult to equip a thicker BGO shield.
- ✓ BGO is also planned to be used as a gamma-ray burst monitor.

7. BGO active shield

◆ Background Remove

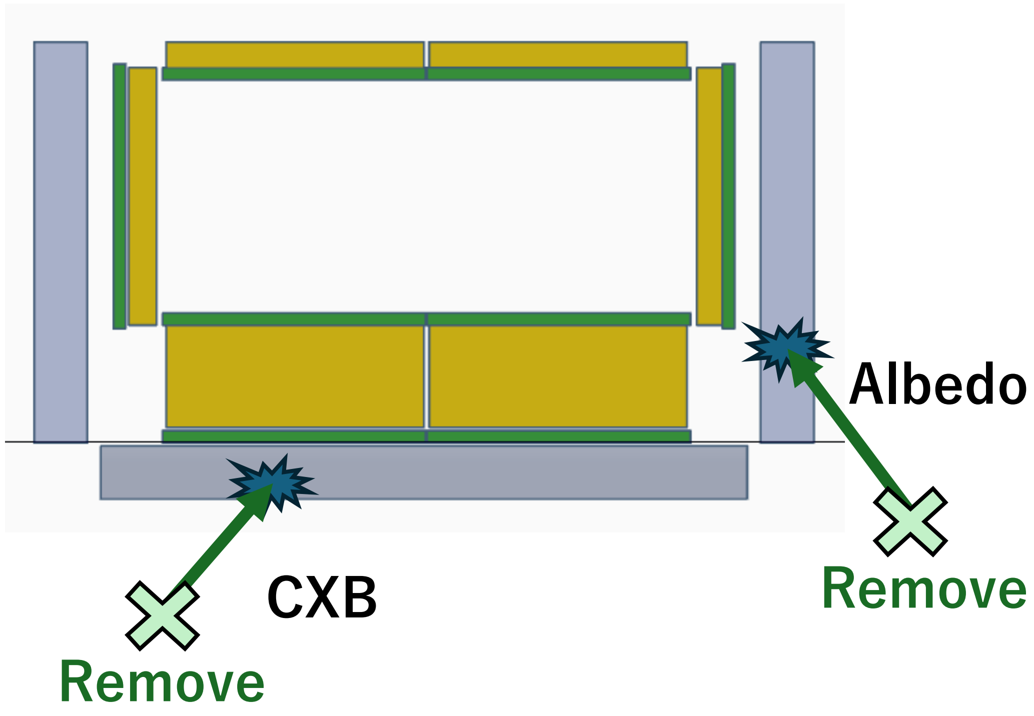

◆ Escape event Remove

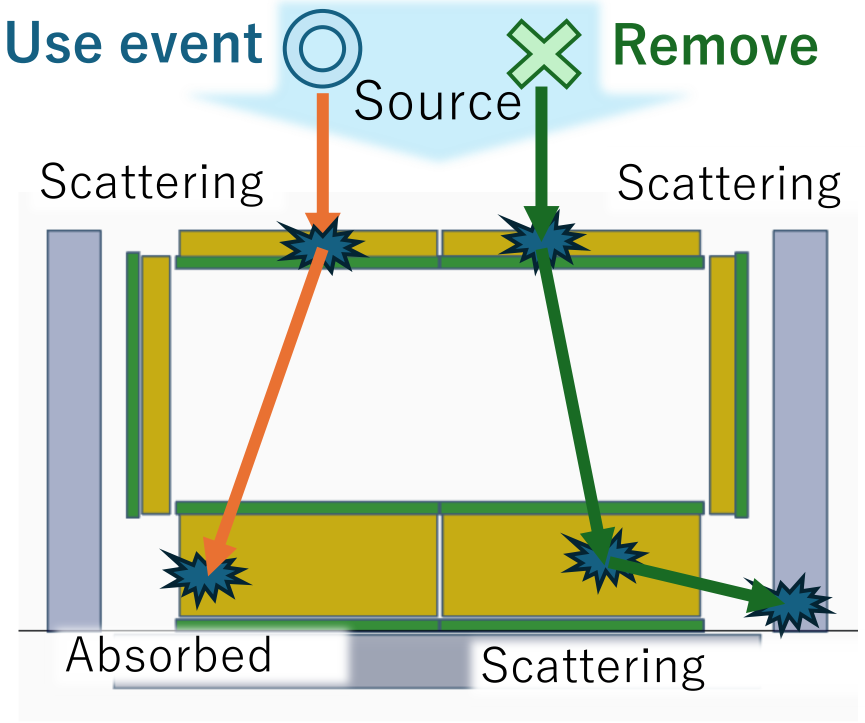

✓ The role of the BGO shield is two.
One is to detect and remove backgrounds such as albedo and CXB.
The other is to eliminate escape events, which occur when particles are not fully absorbed within the Compton camera and escape.

7. INSPIRE : system configuration

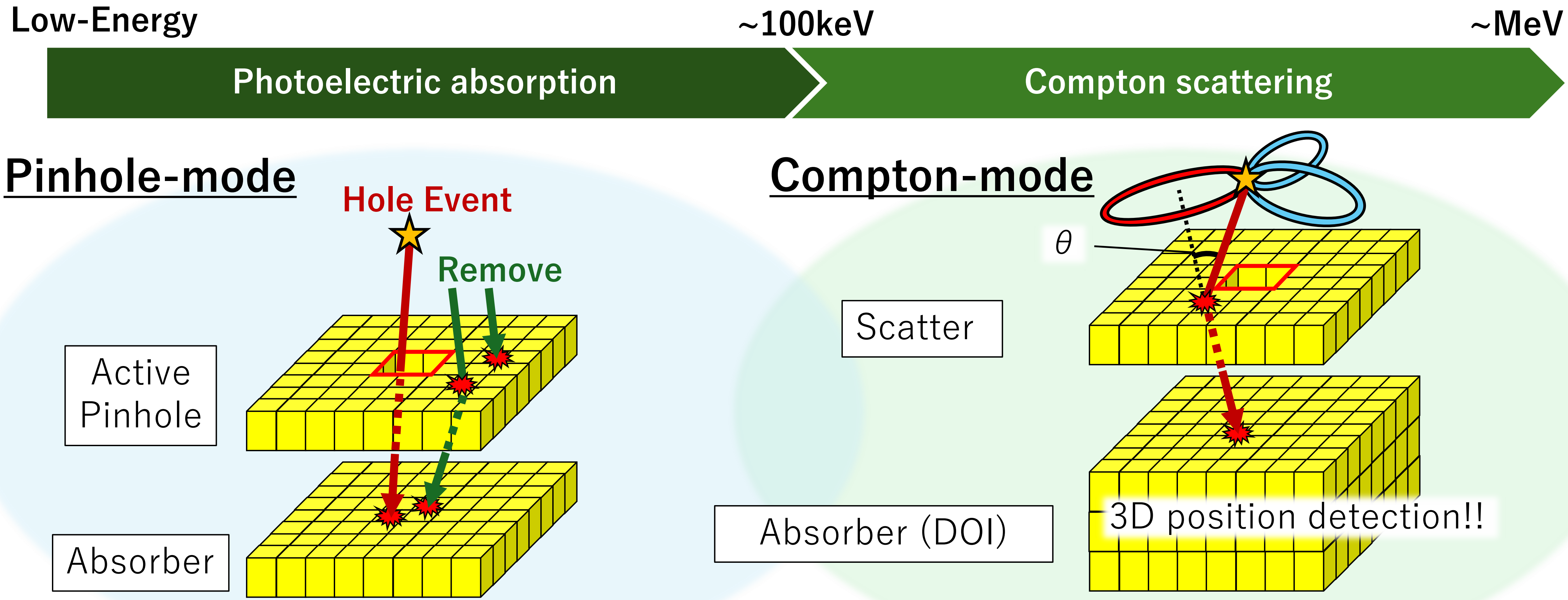

DOI (Depth-of-Interaction)
⇨ Sensitivity up to ~ MeV.

Gamma-ray imaging is possible over a wide energy range from tens of keV to ~ MeV.

7. INSPIRE : system configuration

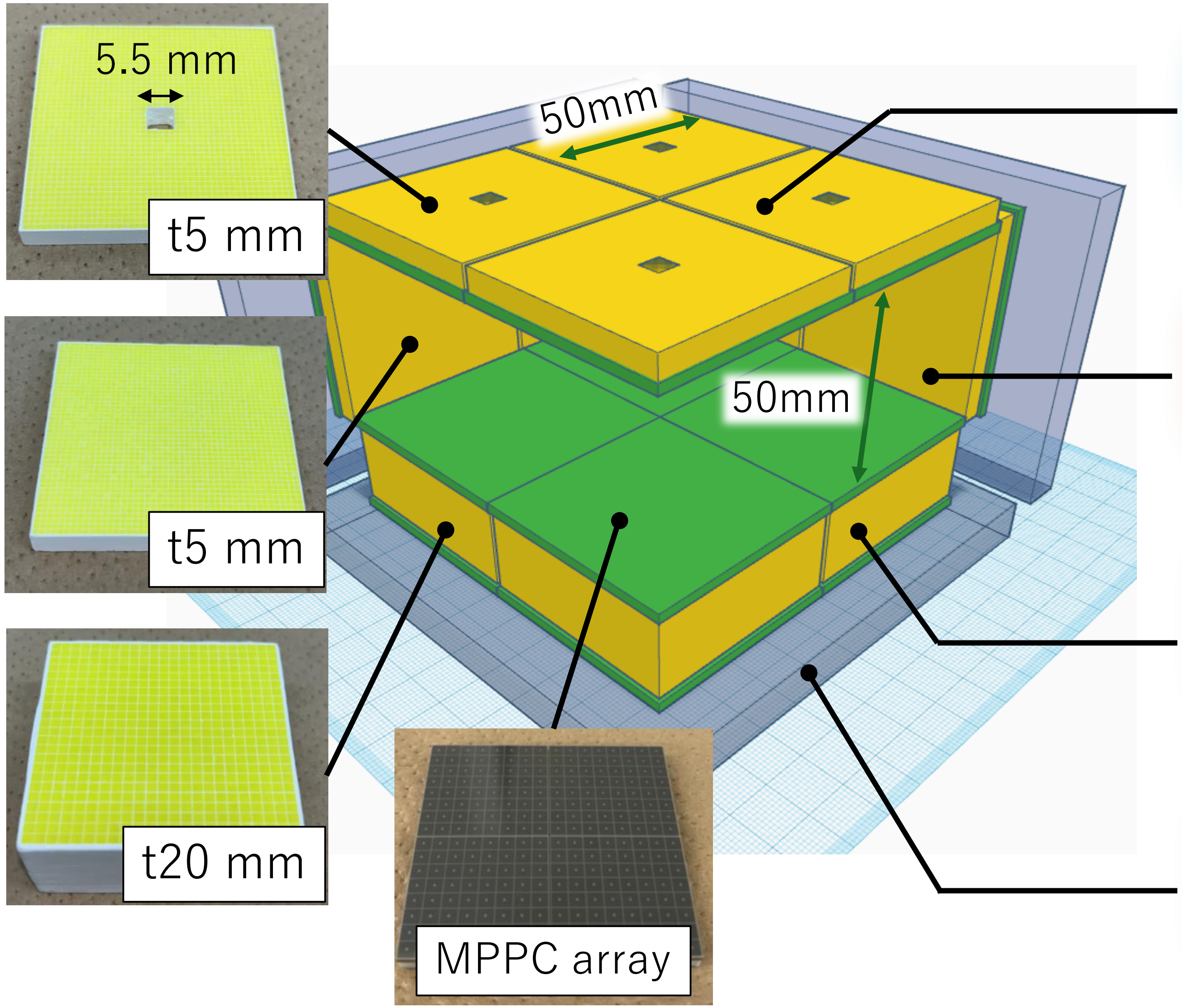

Scatter ：GAGG array + MPPC array

Pixel size： $1 \times 1 \times t5$ mm^3

Hole：5.5×5.5 mm^2

Pixel number：45×45 pixel × 4 array

Side ：GAGG array + MPPC array

Pixel size： $1 \times 1 \times t5$ mm^3

Pixel number：45×45 pixel

Absorber ：GAGG array（DOI）+ MPPC array

Pixel size： $2 \times 2 \times t5$ mm^3

Pixel number：23×23 pixel × 4 layer × 4 array

Shield ：BGO + MPPC

BGO Side, Bottome：t7mm, t10mm

⇨ Background, Fake Event Remove

7. Count rate against background

◆ Detection rate in a background environment (CXB + Albedo)

Initial Energy

CXB: 10keV < E < 10MeV
Albedo: 10keV < E < 100MeV

Threshold

GAGG: E > 30 keV
BGO: E > 50 keV

⇨ Calculation of the count rate for each scintillator.

GAGG Front: 45 × 45 × 5 mm^3 = 10.1 cm^3
GAGG Side: 45 × 45 × 5 mm^3 = 10.1 cm^3
GAGG Rear: 46 × 46 × 20 mm^3 = 42.3 cm^3

BGO Side: 75 × 75 × 7 mm^3 = 39.4 cm^3
BGO Rear: 78.5 × 78.5 × 10 mm^3 = 61.6 cm^3

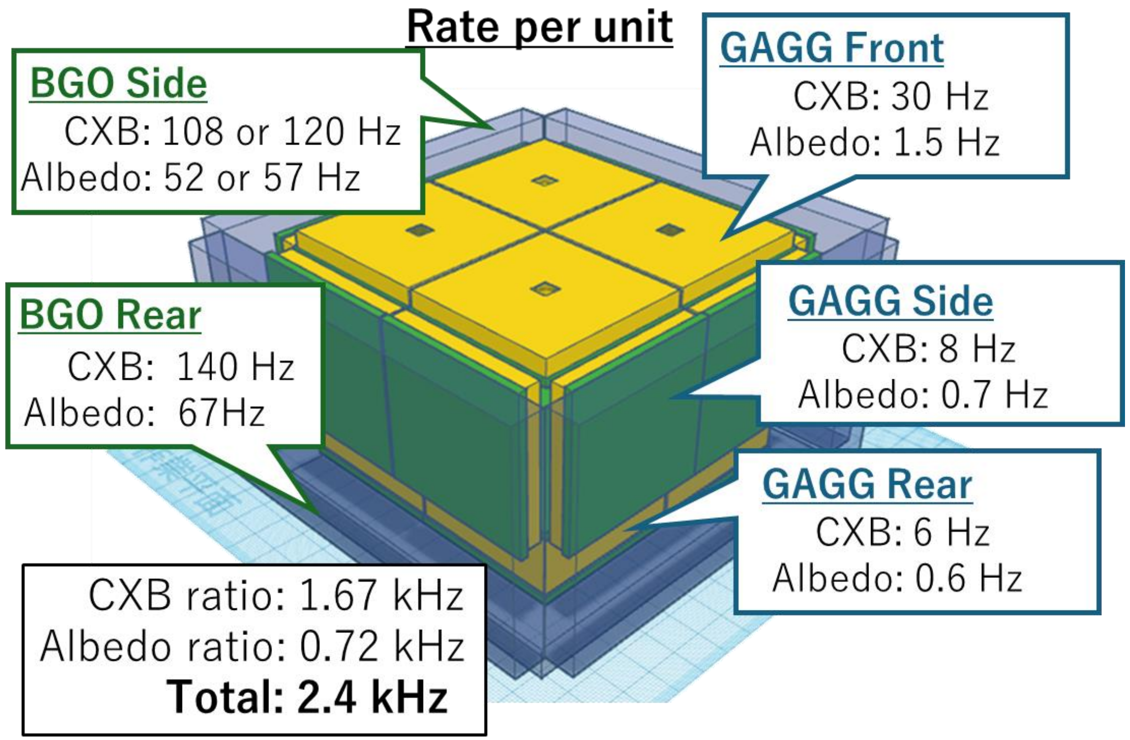

Data acquisition rate(20kHz)>BKG Rate(2.4kHz)

✓ The DAQ board can accurately acquire data at a rate of up to approximately 20 kHz. When simulating CXB and Albedo, the background rate is estimated to be around 2.4 kHz, which is well within the manageable range.

7. Depth of Interaction

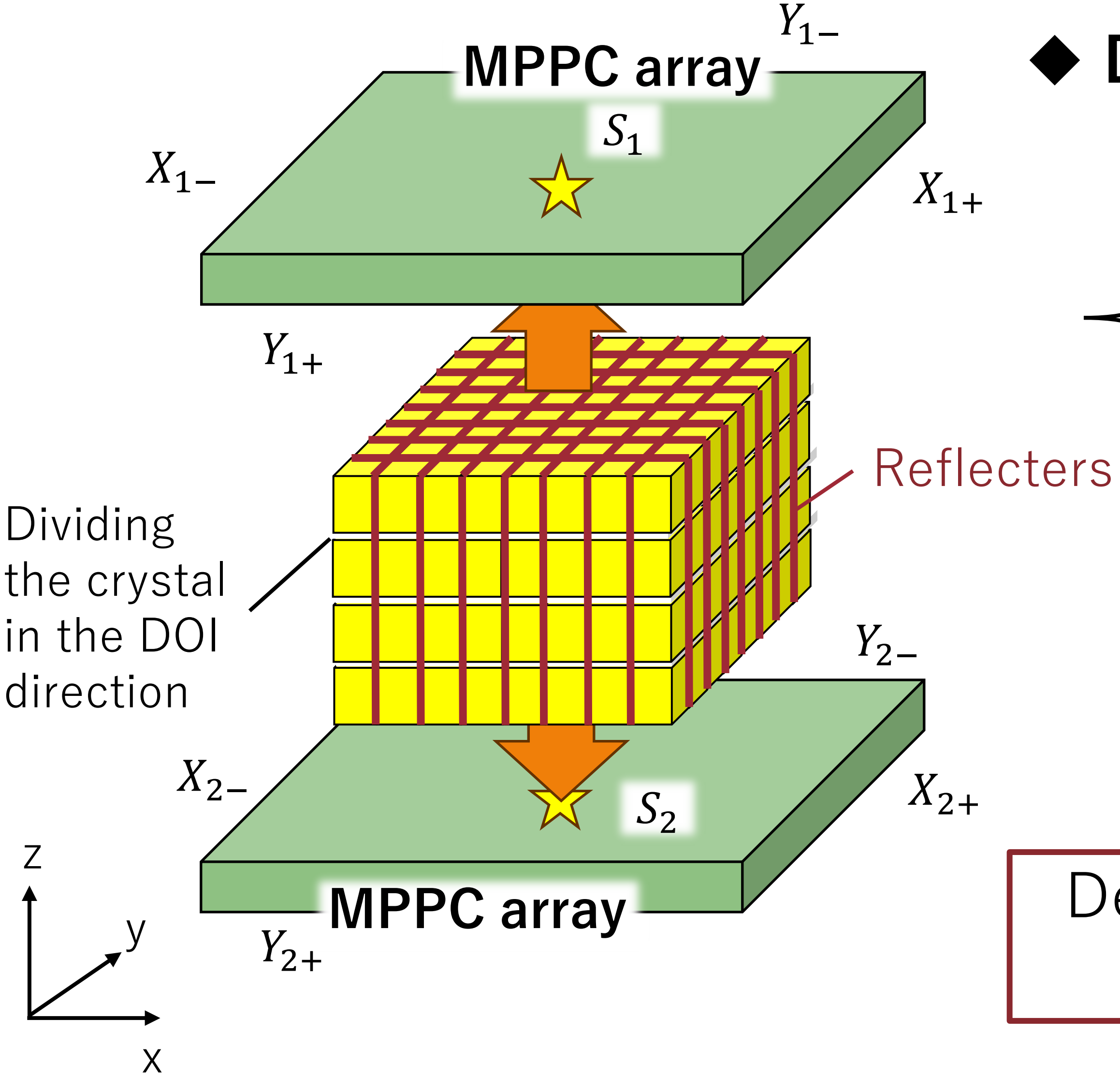

◆ Derivation of 3D position

$$
\begin{cases}
X = ((X_{1+} + X_{2+}) - (X_{1-} + X_{2-}))/(S_1 + S_2) \\
Y = ((Y_{1+} + Y_{2+}) - (Y_{1-} + Y_{2-}))/(S_1 + S_2) \\
Z = S_1/(S_1 + S_2) \times L
\end{cases}
$$

S_1, S_2 : Total output sum of each MPPC

L : Length in the Z direction

Deriving the position along the Z-axis from the output ratio of each MPPC!

7. Scintillater properties

	Ce:GAGG	BGO	NaI(Tl)	CsI(Tl)
density [g/cm^3]	6.63	7.13	3.67	4.51
luminous intensity [photon/MeV]	46,000	9,000	4,1000	6,6000
Energy Resolution@662keV	9	16	7-9	9-11
peak emission wavelength[nm]	520	480	410	565
fluorescence decay time[ns]	88	300	230	1000
self-radioactivity	no	no	present	present
hygroscopicity	no	no	present	present

- ✓ GAGG was selected for its high density, light yield, non-hygroscopic properties, ease of processing, and resistance to cosmic radiation activation.
- ✓ BGO is a high-density crystal that efficiently detects external background, making it commonly used as an active shield.

7. - PMT vs MPPC -

PMT・MPPC ⇨ A detector capable of capturing faint light.

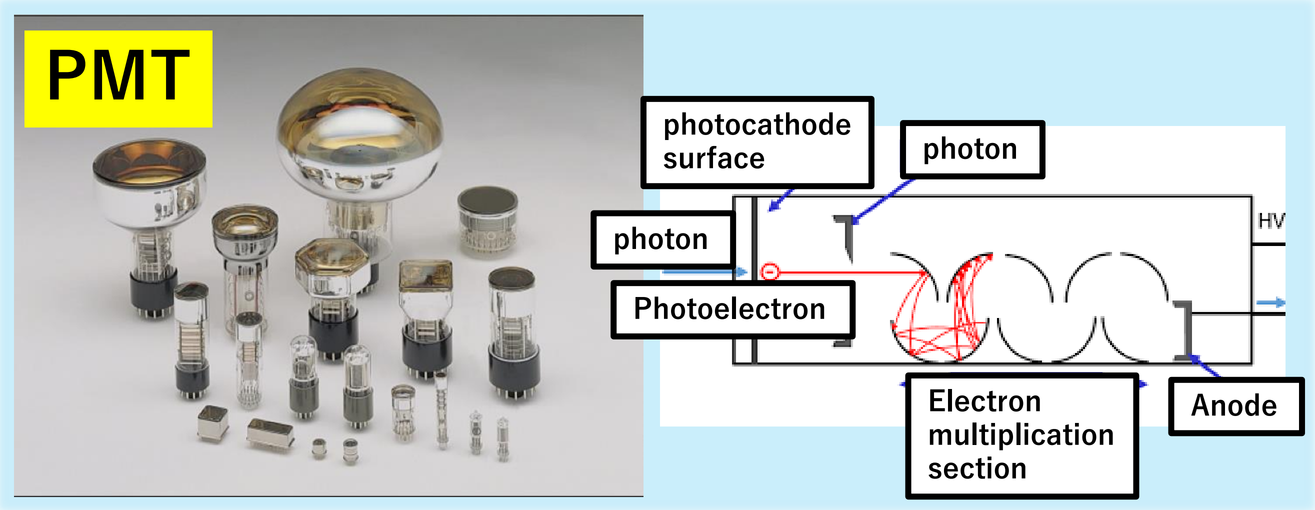

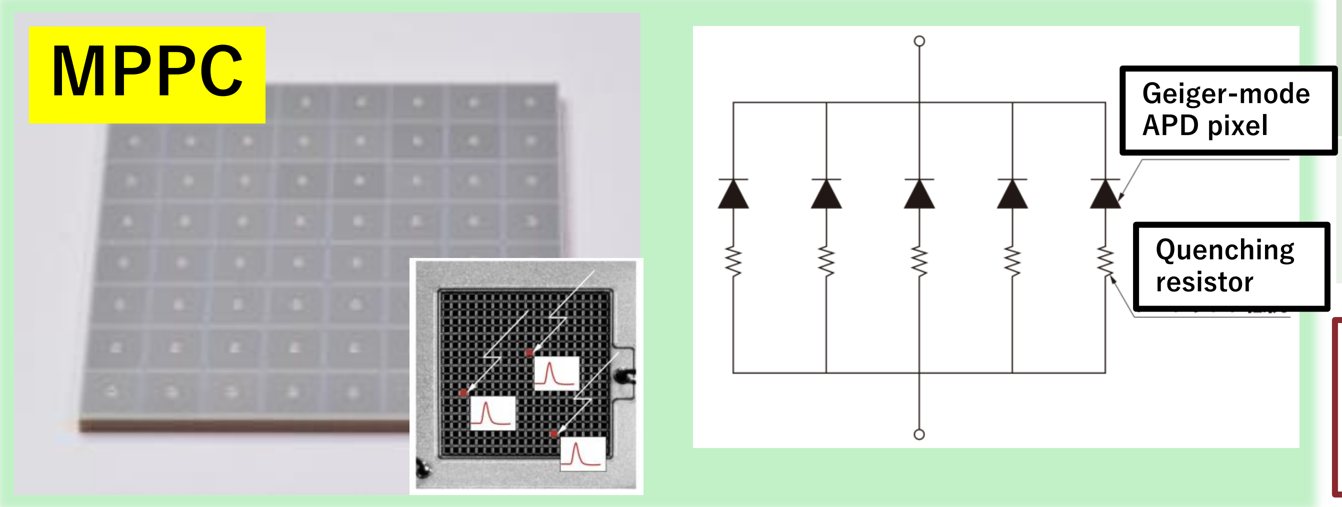

	PMT	MPPC
Gain	$10^6 \sim 10^7$	$10^5 \sim 10^6$
Operating voltage	1000~ V	**~ 50 V**
SIze	Big	**Compact**
Quantum efficiency	20 ~ 30 %	**30 ~ 40 %**
Photon identification	Impossible	Possible
Magnetic field effect	×	◎

Equipped with a low-voltage, compact MPPC (Multi-Pixel Photon Counter)

7. - MPPC -

By applying centroid calculations to the signals read out from the four edges of the MPPC, the reaction position on a two-dimensional plane can be determined.

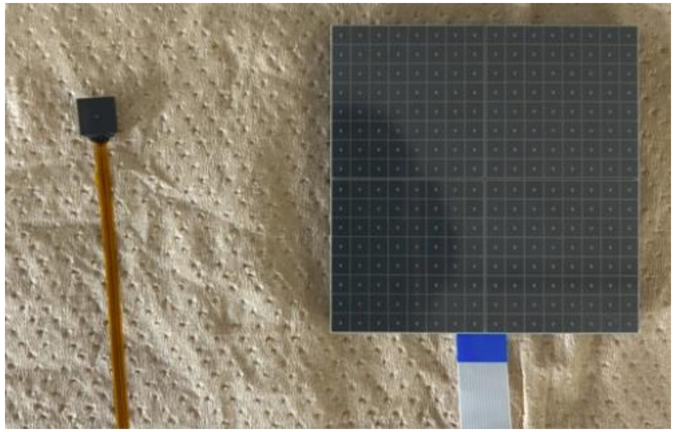

Table 3.2 Structure and Characteristics of S14161-1685
(Ta = 25° C, Vs = ±5V, λ = 700 nm)

Item	Specification	Unit	Item	Specification	Unit
MPPC	S14161-3050HS-08	-	Sensitivity wavelength range	270-900	nm
Number of channels	256 (64 × 4)	ch	Peak sensitivity wavelength	450	nm
Effective photosensitive area	3 × 3	mm/ch	Detection efficiency (450 nm)	50	%
Pixel pitch	50	μm	Breakdown voltage	38	V
Number of pixels	3531	/ch	Recommended operating voltage	V_BR + 2.7	V
Operating temperature range	-10 to +40	°C	Gain	2.5×10^6	-
Storage temperature range	-20 to +50	°C	Terminal capacitance	500	pF
Temperature sensor	LM94021	-	Temperature coefficient	34	mV/°C

8. Performance – angular resolution-

◆ Pinhole mode

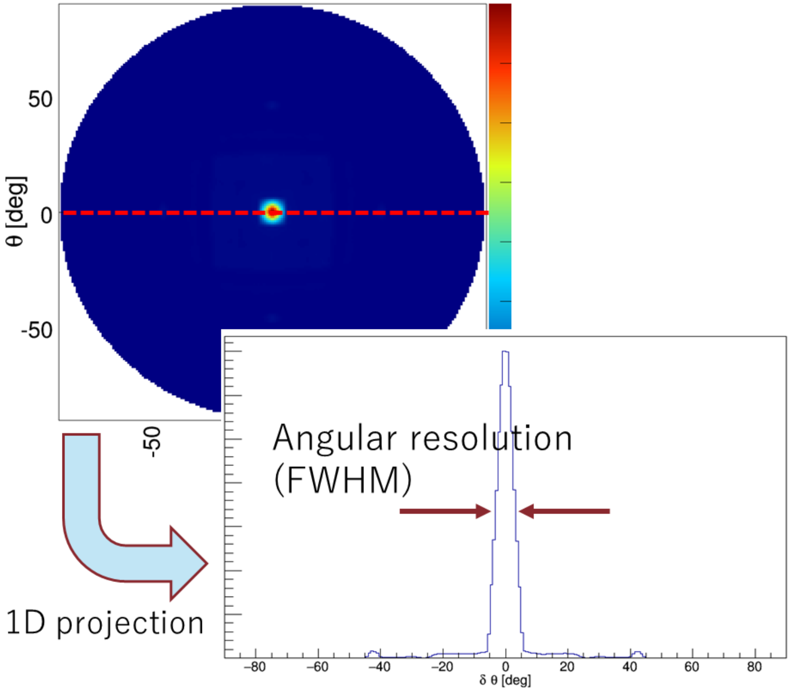

◆ Compton mode

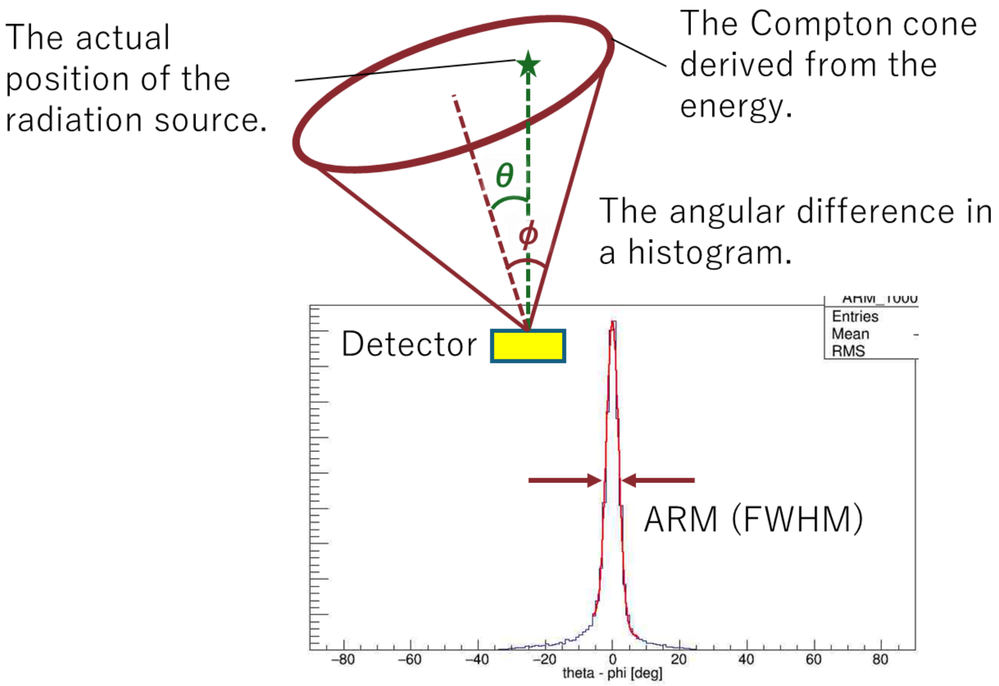

- ✓ In pinhole mode, the FWHM of the 1D projection of the image is used as the angular resolution.
- ✓ In Compton mode, for a point source with a known position, the angle θ is defined as the angle between the source position and the scattering axis of the Compton event, while the scattering angle Φ is calculated from the energy information. The FWHM of the histogram of the differences between θ and Φ is used as the angular resolution.

8. Field of View

◆ Pinhole mode

⇨ The field of view is limited by the detector geometry.

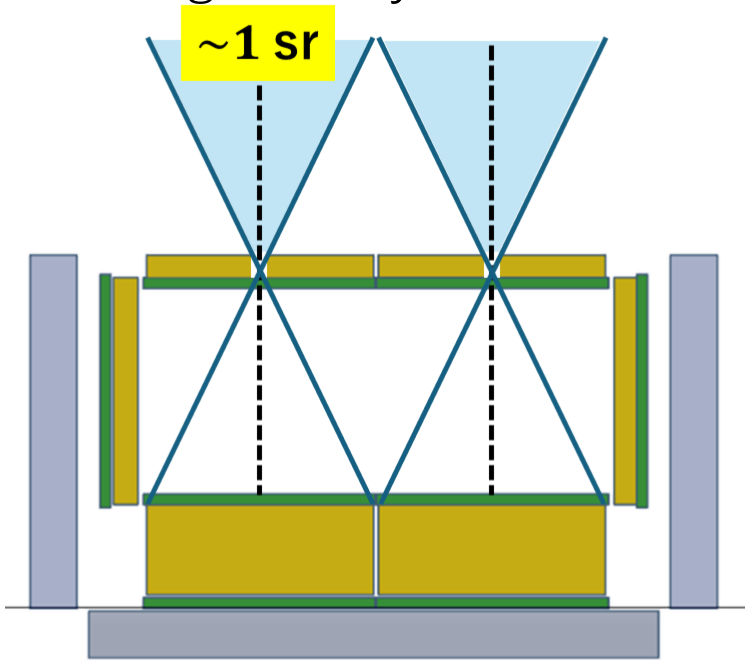

◆ Compton mode

⇨ Derived from the angular dependence of the intrinsic efficiency.

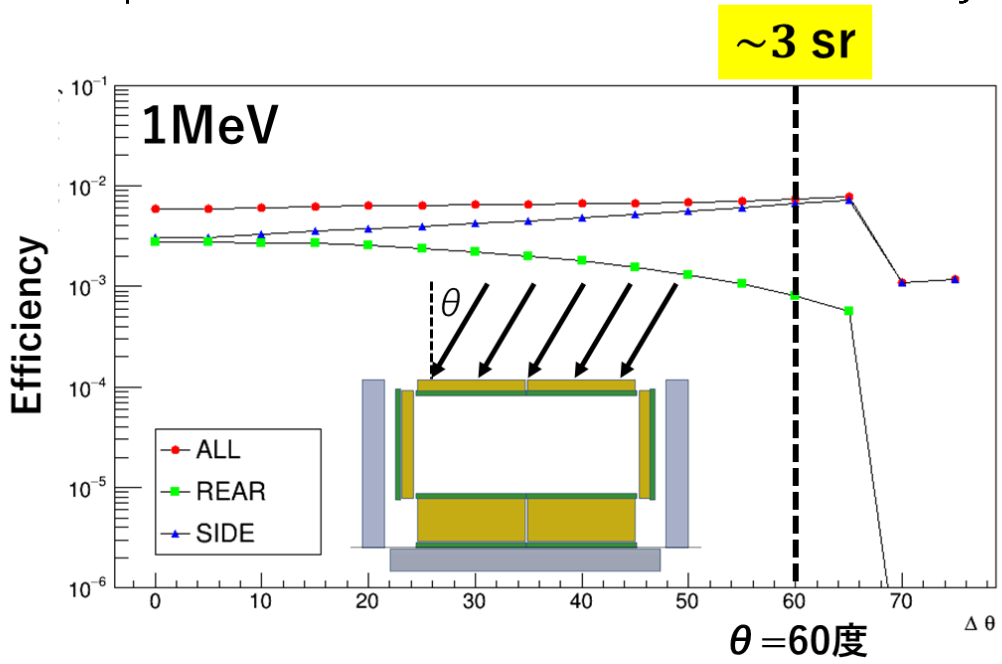

✓ The FOV in pinhole mode is geometrically determined.

✓ On the other hand, the FOV in Compton mode is defined by the angular dependence of the detection efficiency. The angular dependence of the intrinsic efficiency when 10^7 photons are irradiated at 1 MeV is presented.

8. Performance evaluation - Detection sensitivity for point sources -

◆ Evaluation of the intrinsic efficiency in compton mode(**Geant4 Simulation**)

Geant4 simulation

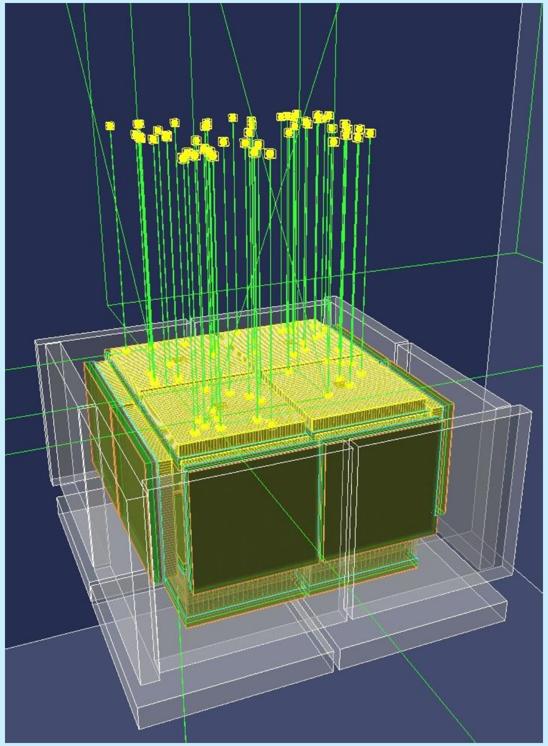

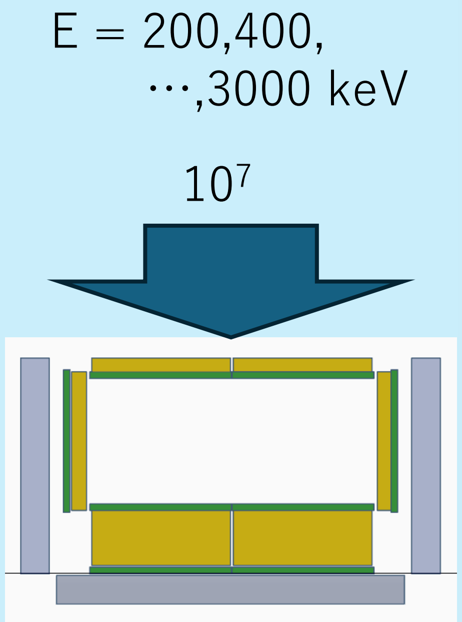

1. Reproduction of GAGG, MPPC, and BGO shield in Geant4.
2. Irradiation of 10^7 gamma photons of each energy from the front.

Count events as pinhole events where the photon "pass through the hole and reacts only with the absorber."

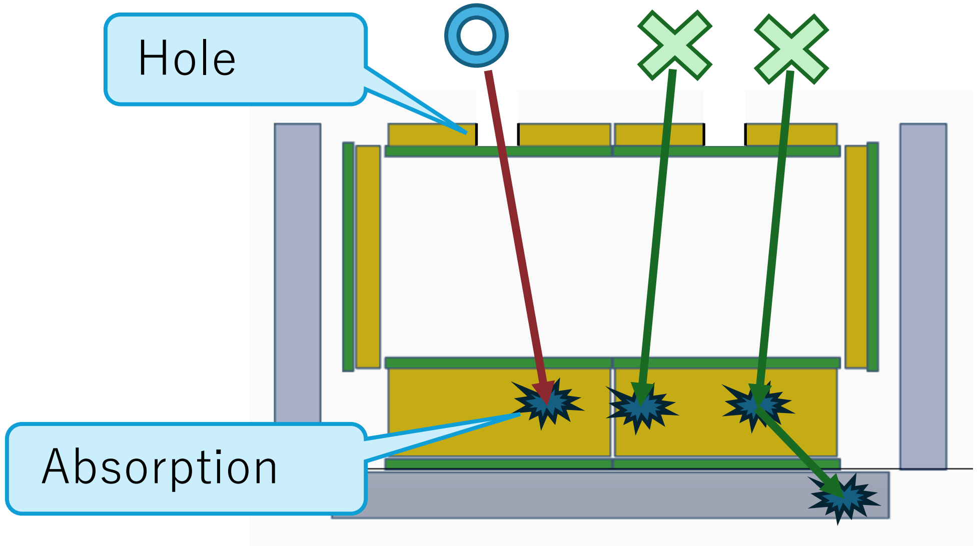

Intrinsic efficiency = pinhole evevt / Number of irradiated gamma photons.

8. Performance evaluation - Detection sensitivity for point sources -

◆ Evaluation of the intrinsic efficiency in compton mode(**Geant4 Simulation**)

Geant4 simulation

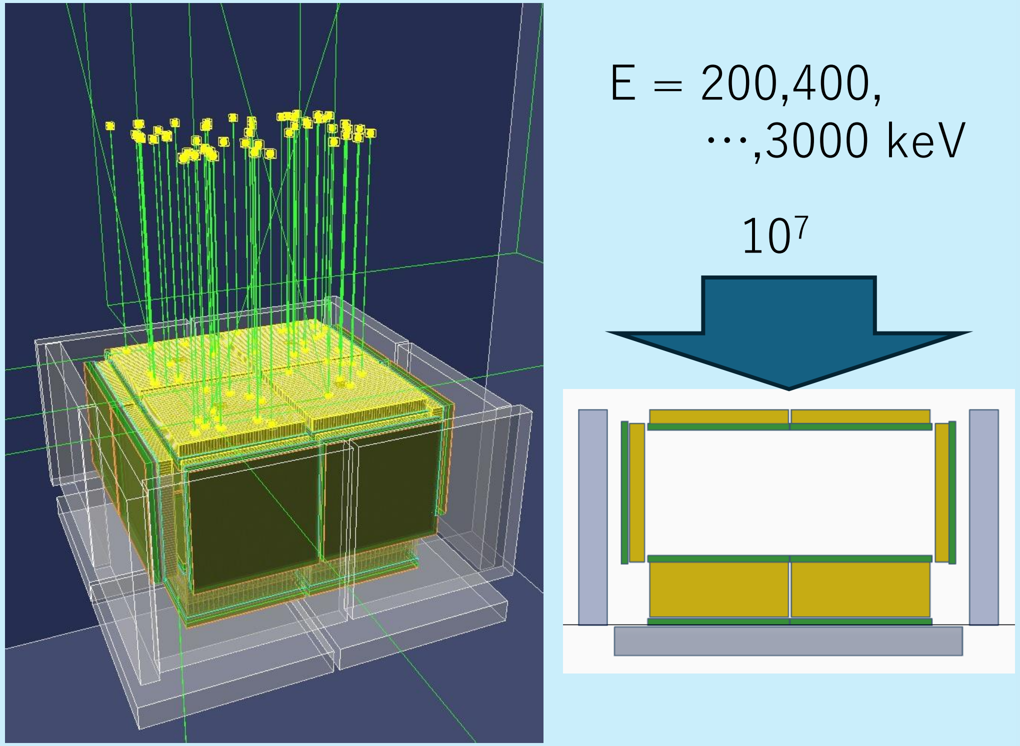

1. Reproduction of GAGG, MPPC, and BGO shield in Geant4.
2. Irradiation of 10^7 gamma photons of each energy from the front.

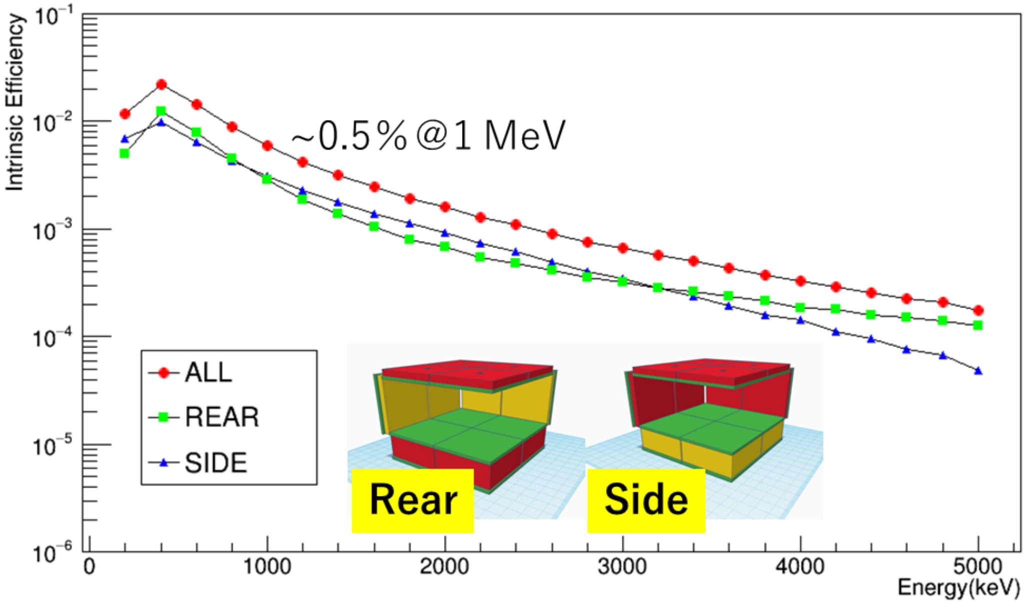

Intrinsic efficiency = compton evevt / Number of irradiated gamma photons.

8. Efficiency

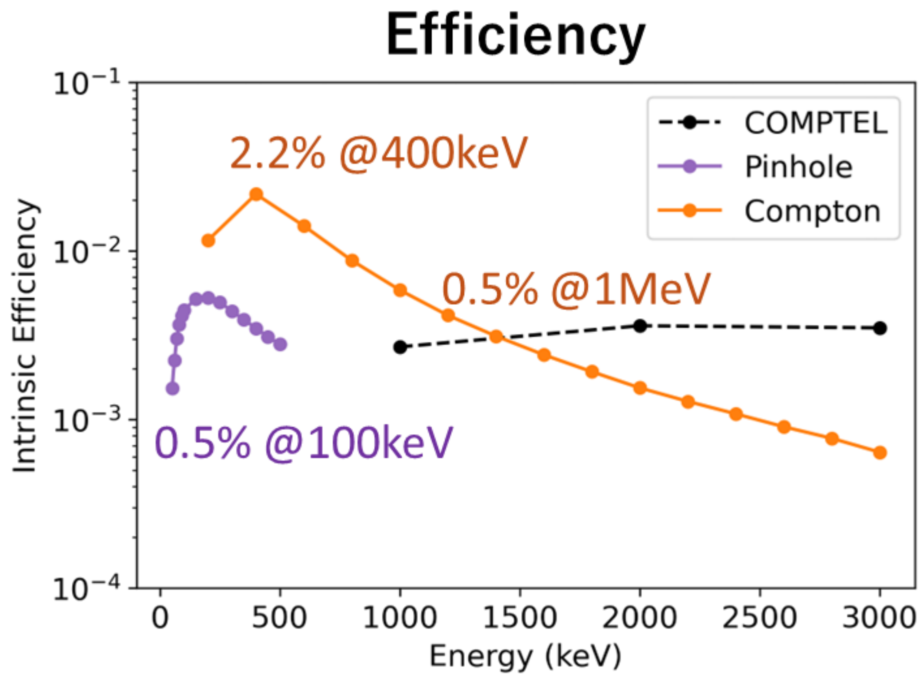

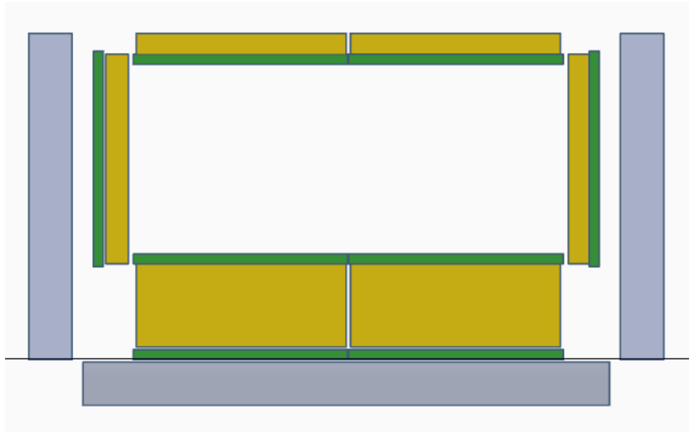

✓ It is observed that the efficiency decreases for lower energies below 100 keV.
⇒ due to the MPPCs located directly behind the hole or in the absorber interacting with low-energy gamma rays.

✓ On the other hand, above 100 keV, the sensitivity is expected to decrease at higher energies, as events involving Compton scattering in the absorber increase.

9. Compton Camera Principle

Gamma-ray Detection Methods

Gamma-ray Detection with 『 **Scintillator** + **MPPC** 』

Gamma rays

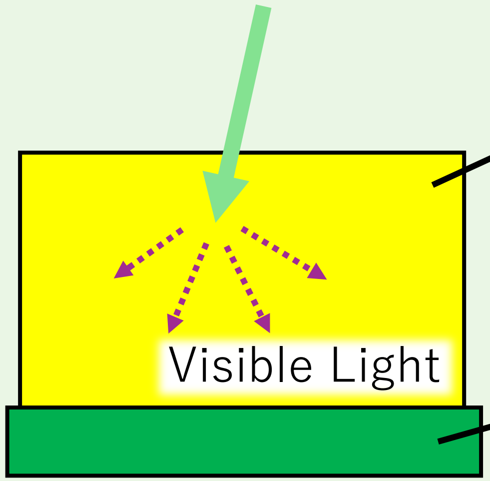

Scintillator
Photon emission corresponding to gamma-ray energy

MPPC
Measure the number of photons

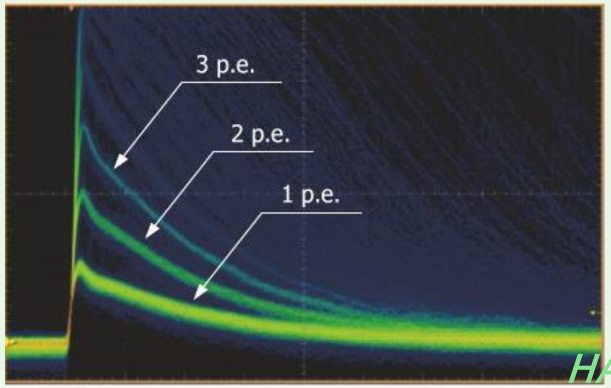

Compton Reconstruction

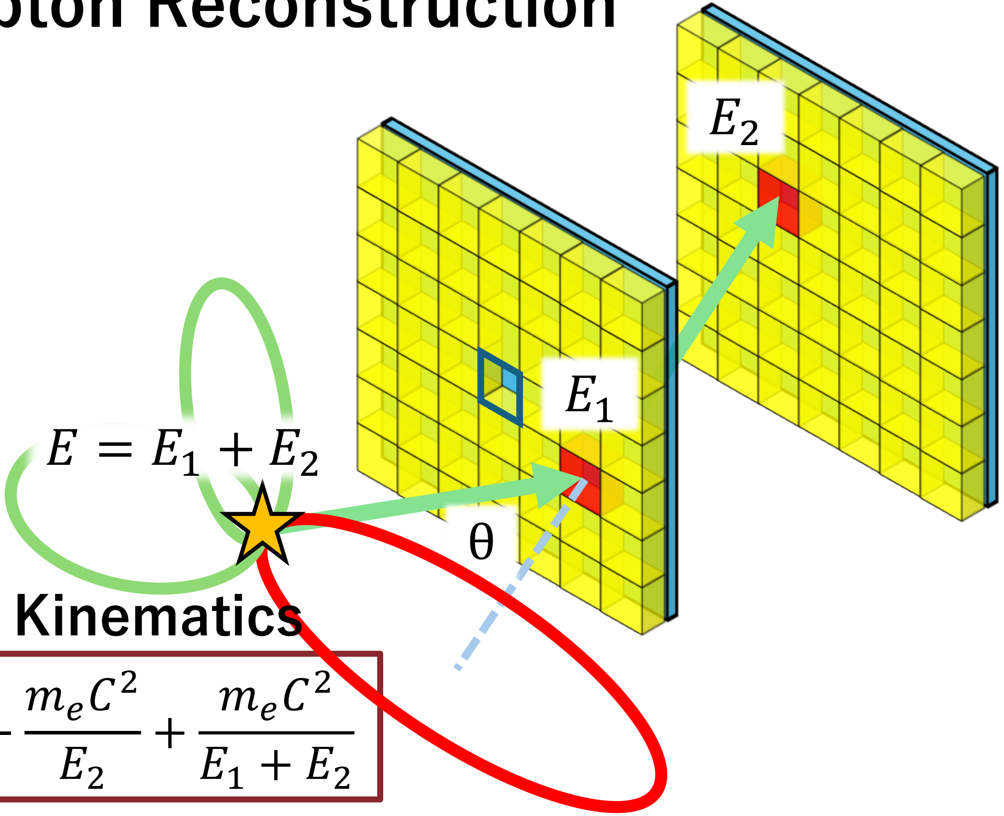

Compton Kinematics

$$\cos\theta = 1 - \frac{m_e C^2}{E_2} + \frac{m_e C^2}{E_1 + E_2}$$

Measure the interaction time, interaction position, and energy of gamma rays.

⇨ Determine the arrival direction of gamma rays.

9. Event Selection

Pinhole mode

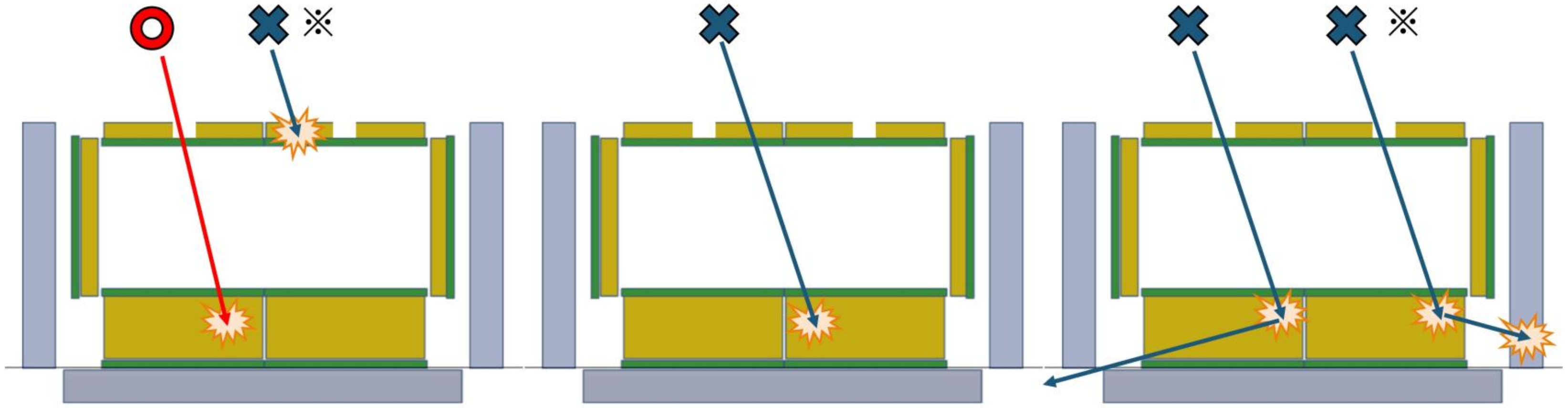

Signal event

Scatterer Transmission Event

Escape Event

Compton mode

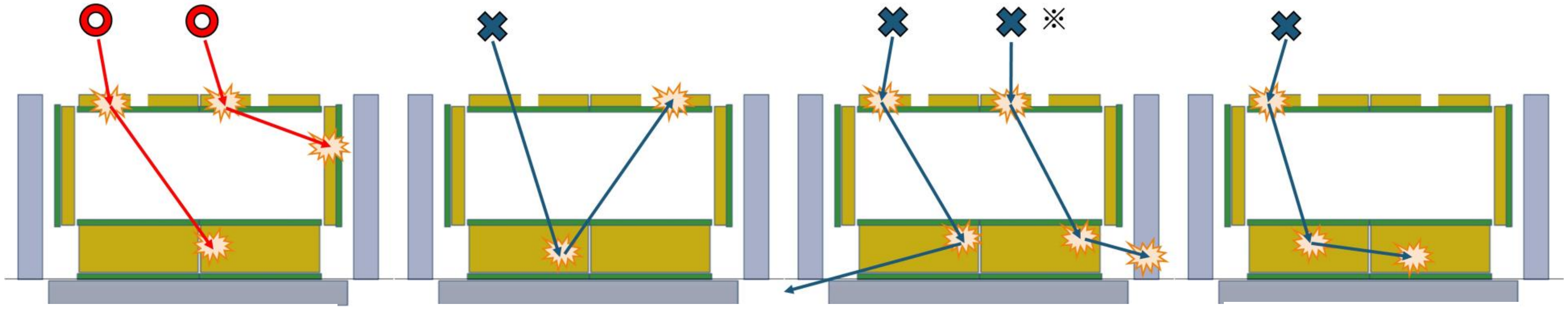

Signal event

Backscattering

Escape Event

Multiple scattering

9. Event Selection

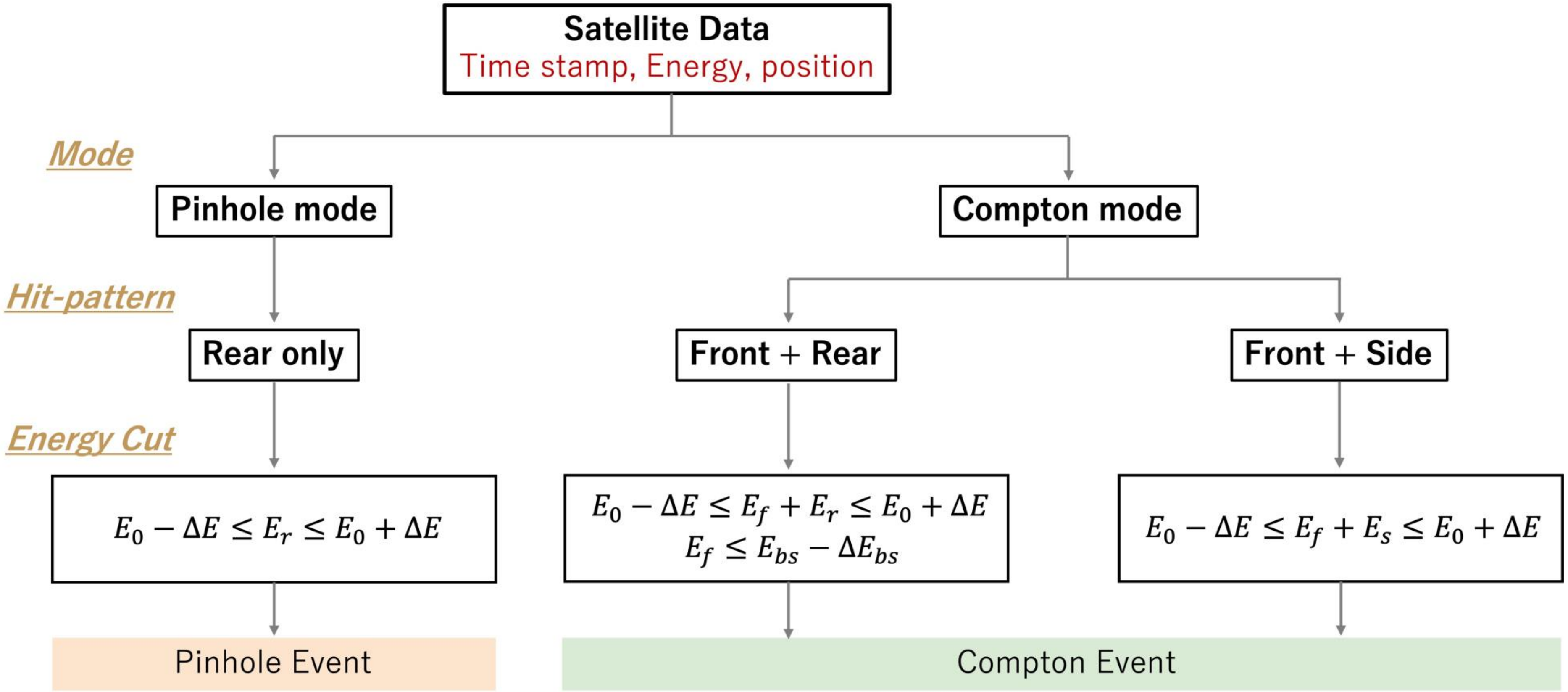

- E_0: Photon energy
- ΔE: Energy resolution width
- E_{bs}: Back-scatter energy
- E_f: Energy deposited in the scatterer
- E_r: Energy deposited in the absorber
- E_s: Energy deposited in the side scatterer

9. Event Selection -compton event-

Rear Event selection

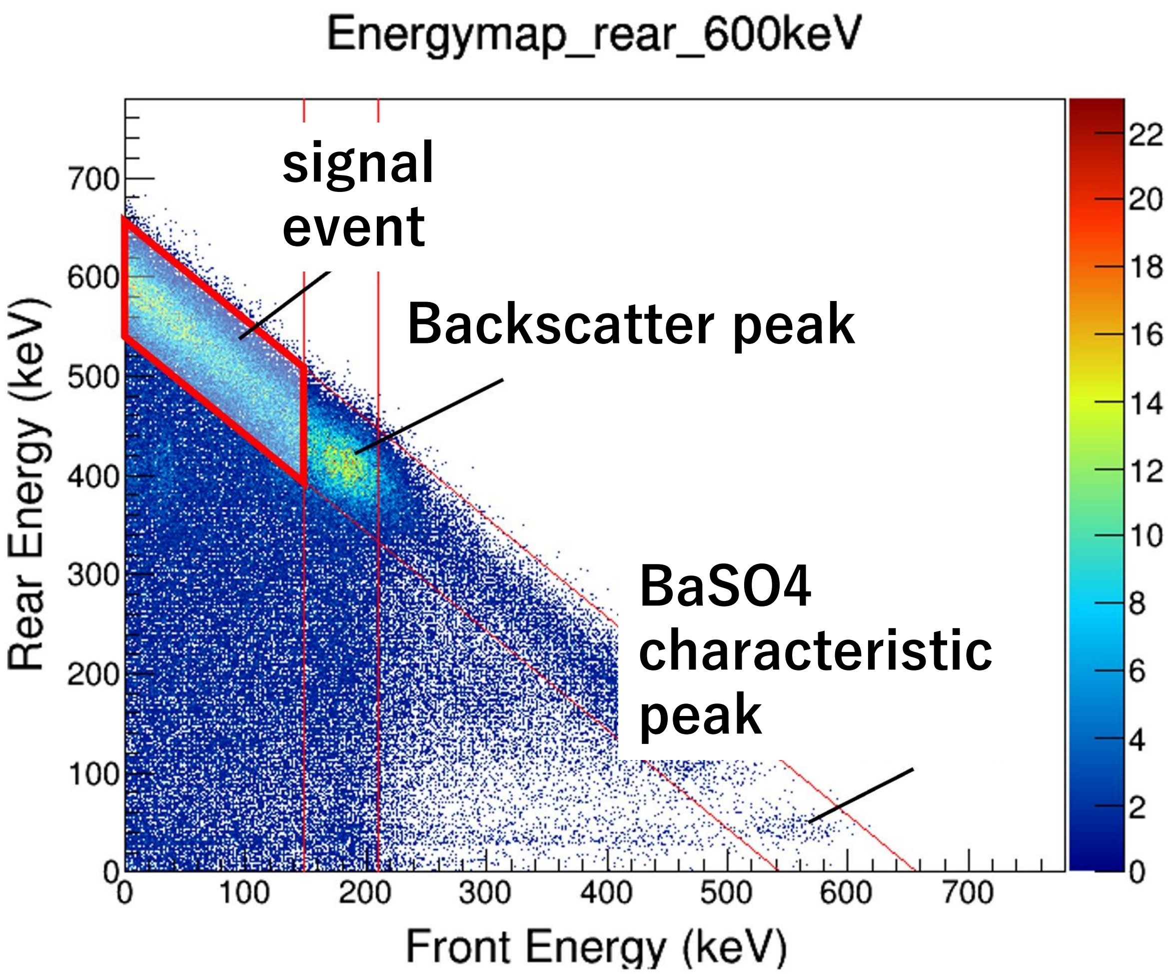

Side Event selection

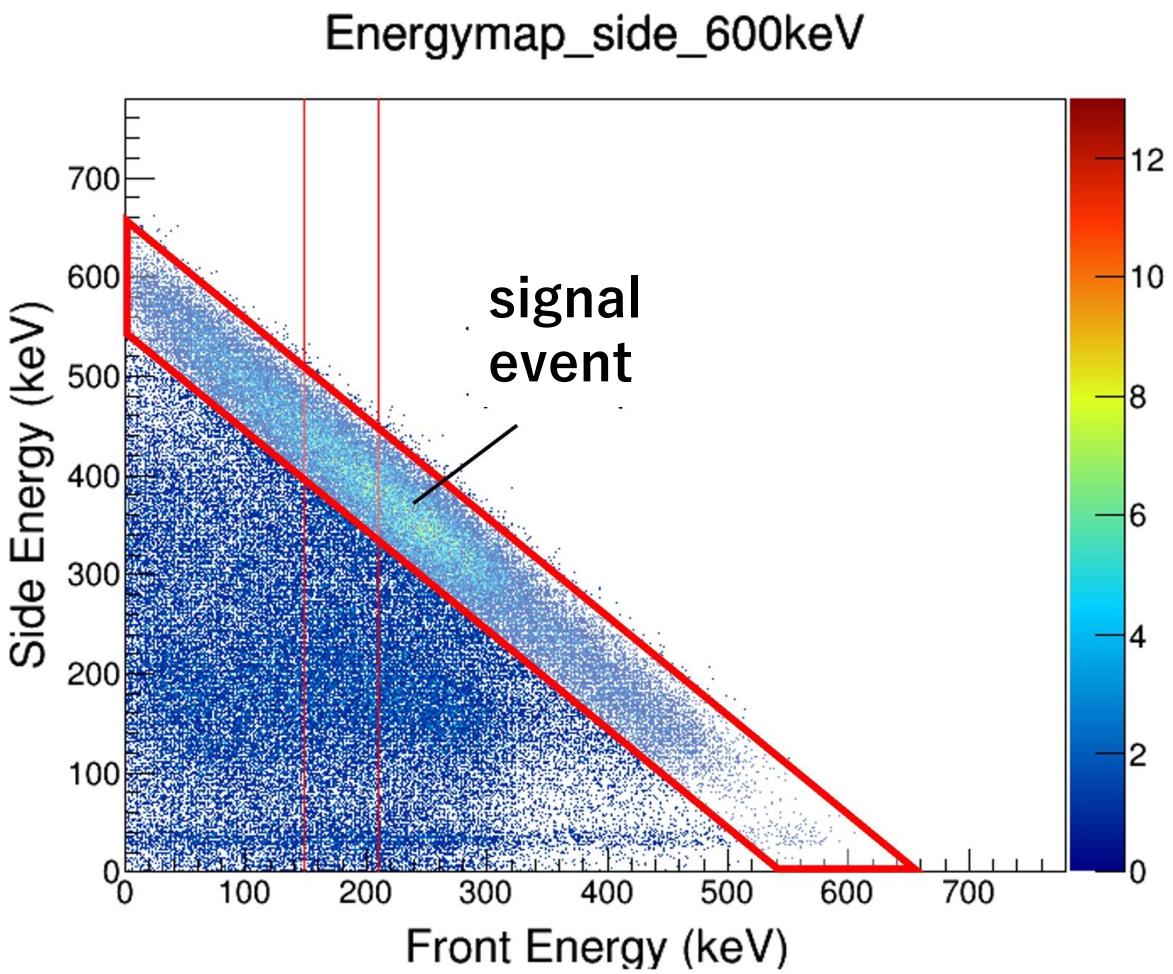

9. Angle dependence of the Side Energy map

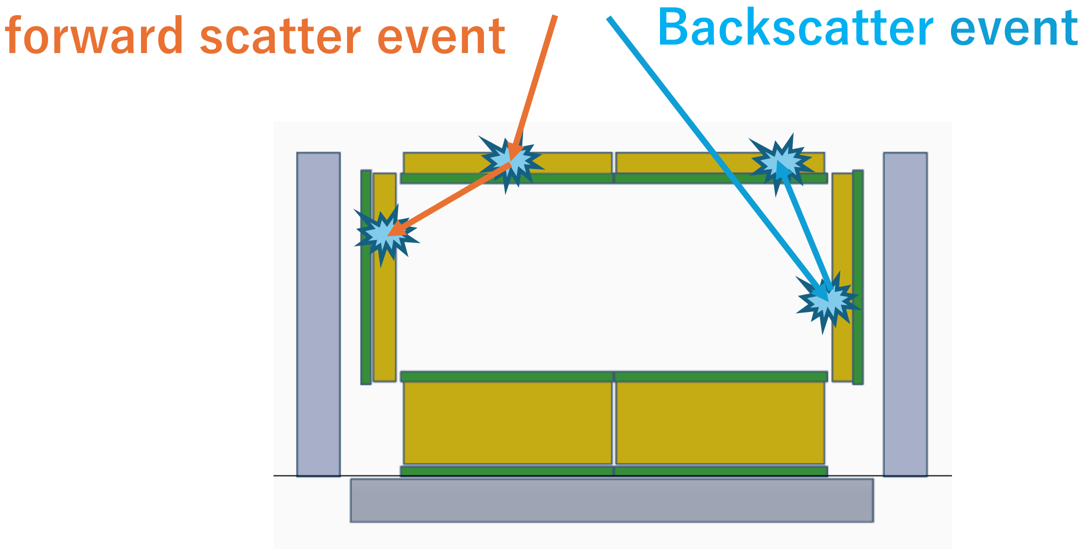

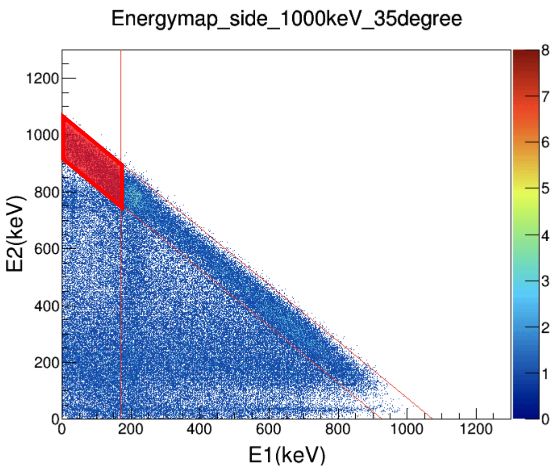

w/o Backscatter

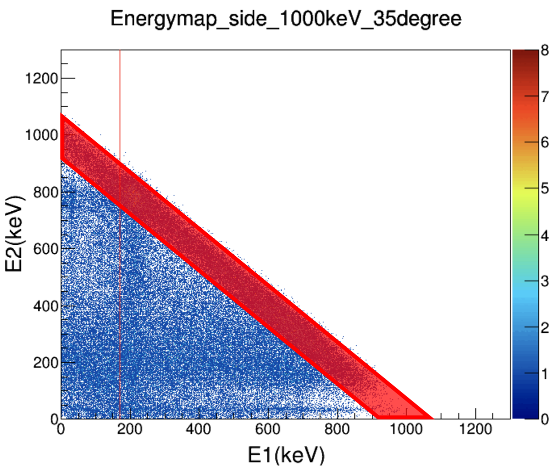

w/ Backscatter

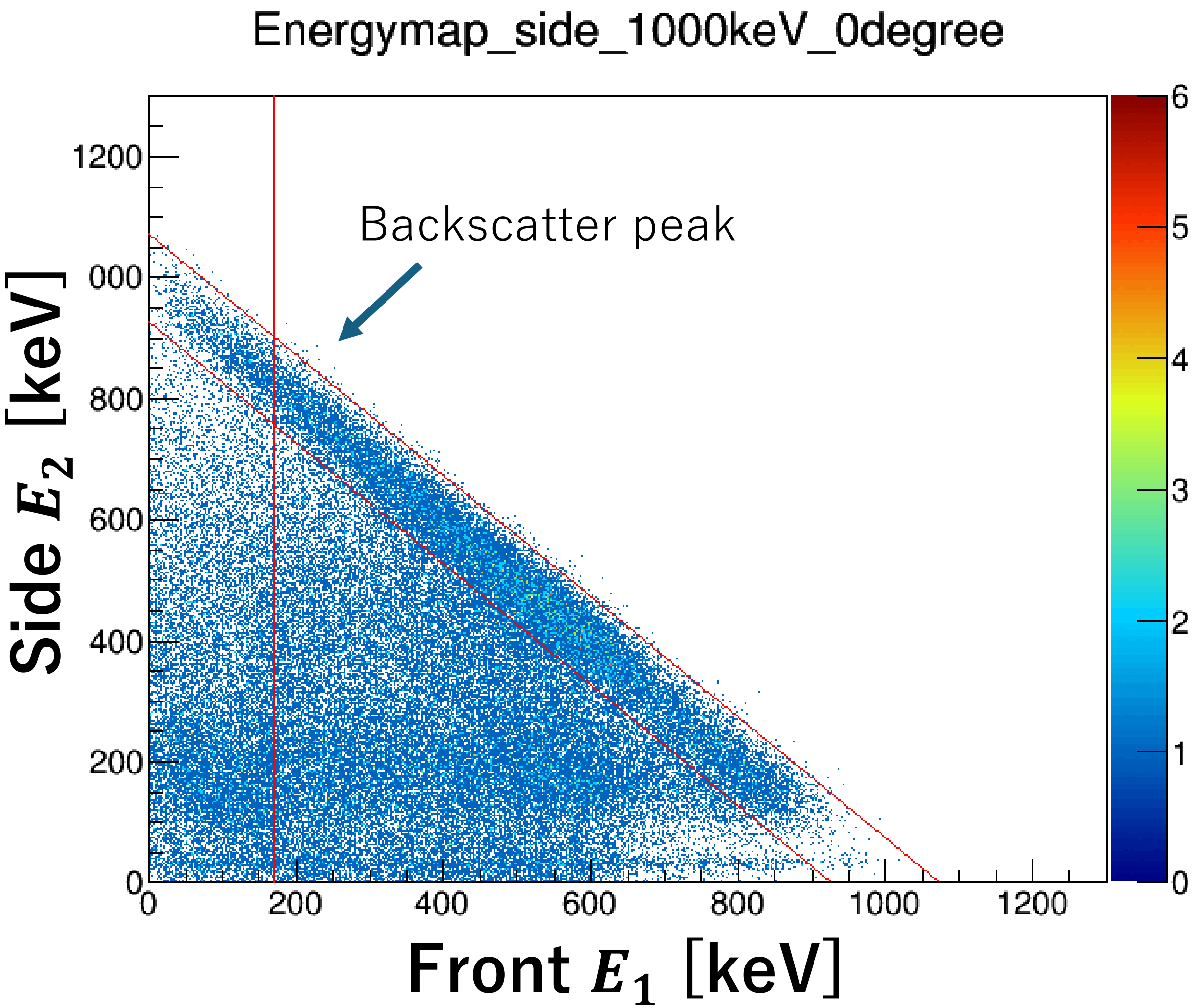

Large angle θ ⇨ A backscatter peak appears on the side.

9. Side Energy cut

w/ backscatter

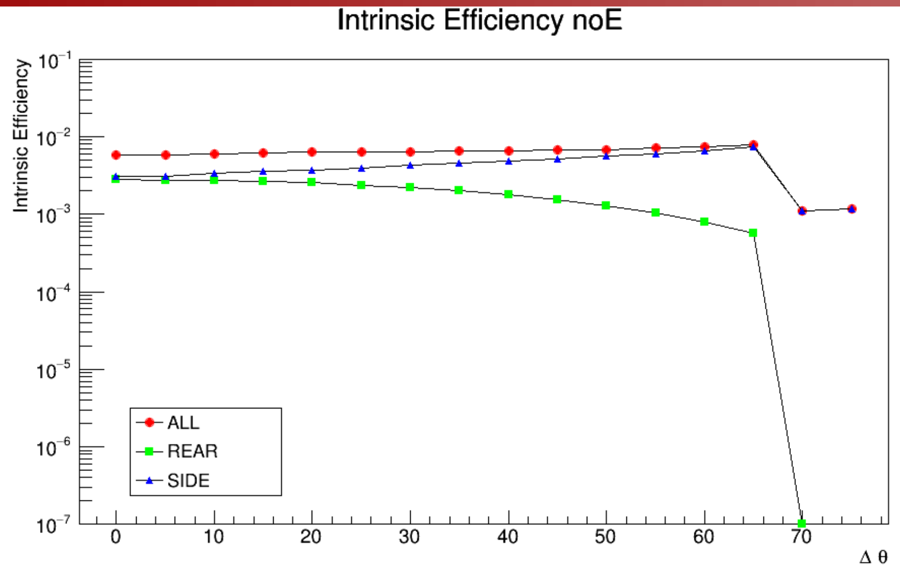

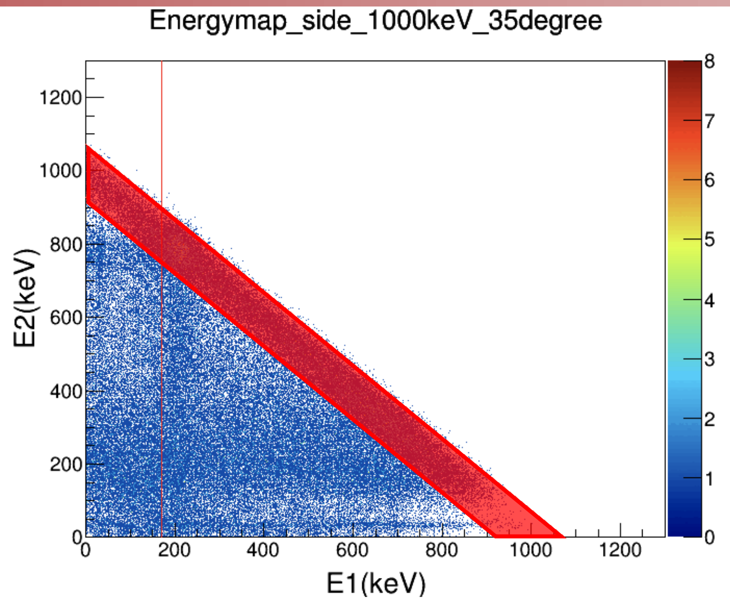

w/o backscatter

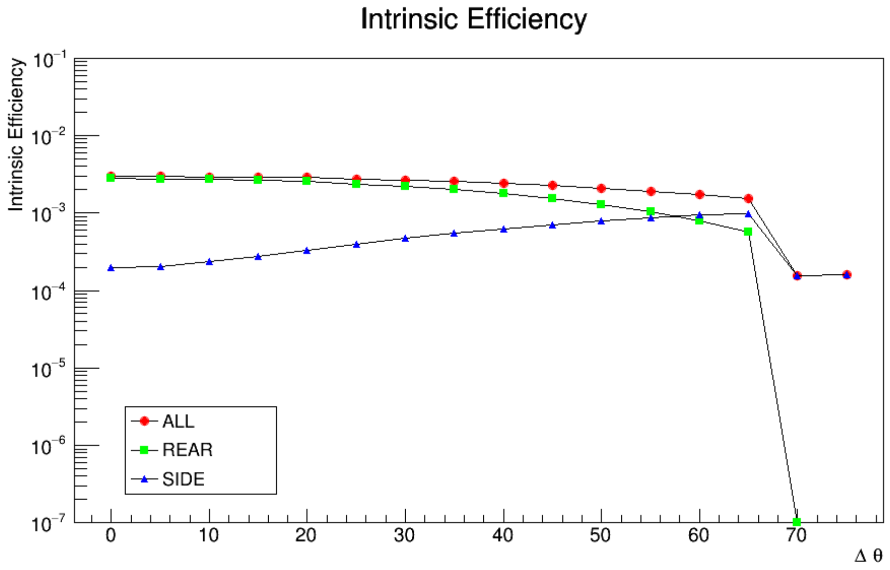

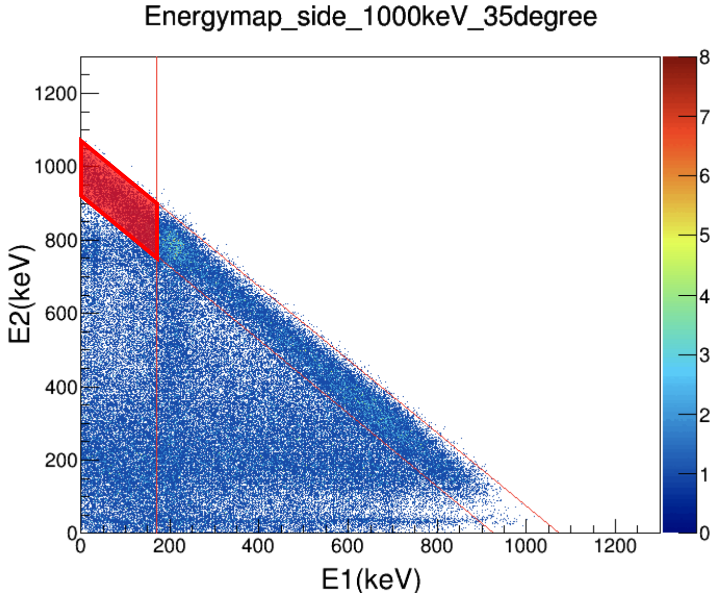

9. Imaging - Pinhole mode -

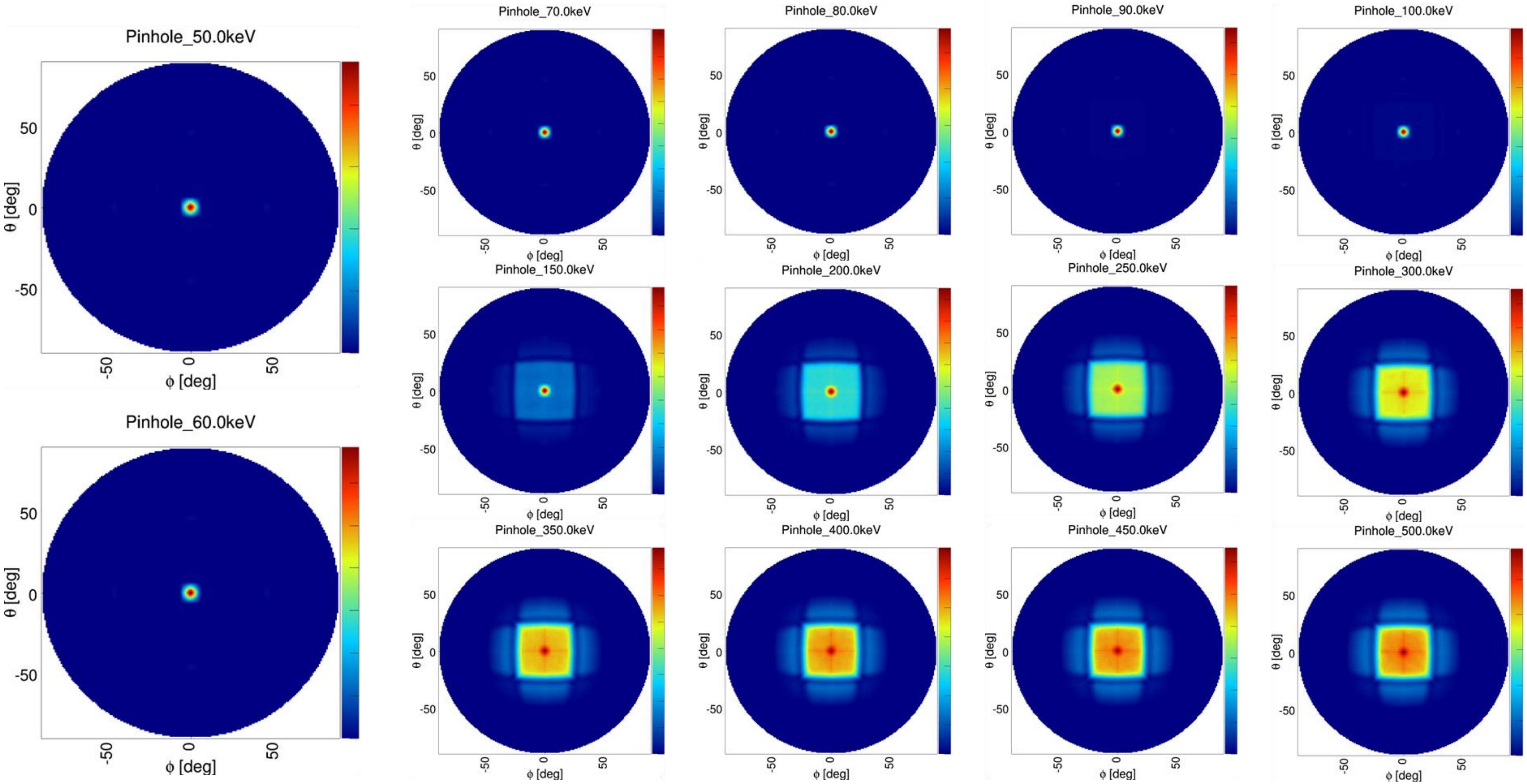

9. Imaging - Pinhole mode -

■ **Imaging of a tilted point source**

⇨ Appearance of artifacts

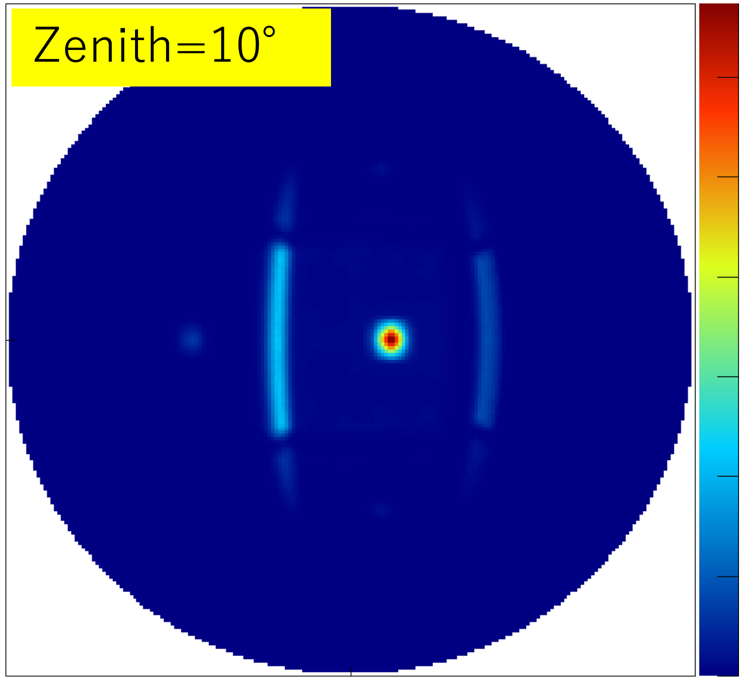

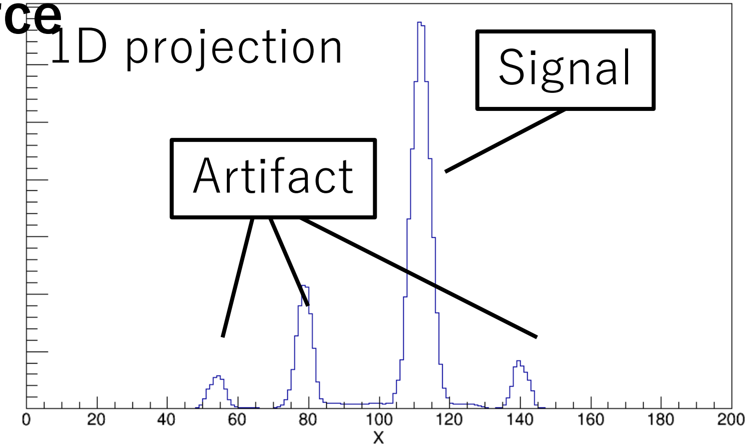

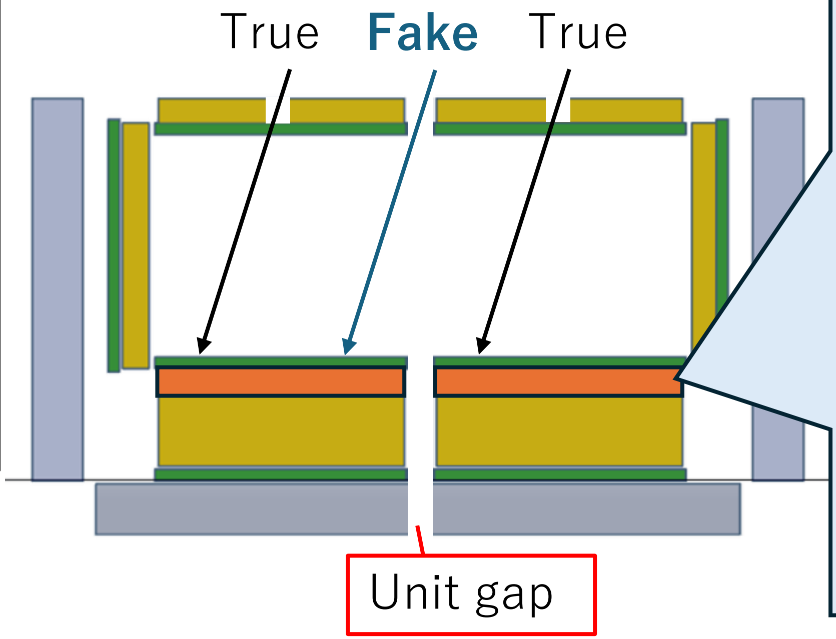

Count rate of the first layer of the absorber

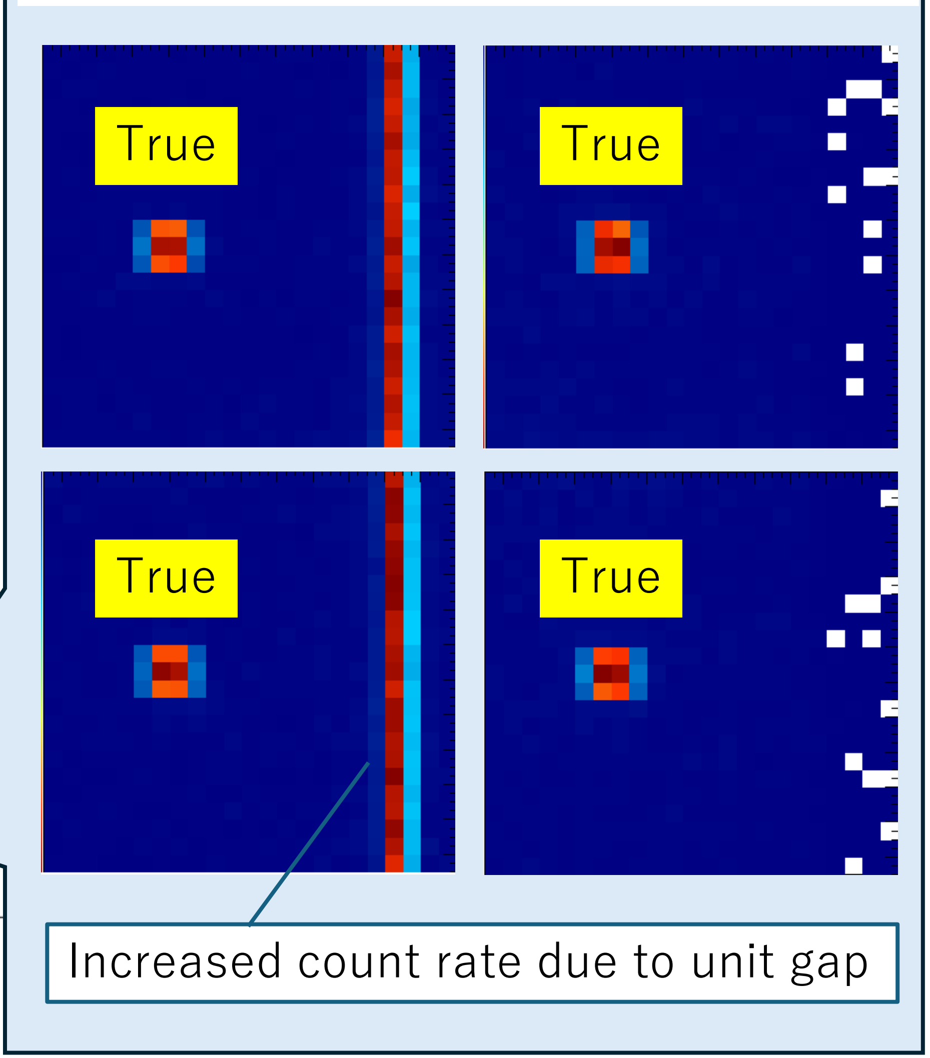

9. Imaging - Compton mode -

Law Energy

High Energy

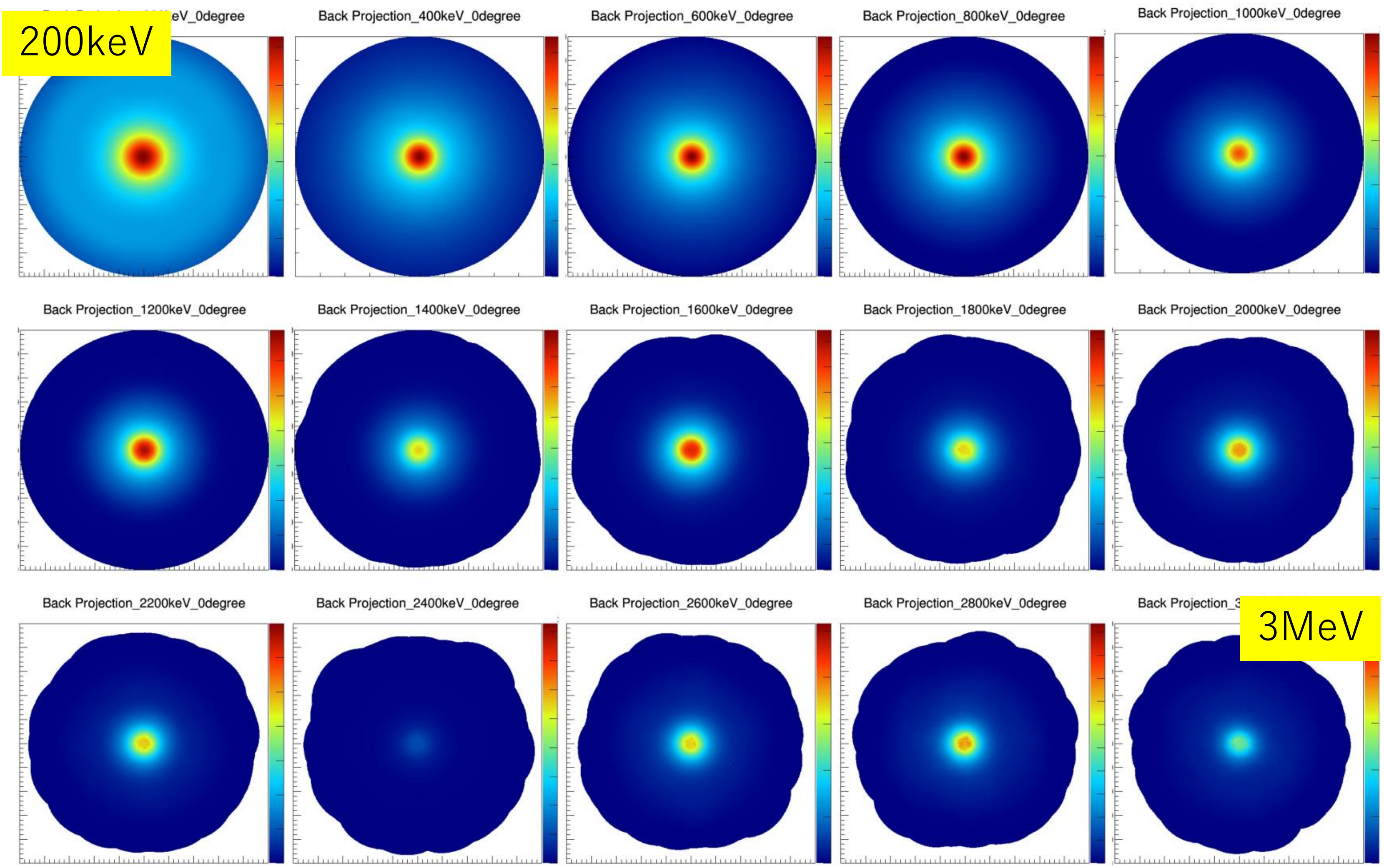

9. Imaging - Compton mode -

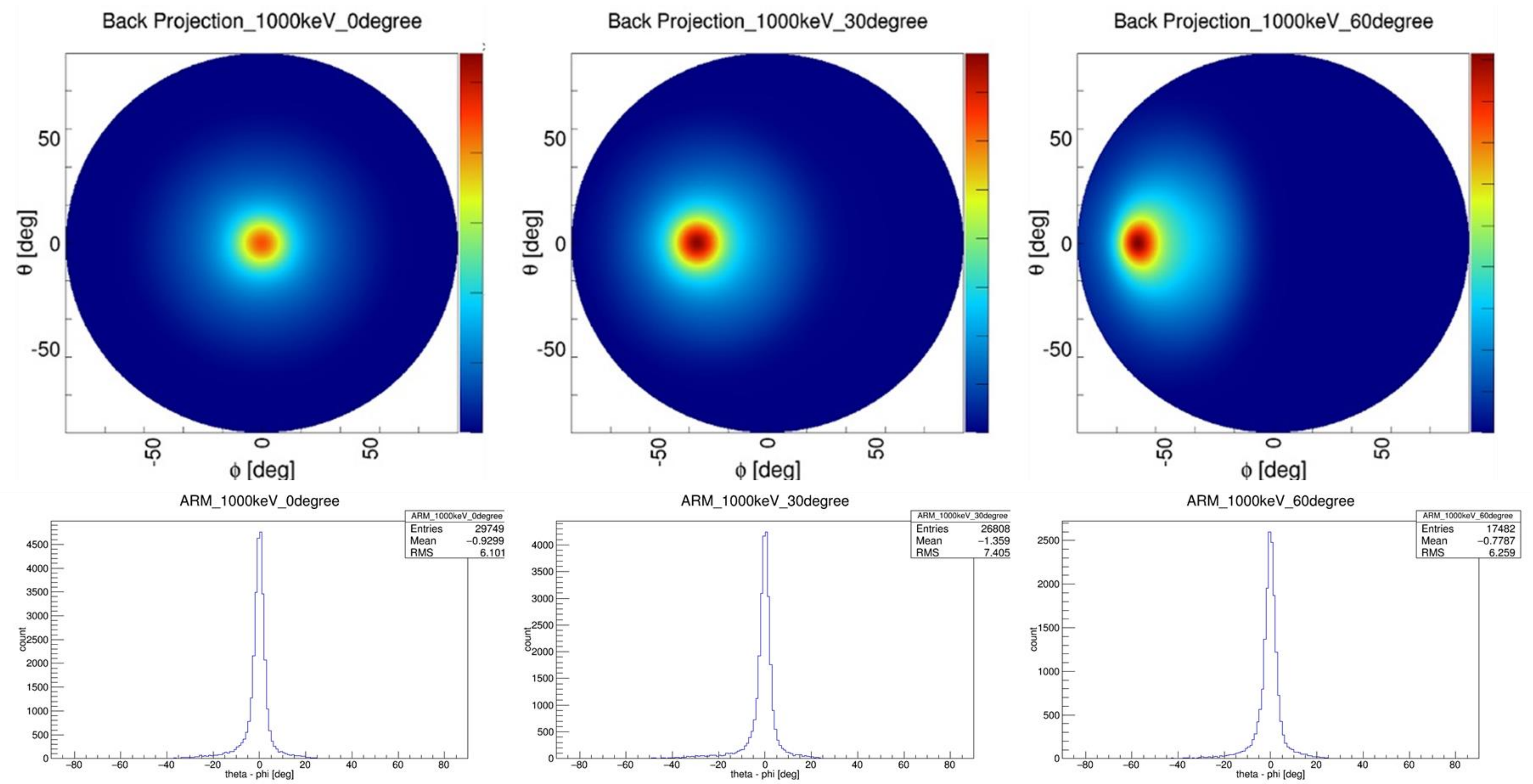

14A. Performance evaluation - Detection sensitivity for point sources -

◆ Sensitivity evaluation.

$$S(E) = \frac{f}{\eta(E)}\sqrt{\frac{b(E)}{A\,\Delta E\,T}}$$

$S(E)$: Detection sensitivity [ph cm^{-2} s^{-1} keV^{-1}]
f : Detection limit in terms of σ
$\eta(E)$: Detection efficiency
$b(E)$: Detector background [cnt cm^{-2} s^{-1} keV^{-1}]
A : Detector area [cm^2]
ΔE : Energy resolution
T : Observation time [s]

Assumptions:

$A = 100\ \mathrm{cm}^2$, $f = 3$ (3 σ detection),
$\Delta E = 0.5E$ [keV], $T = 10^6$ [s]

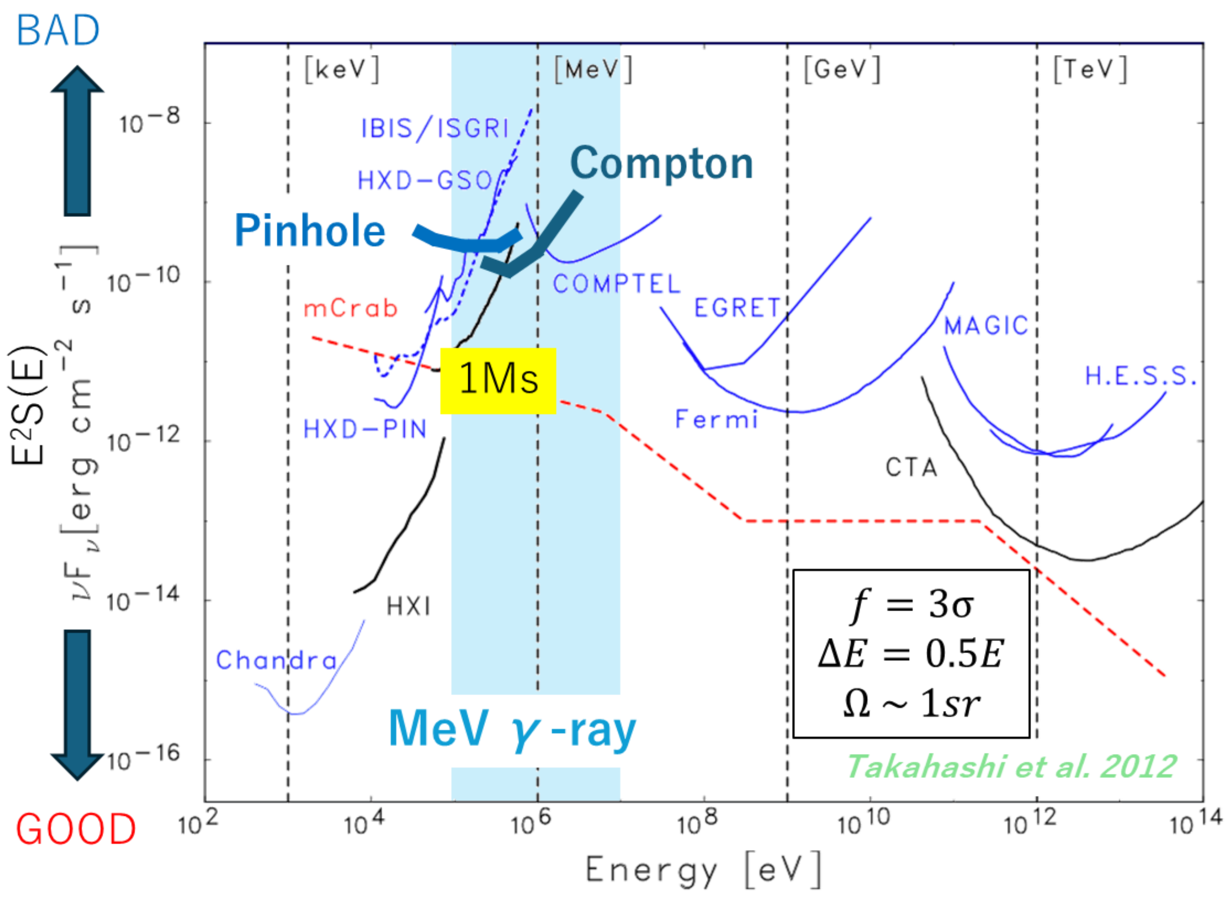

Due to its high intensity and low outgassing properties, which help minimize light loss, **the two-part epoxy adhesive EPO-TEK301**, certified by NASA Lowoutgassing ASTM E595, was chosen.

Calibration Result

- **Energy Resolution Evaluation**
  Right figure: Spectrum (Energy)
  Left figure: Pixel map viewed in the range of 662±50 keV

FRONT：7.5%@662keV
SIDE1：6.9%@662keV
SIDE2：6.8%@662keV

FRONT

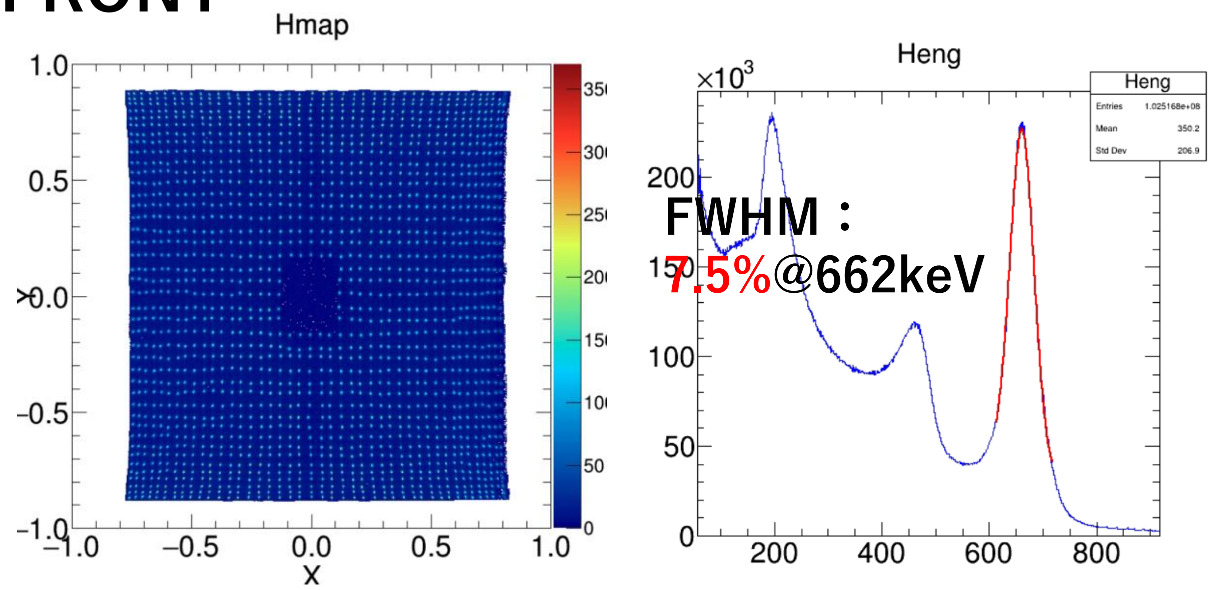

SIDE1

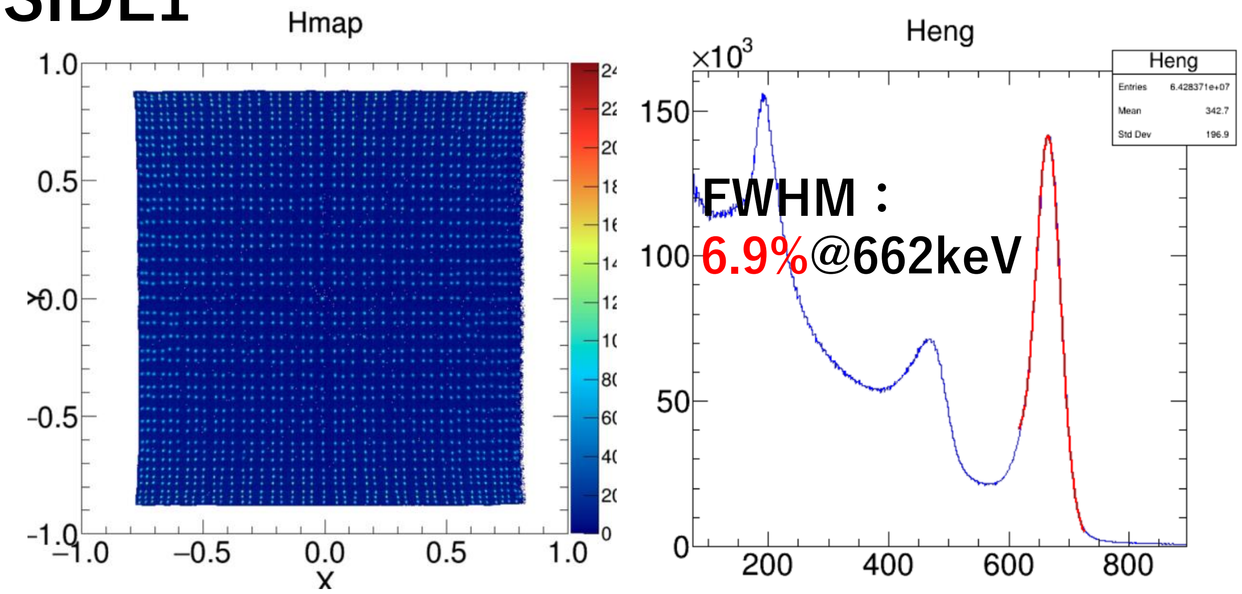

SIDE2

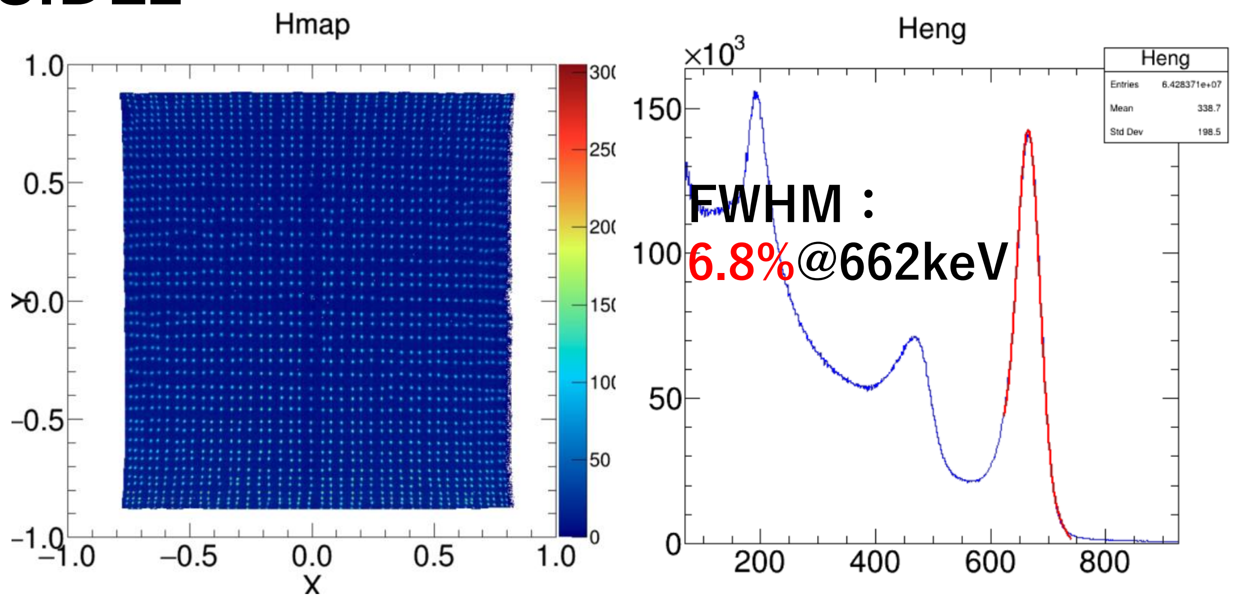

DOI (3d position map)

DOI

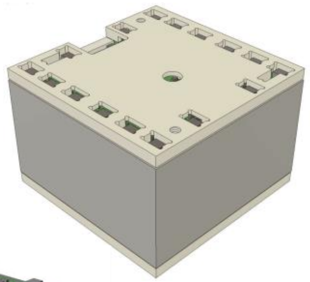

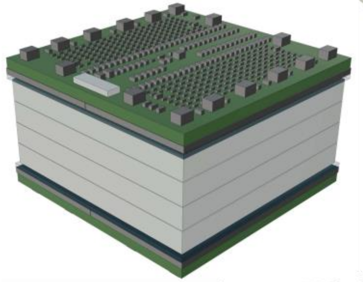

DOI（EM）

3d position map

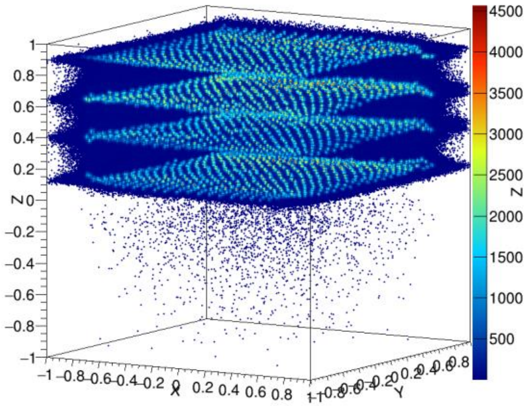

x-z map

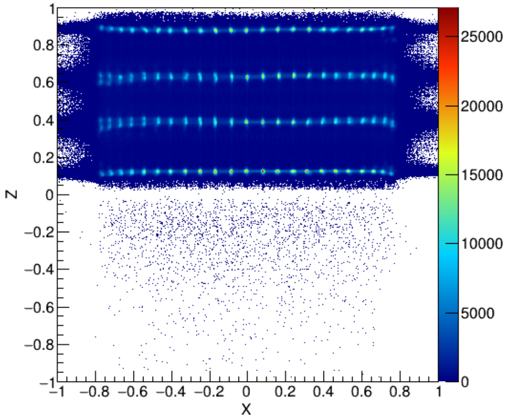

layer1

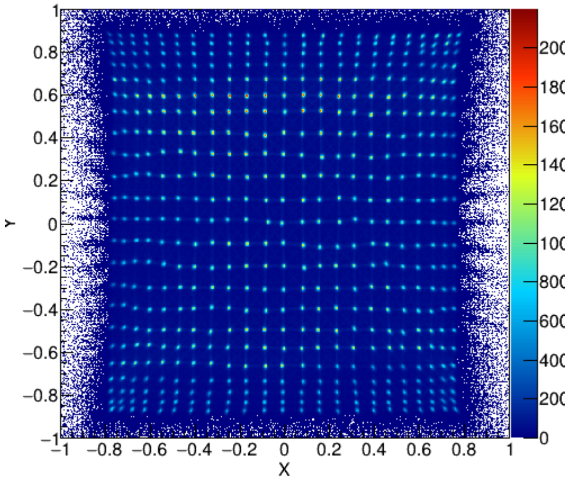

layer2

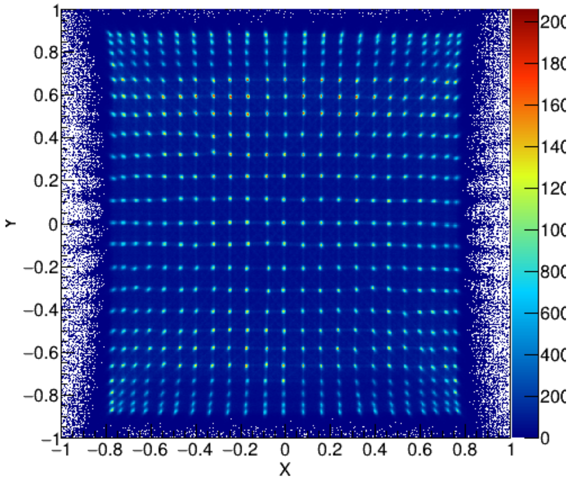

layer3

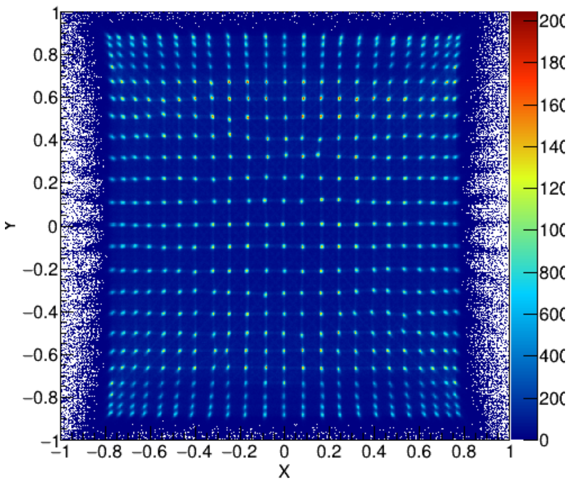

layer4

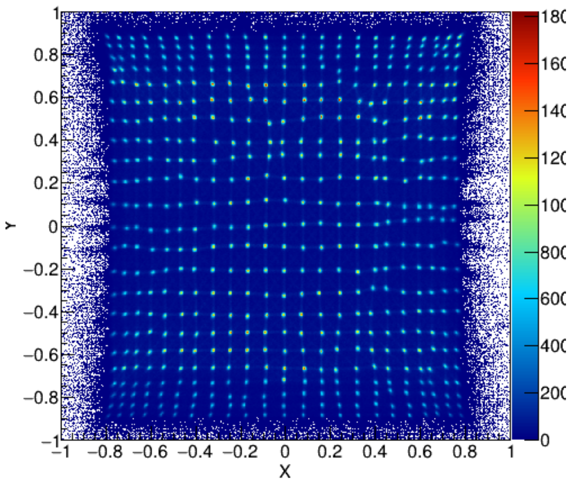

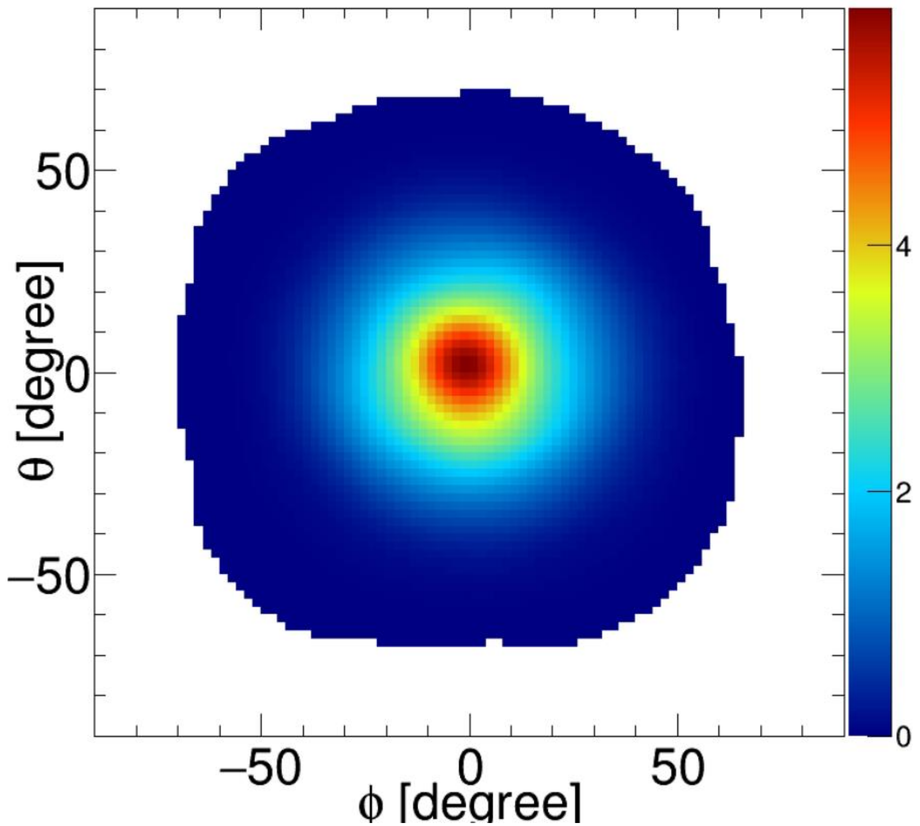

θ [degree]
ϕ [degree]
50
0
−50
4
2
0

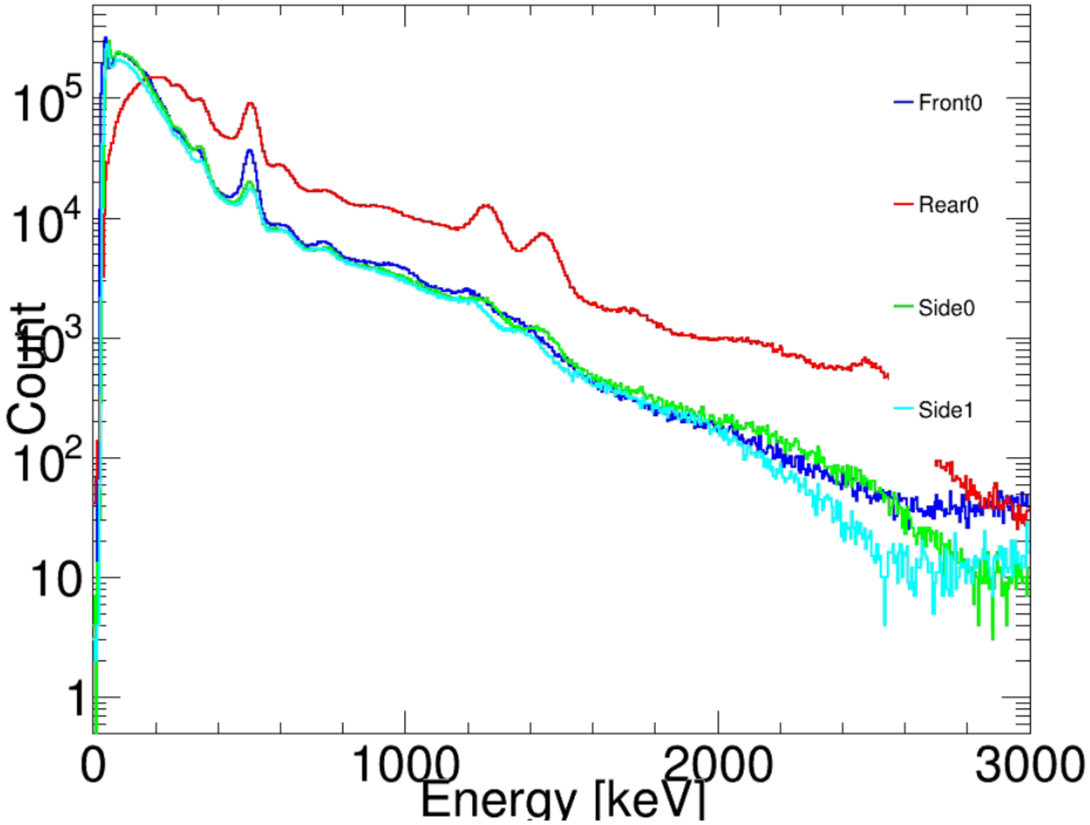

Count
Energy [keV]
10^5
10^4
10^3
10^2
10
1
0
1000
2000
3000
Front0
Rear0
Side0
Side1

12. Radiation damage to MPPC

Nakamori et al 2013, ICRC

10krad

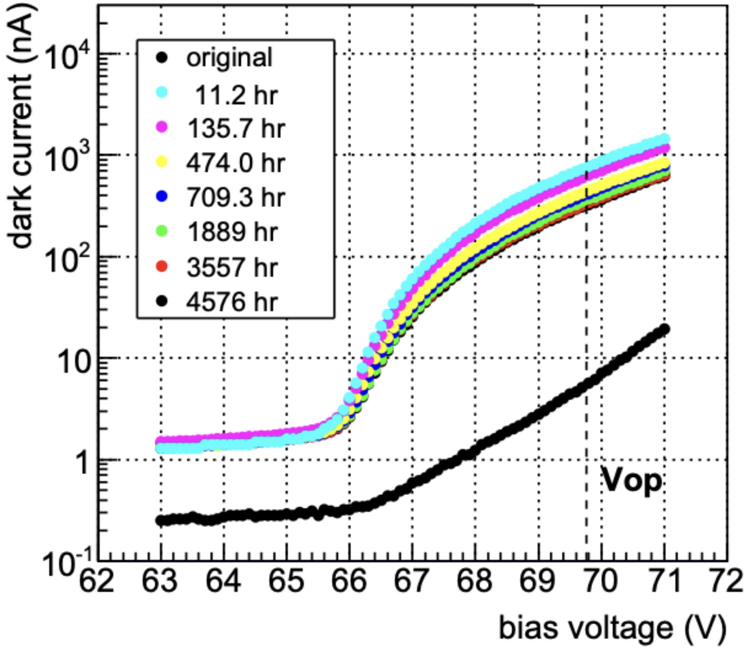

100krad

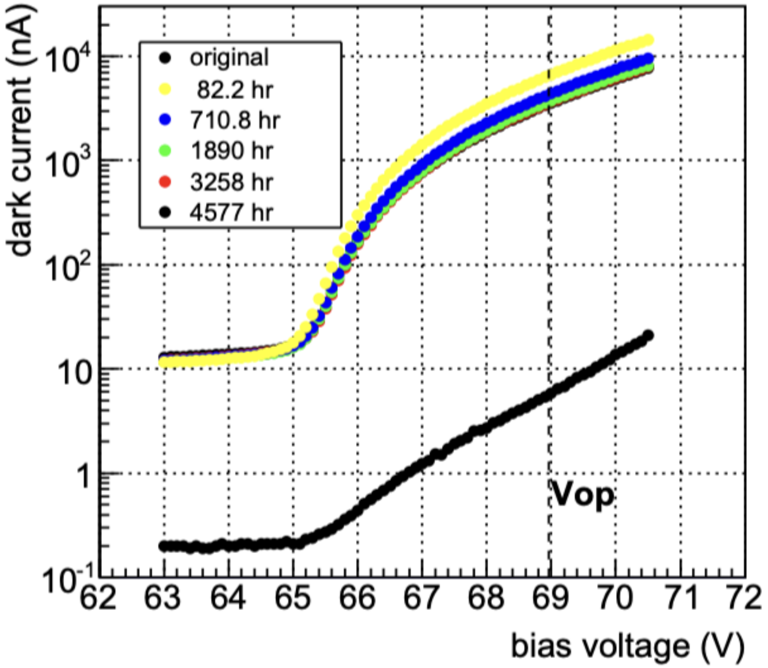

・In orbit ：~1krad/year
・Bulk damage and charge trapping due to ionization processes ：Increase in dark current
⇒The low-energy range around ~50 keV may become indistinguishable from noise.

12. Power supply test

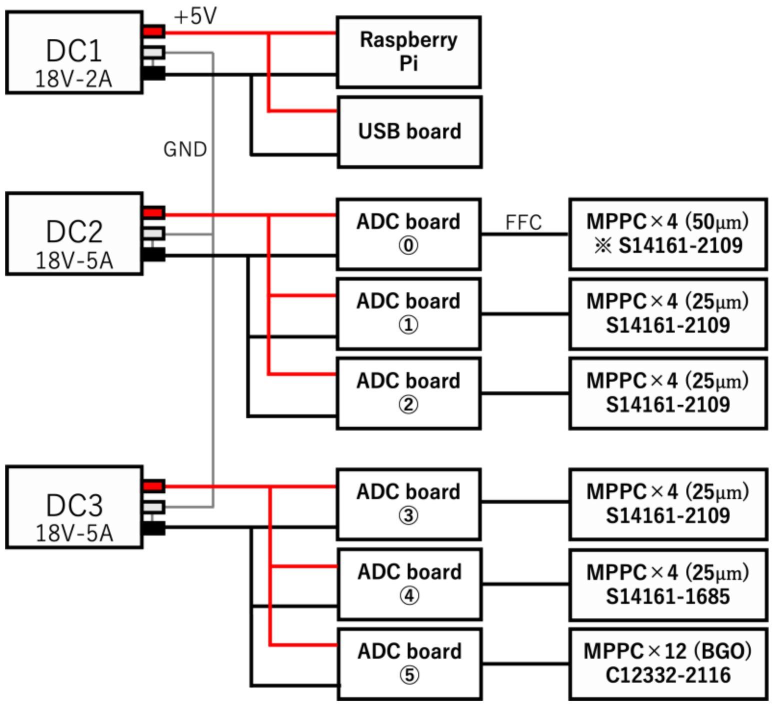

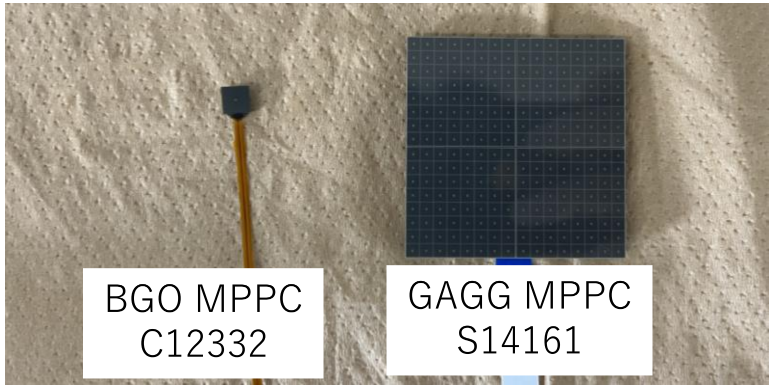

DC1 → DC2 → DC3

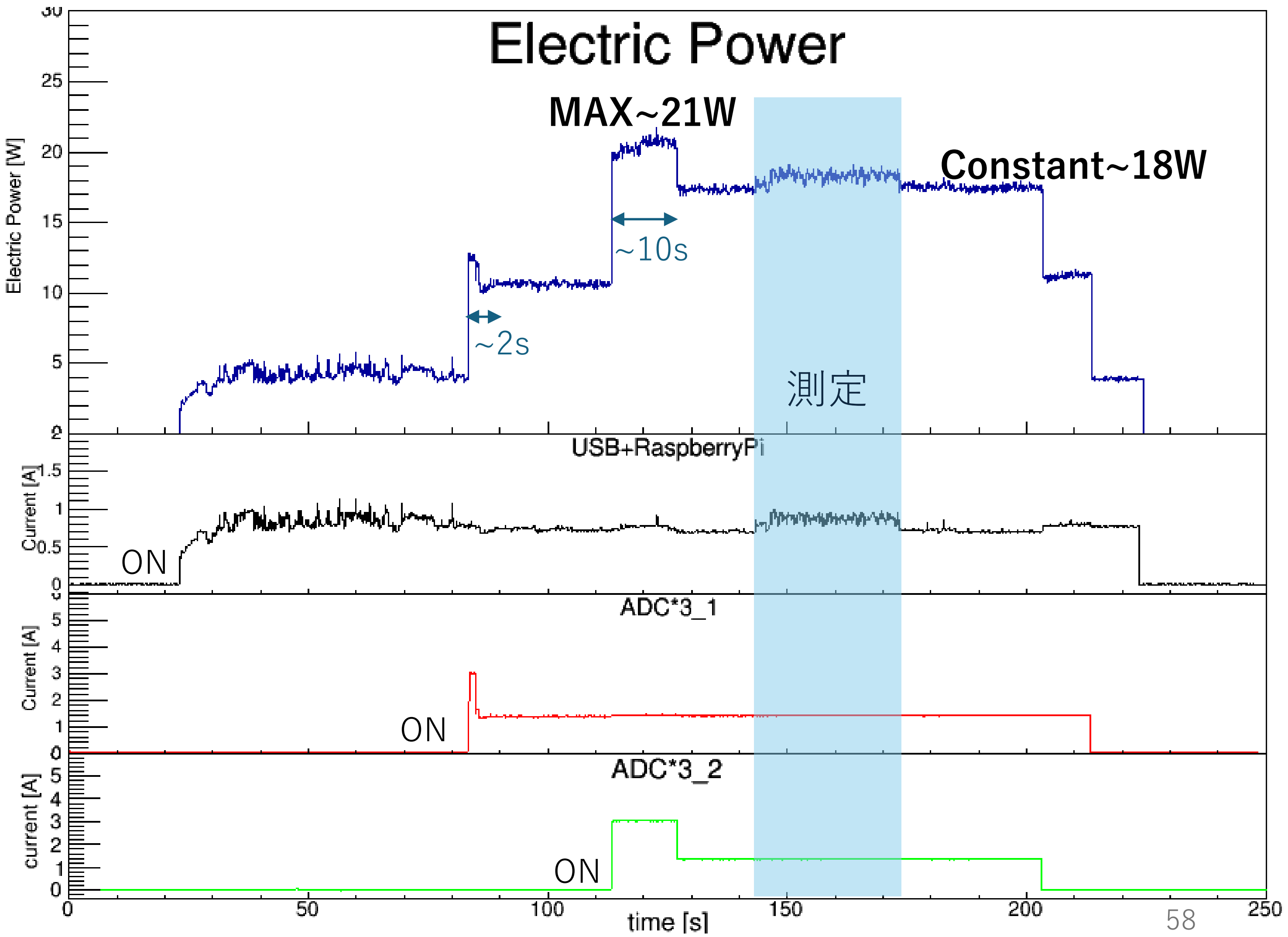

12. DAQ Part

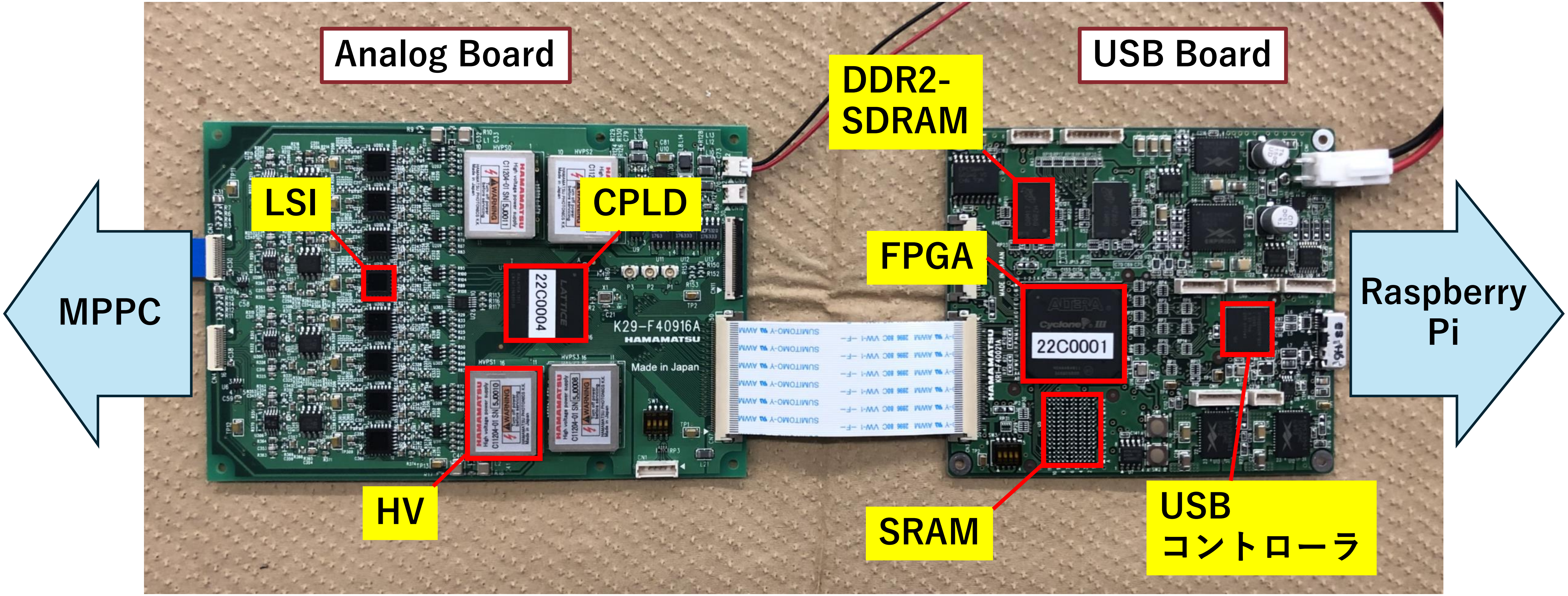

Analog Board
USB Board
DDR2-SDRAM
LSI
CPLD
FPGA
MPPC
Raspberry Pi
HV
SRAM
USB コントローラ
22C0004
22C0001
K29-F40916A
HAMAMATSU
Made in Japan

12. Radiation test

Irradiation position	Total irradiation duration	Hard error	Soft error	Sum
FPGA・SRAM	2.7	3	0	3
DDR2-SDRAM	1.0	1	1	2
USBコントローラ	0.4	0	1	1
CPLD	8.0	0	0	0
LSI	7.0	0	0	0

- ✓ The ADC board experiences both hard and soft errors on a timescale of several months.
  ⇨ It has been confirmed that restarting the system restores normal operation.
- ✓ No critical errors have been observed on the USB board.
- ✓ Protons hitting circuit boards can cause Single Event Upsets (SEUs) or Single Event Latch-ups (SELs).
  SEUs flip bits in memory or flip-flop circuits, while SELs cause excessive current in thyristor structures, risking permanent damage. Prompt overcurrent detection is essential to mitigate SELs.

galactic plane observation

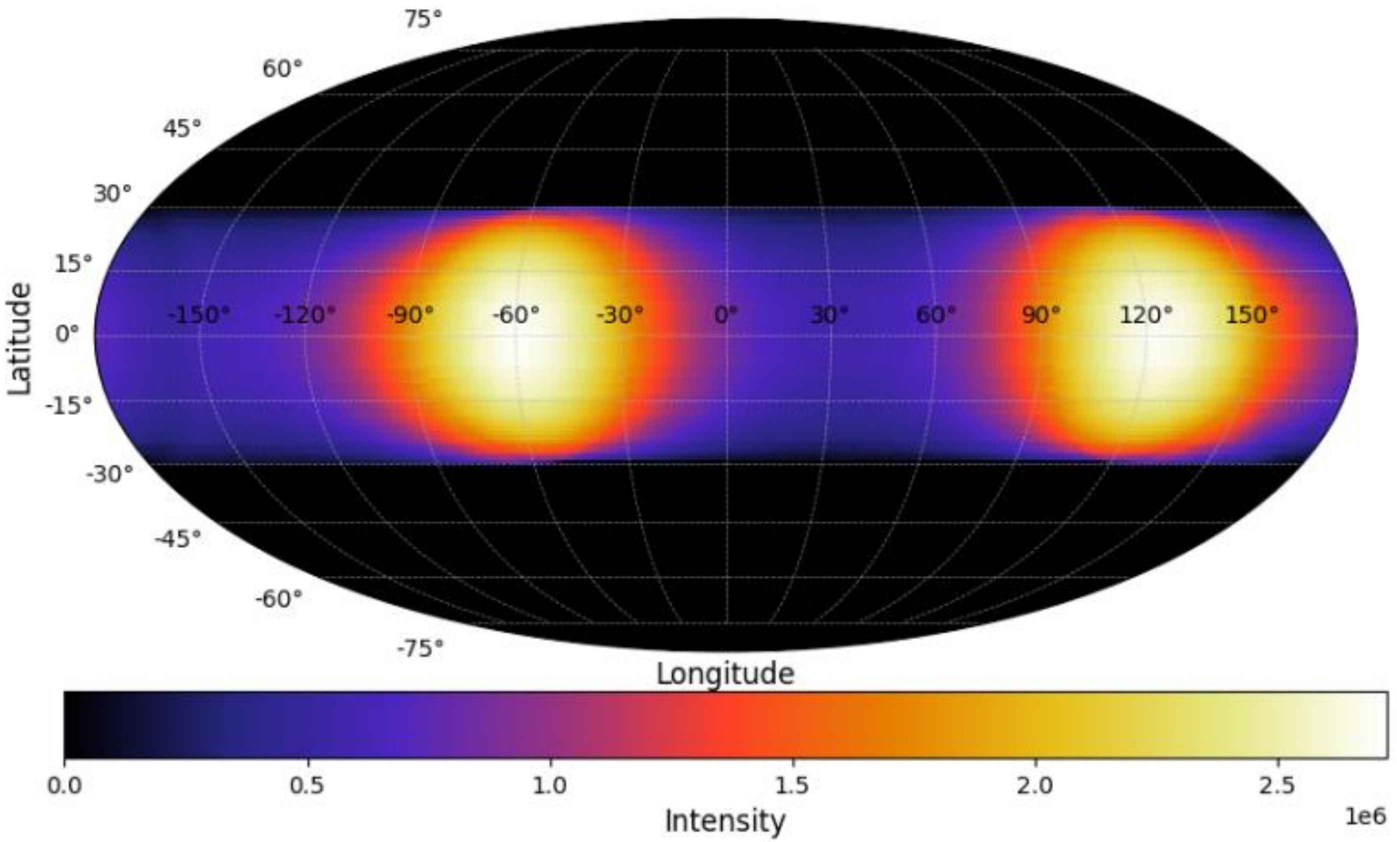

Exposure Map (1year)

Orbit

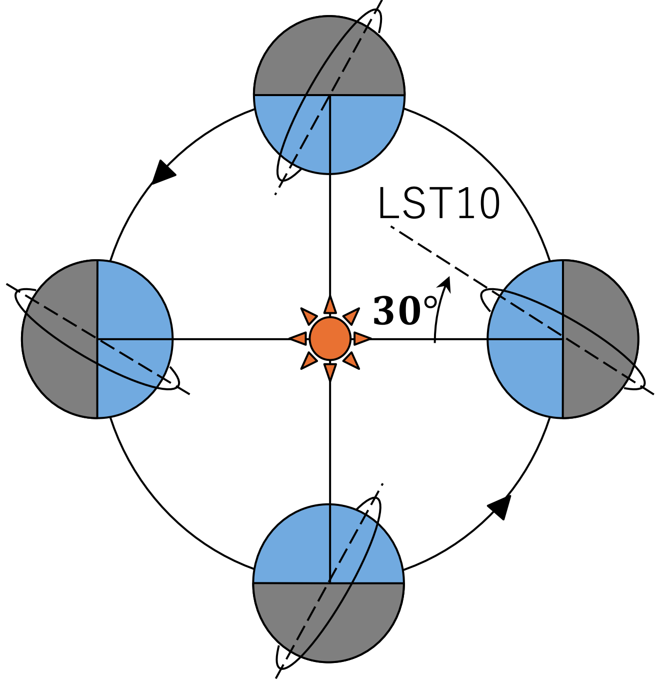

Sun-synchronous orbit

(LST10/550km Altitude)

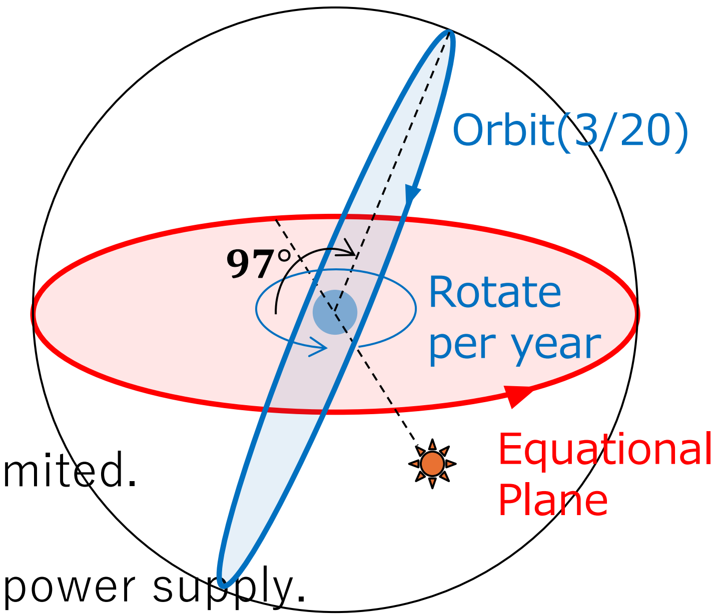

Merit

The angle between the satellite's orbital plane and the direction of the sun remains almost constant throughout the year

- Thermal design is easier because the thermal environment can be limited.
- Easy equipment placement in terms of field of view.
- The sun angle is almost constant, so it is easy to secure a constant power supply.

https://www.jstage.jst.go.jp/article/kjsass/55/639/55_113/_pdf/-char/ja

Observation method

Out-of-plane offset observation

equational coordinates
equational longitude···anti-solar
equational latitude···galactic plane
→**Mapping the galactic plane in one year**

Merit

Facing anti-solar direction, which is advantageous for power generation

Restriction

No observation when the earth is in the Compton camera's field of view(60°)

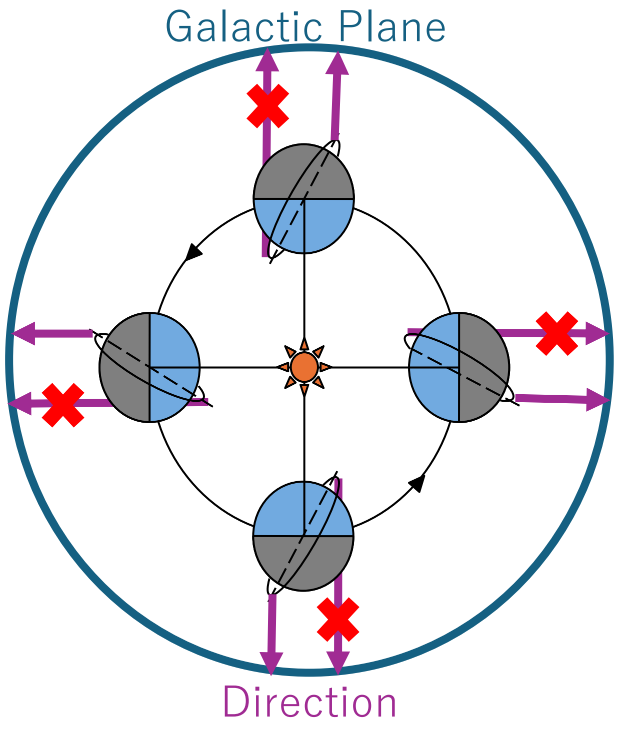

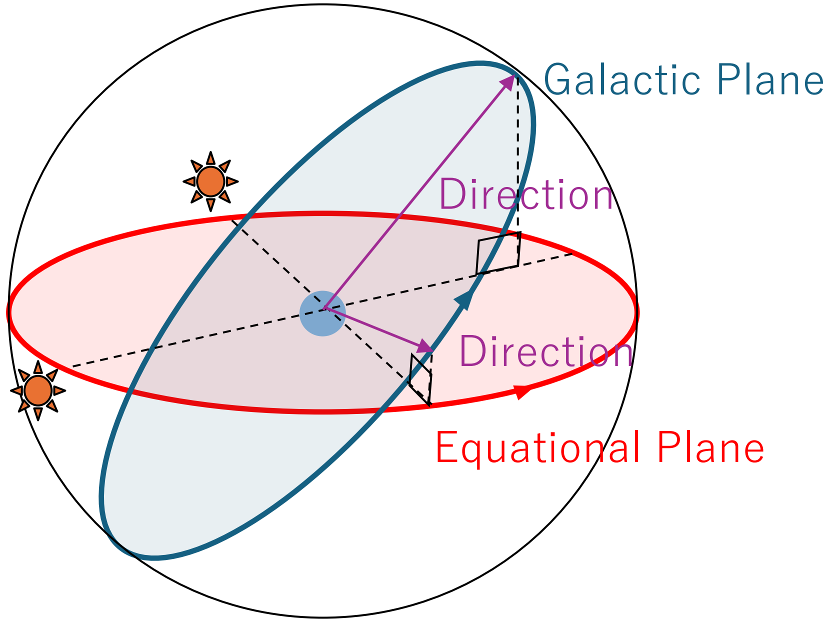

How to calculate Observation time

In Galactic Plane,
Direction $\pm 30°$ is counted(pinhole FOV)

※Constant velocity at the equatorial plane
→Coarse and dense observation time